UNIVERSITY OF CALIFORNIA,

IRVINE

Energy optimization of secondary treatment in WRRFs via off-gas and respirometric measurements

DISSERTATION

submitted in partial satisfaction of the requirements

for the degree of

DOCTOR OF PHILOSOPHY

in Engineering

by

Federico Pasini

Dissertation Committee:

Professor Diego Rosso, Chair

Professor Sunny Jiang

Professor Brett Sanders

2019

DEDICATION

to my parents who always believed in me

to me, because I believed them

TABLE OF CONTENTS

LIST OF FIGURES

LIST OF TABLES

ACKNOWLEDGMENTS

First and foremost, I would like to acknowledge my parents, who taught me all I needed to know to carry on during this experience. I am grateful to my advisor and committee chair, Professor Diego Rosso, for sharing his knowledge and teaching me how to be an independent and critical mind. A special thanks to the committee members, Professor Sunny Jiang and Professor Brett Sanders for their useful comments and advice which helped me grow over my preliminary, qualifying and final examinations.

I would like to thank Manel Garrido for the constant help and support, Graham McCarthy and Igor Bindi for sharing with me never-ending days of experimental work, all my friends and co-workers in EPL lab for all their friendship and kindness throughout these years. Furthermore, I would like to acknowledge who made this dissertation possible through their financial support: DOE CERC-WET project, NSERC Government of Canada, Trojan Technologies, Southern California Edison, Los Angeles Sanitation District (LACSD), Inland Empire Utilities Agency and the UCI Wex Center. Finally, I would like to acknowledge Travis Sprague, Pietro Cambiaso and all operators and engineers from IEUA for their kindness and support.

CURRICULUM VITAE

Federico Pasini

2012 – B.S. in Civil and Environmental Engineering, Universita' Politecnica delle Marche, Ancona, Italy

2015 – M.S. in Civil and Environmental Engineering, Universita' Politecnica delle Marche, Ancona, Italy

2019 – Ph.D. in Engineering, University of California, Irvine
with concentrate in Civil and Environmental Engineering

FIELD OF STUDY

Energy optimization of wastewater sanitation

PUBLICATIONS

Pasini F., Garrido-Baserba M., Ahmed A., Nahkla G., Santoro D., Rosso D. Oxygen transfer and plant-wide energy assessment of primary screening in WRRFs. *Water Environment Research* (in revision).

Pasini F., Garrido-Baserba M., Sprague T., Cambiaso P., Rosso D. Quantification of energy and cost reduction from decreasing DO levels in full-scale WRRFs. *Environmental Science and Technology* (in preparation).

Pasini F., Garrido-Baserba M., Rosso D. Real-time off-gas and respirometric measurements to optimize secondary treatment in WRRFs. *Water Research* (in preparation).

Pasini F., Garrido-Baserba M., Ahmed A., Nahkla G., Giaccherini F., Santoro D., Wessel C., Marcelis P., Kras. R., Rosso D. Analysis of activated sludge aeration systems following primary filtration. (2018) Weftec, 91st, New Orleans, Lousiana.

Pasini F., Garrido-Baserba M., Sprague T., Cambiaso P., Bindi I., Mc Carthy G., Rosso D. Long Term Aeration Power and Energy Monitoring Via Fully Automated Telemetric Off-Gas Analysis. (2019) Weftec, 92nd, Chicago, Illinois.

ABSTRACT OF THE DISSERTATION

Energy optimization of secondary treatment in WRRFs via off-gas and respirometric measurements

by

Federico Pasini

Doctor of Philosophy in Engineering

University of California, Irvine – Fall 2019

Professor Diego Rosso, Chair

Water resource recovery facilities (WRRFs) are responsible for a significant portion of the municipal energy consumption and related GHG emissions. Most of the energy demand for water sanitation (up to 80%) is commonly required in the secondary stage of the treatment, where aeration is provided to the tank through a range of technological solutions (mechanical aerators, coarse to fine bubbles diffusers, etc.) to ensure aerobic conditions in the aerated stage of activated sludge process (AS).

Despite the high cost of aeration, the best science describing the mechanics of oxygen transfer is affected by dynamic process conditions has not yet been fully integrated into the considerations for control, design, and modelling of secondary treatment in WRRFs. First, effluent quality and process stability are prioritized over the cost of treatment; second, the capability of existing facilities to adapt the air supply to transient oxygen demand over the daily fluctuation is often limited by dated design and/or equipment; third, whereas energy rates are often time-based,

this results in the highest cost of treatment correspondent to the lowest efficiency in air use from the blowers.

Hence, the objective of the dissertation is to investigate the potential of continuous characterization of process dynamics and aeration efficiency indicators as a diagnostic tool to optimize energy efficiency in WRRFs. Extensive off-gas and respirometric measurements were used to define temporal and spatial fluctuations of aeration dynamics in secondary treatment and correlate biological oxygen uptake rate (OUR) with oxygen transfer efficiency (OTE).

Additional insights were provided by the adopted methodology, as the coupling of online respirometric and off-gas monitoring with power metering allowed to create redundancy in the measurement of OUR and power demand for aeration. This ultimately served to extract more information about oxygen supply efficiency and mechanical efficiency of the blowers, compared to the standard practice.

Overall, the results confirmed how significant reduction of power demand for aeration (20-50%) can be achieved while ensuring effluent quality by strategically modifying process operations (carbon diversion in primary treatment, DO reduction in secondary treatment, flow equalization, etc.).

In addition, this study finds that better understanding of site-specific process dynamics using a validated and optimized WRRF model can significantly reduce aeration power demand. Finally, an approach to characterize process operations and highlighting optimal and critical points through the analysis of key state variables is proposed for design, modeling and process control of WRRFs secondary treatment.

1. Introduction

Water and energy are deeply intertwined. Whereas the reduction of energy demand is recognized among the main contributors to mitigate global climate change, understanding the water-energy nexus is of utmost importance to achieve this goal. First, the energy required for water distribution and sanitation from water resource recovery facilities (WRRFs) is estimated around 2% of the total world electricity consumption and up to 20% the energy demand for municipalities. This translates in high environmental impact and substantial GHG emissions to operate water services ((Racovicenau 2013), (Olsson 2015)).

The analysis of the interaction between water and energy as basic services within the public infrastructure is fundamental tool for policymakers as it involves many socio-economical aspects (Sorrell 2015), whereas the role of civil and environmental engineers in the optimization of energy efficiency for water services it is of utmost importance to guarantee a sustainable development of public infrastructure. (Cosgrove and Loucks 2015). Second, due to the nature of electricity and water as highly subsidized goods, the collection of adequate revenues to cover O&M costs and invest in future improvements may be challenging for many utilities (Griffin 2016). Water and energy consumption are often priced following a set of structures established to promote a rational use of the existing infrastructure. Whereas conservation is generally favored by high prices for high consumption, this strategy may fail in ensuring an equitable distribution of the service to different income level of customers or, contrarily, fail to generate enough revenues to cover costs in the case a significant reduction of demand occurs among customers ((Banerjee et al. 2010); (Lago and Mysiak 2015); (Dinar 2003)). Hence, reducing cost of operations may be a viable option

to sustain capital investment for energy optimization without jeopardizing the equity or sustainability of the tariff (Pajares, Valero, and Sánchez 2019).

Third, it is common interest of large energy consumer such as WRRFs and energy providers to reduce peaks in power demand. A study showed how a minor (1%) shift in power demand would result in savings in the order of billions of dollars at system level (Spees, 2008). On the energy provider side, this was favored by establishing rebates and customized energy tariffs incentivizing the reduction of power demand during targeted periods of the day from large utilities (Thompson and Piette 2009). On the utility side, new energy practices were concurrently implemented and often coupled with rebates and customized tariffs from the energy provider. Demand side management (DSM) is the definition of a portfolio of measures aimed to optimize the energy system by modifying the consumption over the day, based on price and peak demand constraints. Generally, those strategies are not singularly aimed to reduce energy consumption rather than curb the demand during critical time of the day (Palensky and Dietrich 2011).

With focus on our case, it is largely highlighted how energy efficiency of WRRFs is dependent on several factors, ranging from the size and characteristics of the facility such as the equipment and the energy intensity of the adopted process (activated sludge, ultra-filtration, reverse osmosis, etc.) as well as the type of the treated wastewater (domestic, industrial, etc.), the end-use of the produced water (re-use, discharge limits for final receptor, etc.) ((Metcalf & Eddy 2014); (Olsson 2015)). Because activated sludge (AS) is a commonly adopted to perform biological secondary treatment in WRRFs, the cost of providing air to ensure aerobic conditions for microbiological activity is often the main component of the overall energy demand, up to 75% of the total from the WRRF ((Reardon 1995); (Rosso, Iranpour, and Stenstrom 2005)). As WRRFs operations undergo significant variability during the day and among different seasons due to the transient nature of

influent flows, contaminants concentration and temperatures effecting process biochemistry ((ASCE 2007); (Henze et al. 2008); (Metcalf & Eddy 2014); (Stenstrom and Gilbert 1981)), this results in variable energy requirements as well as energy efficiency. Commonly, aeration tanks in WRRFs are operated with scheduled air flow rates or controls based on dissolved oxygen setpoints, often coupled with ammonia sensors to maintain targeted DO concentrations over the tank length and ensure adequate air supply to match varying oxygen requirements. However, whereas this provides a more responsive behavior of the air supply to the fluctuating oxygen requirements, it does not provide insights about the efficiency of the air use (i.e, transfer efficiency). In the last 30 years, the development of testing methodologies such as off-gas test allowed to quantify the oxygen transfer efficiency (OTE%) and correlate transient conditions to the efficiency of air use ((Redmon et al. 1983); (ASCE 1997)). The negative effect of contaminants on oxygen transfer is quantified by the alpha factor (α), which expresses the suppression of oxygen transfer compared to clean water conditions ((Metcalf & Eddy 2014); (ASCE 1997)). Several are the studies confirming the effect of process conditions on oxygen transfer efficiency: turbulence, flow regime and type of diffusers (e.g. (D. Rosso, Iranpour, and Stenstrom 2005); (Gillot and Héduit 2008)), presence of surfactants (Diego Rosso and Stenstrom 2006), rheological characteristics of the activated sludge and mean cell retention time (MCRT) ((Gillot et al. 2005); (Germain et al. 2007); (Fabiyi and Novak, 2008); (Racault et al. 2011); (Ratkovich et al. 2013), (Durán et al. 2016); (Jochen Henkel et al. 2009); (Wagner et al. 2002); (Krampe and Krauth 2003)).

Two are the main factors resulting in high environmental impact of secondary treatment: first, the efficiency of oxygen transfer from gas to liquid phase is variable under process conditions, where highest suppression of oxygen transfer corresponds to periods of highest concentration of contaminants and least efficient air supply ((Olsson 2015);(Rosso 2018)). Second, the cost of

aeration is additionally amplified by the energy tariff structure, which prices can be almost 25% more expensive during peak hours, where energy consumption in secondary treatment can reach up to 4 times the energy demand required off-peak (Emami, Sobhani, and Rosso 2018). The efficiency of AS operations is therefore usually the lowest during peak-hours, when highest influent results in the circadian amplification of air flow rate supplied to the tank, resulting in energy consumption and concurrent GHG emissions. Nonetheless, aeration systems in WRRFs are yet partially able to effectively adapt air supply to the varying oxygen demand for transient hydraulic and organic loads due to dated equipment and design of the plants. Whereas ensuring effluent quality is always prioritized to energy efficiency in order to avoid liability for non-complying to discharge limits, inefficient operations and excessive cost of treatment are often overlooked by WRRFs (Åmand, Olsson, and Carlsson 2013).

Thus, the capability to implement targeted periods of high and low power demand for WRRFs would result in significant savings for cost of treatment, whereas energy requirements for treatment can be tailored during the day ((Amaral et al. 2016); (Beltran et al. 2012); (Grau et al. 2007); (Åmand et al. 2013); (Ingildsen and Olsson, 2015)). Nevertheless, most of the applications of off-gas testing provided punctual or overall limited datapoints, corresponding to specific loading and operating conditions and overlooking daily and seasonal fluctuations. Hence, despite the application of the standard off-gas test methodology (ASCE 1997) is largely recognized as a powerful diagnostic tool, continuous off-gas monitoring would offer higher detail in the process dynamics characterization ((Schuchardt et al. 2007); (Leu et al. 2009); (Amerlinck et al. 2016)). In the last fifteen years, the implementation of aeration dynamics monitoring for energy optimization was investigated.

Several are the studies performed via benchmark modelling ((Åmand, Olsson, and Carlsson 2013); (Garrido-Baserba et al. 2017)) while few are the examples of full-scale implementation of optimization measures based on aeration efficiency indicators ((Jenkins et al. 2008); (Schuchardt et al. 2007)). Results confirmed the importance of the continuous diagnostic of aeration efficiency to achieve energy and cost savings for aeration ((Pittoors, Guo, and Van Hulle 2014);(Åmand, Olsson, and Carlsson 2013)).

Nonetheless, the uncertainty about the mechanistic phenomena affecting oxygen transfer yet partially allows to extend site-specific datasets. Whereas the state of art is still evolving to understand and apply process modifications and reduce energy footprint, the thorough characterization of process dynamics is highly regarded as a fundamental step to achieve this goal ((Amaral et al. 2016); (Beltrán et al. 2012); (Gernaey et al. 2001)). Thus, a more extensive application of off-gas monitoring coupled with other methodologies is required to consolidate its potential as diagnostic tool and accurately predict aeration system dynamics independently from site-specific conditions.

In this study, off-gas monitoring was coupled with real-time respirometric measurements. This was to investigate a surrogate parameter able to globally describe the effect of contaminants and biomass concentration on oxygen transfer. The development of a correlation between respiration rates and oxygen transfer efficiency would allow to define optimal oxygen supply to match the microbiological demand while targeting highest aeration efficiency. Moreover, the long-term off-gas monitoring would highlight the varying performances of the aeration system during the daily cycle and allow to highlight optimal operating conditions (dissolved oxygen setpoints, air flow rate, etc.). Finally, the additional measurement or respirometric rates, power demand for aeration and water quality would allow calibrate off-gas calculations in real time as well as provide

additional insights on the process conditions. Hence, the goal of this doctoral study is to investigate a portfolio of operational solutions to minimize energy wastage and maximize treatment capacity based on off-gas and respirometric methodologies, at pilot and full-scale. The results collected during the experimental campaigns were implemented in site-specific models to improve the accuracy in the evaluation of optimization strategies. Different aspects of daily operations of WRRFs were investigated to provide a range of solution independent from site-specific conditions.

In chapter 1, the introduction of targeted solid removal upstream the aeration tank is evaluated. This was to quantify the potential energy savings in secondary treatment resulting from carbon-diversion in primary treatment. The first phase of the study was performed at both pilot and full-scale and allowed to highlight the differential performances of two identical biological reactors operated with pre-screened and raw primary influent, respectively. Results from off-gas and respirometric tests confirmed the beneficial effect of primary screening on cost for aeration, as oxygen requirements were reduced for pilot and full-scale resulting in the reduction of biomass respiration rates. The collected results were implemented in a series of plant-wide models consisting of primary treatment, secondary treatment, sludge dewatering and anaerobic digestion. Different technological solutions were evaluated to simulate primary treatment. Primary clarifiers and screens/RBFs were compared in the model to evaluate the advantages of targeted and flow-independent solid removal. Different time periods over the daily influent variability and different solids removal performances were implemented to define a plant-wide energy balance and evaluate cost and benefit of carbon diversion through primary screening. Overall, results showed how 15% energy savings could be achieved by the concomitant effect of the reduction of air requirements in secondary treatment and enhanced biogas production in anaerobic digestion.

In chapter 2, long-term monitoring of aeration efficiency indicators is presented as a tool to continuously characterize process dynamics. Commonly, off-gas testing is performed manually, hence existing data are limited to a narrow range of operating conditions as manual labor is required to perform the measurements. To overcome this limitation, a fully automated off-gas sampling equipment was installed with a fixed sampling hood at the side of the aeration tank to capture process air leaving the tank surface. The position was selected after a full tank characterization to define a section representative of the whole aerated area. One full year of characterization in the aeration tank of a WRRF allowed to collect the fluctuation of process dynamics and aeration efficiency indicators for daily and seasonal variability. The collected results were implemented in a series of models to evaluate optimization strategies and quantify savings for cost of aeration associated with optimization strategies (flow equalization, DO setpoints reduction, etc.). One of the modelled strategies was validated at full-scale and confirmed the potential of targeted DO setpoint decrease to reduce energy footprint and optimize treatment capacity. When the setpoint was decreased in the first aerobic section of a WRRF from 1.9 to 1.7 mg l^{-1}, the aeration control system responded by redistributing the air supply along the tank length, which resulted in up to 20% of savings for power demand as OTE% increased and excessive aeration was minimized, maintaining effluent quality unvaried.

In chapter 3, a similar methodology based on off-gas monitoring is integrated with real-time respirometric measurements. This allowed to profile process parameters along the tank length and highlight the space-time variability. The biomass respirometric rates were coupled with water quality analysis to define loading ratio between oxygen demand and oxygen requirements, settling characteristics and aeration efficiency indicators. Two WRRFs with different size and secondary

treatment layout (single feed, step-feed) were investigated with a multi-points sampling campaign to quantify time and spatial variability of process parameters under dynamic conditions.

Results showed how a correlation between biomass respirometric rates and oxygen transfer efficiency could allow to predict aeration efficiency independently from site-specific data sets. Moreover, by coupling off-gas and respirometric measurements, the calculation of oxygen uptake rate can be performed independently and provide additional insights on the process conditions. A methodology to characterize the dynamics of aerobic processes in secondary treatment and suggest optimization strategies is proposed. This would support operative decision-making, improve the accuracy of process dynamics modelling, provide information about diffusers maintenance schedule, blowers operations and could be adopted for process control, model calibration and design of secondary treatment.

Following is a summary of the process state variables proposed for characterization, modelling, design and control of the secondary treatment. In Table 1.1 different testing methodologies are proposed to diagnose process conditions and evaluate process performances. In Table 1.2 is summarized a set of rules to be implemented for process control, as a soft-sensor alarm to detect process criticalities, evaluate long-term predictions for maintenance (diffusers cleaning) and equipment selection.

Table 1.1 - Summary of testing methodologies.

Methodology	Application	Sampling	Measured variables	Results	Historical data
Static off-gas (ASCE 1997)	Aeration tank mapping	>2% of the aerated surface	Air flow rate, air flux Dissolved oxygen O_2% process air CO_2% process air	- αSOTE% - SOTR - OUR - BHP (Adiabatic formula, kW) - SAE	Tank avg: - <αSOTE%> - <SOTR> - <$OUR_{off-gas}$> - <kW> - <SAE>
Dynamic off-gas	Process dynamics characterization	1 position mid-tank; 2 positions preferred in case of variable diffusers density and air supply (influent, mid-tank)	Air flow rate, air flux Dissolved oxygen O_2% process air CO_2% process air	- αSOTE% - SOTR - OUR - BHP (Adiabatic formula, kW) - SAE	Hourly avg per sampling position: - <αSOTE%> - <SOTR> - <OUR> - <kW> - <SAE>
On-line respirometry (with grab samples for water quality analysis)	Loading conditions characterization	2 positions preferred in case of variable DO setpoints over the tank length	Dissolved oxygen MLSS MLVSS COD NH_3-N	- sOUR for carbon oxidation - sOUR for nitrification - Half-velocity coefficients ks_{Cox} and ks_{NH3-N} - Min ATU inhibiting concentration ATU_{min}	Hourly avg per sampling position: - <$sOUR_{Cox}$> - <$sOUR_{Nitr.}$> - <ks_{Cox}> - <ks_{NH3-N}> - <ATU_{min}>
Standard methods for TSS	Biomass characterization	RAS	MLSS MLVSS MCRT	- MLVSS/MLSS, f(MCRT)	Monthly avg: - <MCRT> - <MLVSS/MLSS>
Power metering	Power demand dynamic characterization	1 meter per blower, if possible	Voltage, current	- kW - kWh - kVAR	Hourly avg: - <kW> - <kWh> - <kVAR>

Table 1.2 - Summary of logic rules for process control.

Real-time variable	Historical avg for comparison	New output variable	Constraints	Time-scale
Process control				
αSOTE%	<αSOTE%> (Hourly avg)	Recalculate air flow rate	<SAE>	~ 2 hours
SOTR	<SOTR> (Hourly avg)	Recalculate DOspt	<SAE>, <SOTR>	~ 2 hours
sOUR for C_{ox}	<sOUR C_{ox}> (Hourly avg)	Recalculate air flow rate Recalculate DOspt	<SOTR>	~ 1 hour
sOUR for Nitr.	<sOUR Nitr.> (Hourly avg)	Recalculate air flow rate Recalculate DOspt	<SOTR>	~ 1 hour
Maintenance schedule				
αSOTE%	<αSOTE%> (Tank, hourly avg)	Estimate fouling effect	$\frac{Cost\ of\ cleaning}{Loss\ in\ efficiency}$	~3 to 6 months
SAE	<SAE> (Tank, hourly avg)			
kW	<kW>			
Biomass characterization				
sOUR for Cox	< ksC_{ox} > (Tank, hourly avg)	ksCox	Variation in biomass composition (Nitrifiers, heterotroph) Optimal nitrification rate	~ 3 <MCRT>
sOUR for Nitr.	< $ksNH_3$-N.> (Tank, hourly avg)	ksNH3-N		
ATU dosage	<ATUmin>	New inhibiting ATU <ATUmin>		
MLSS, MLVSS	<MLVSS/MLSS>	Optimal MCRT		
MCRT	<MCRT>			

References

Åmand, L., G. Olsson, and B. Carlsson. 2013. "Aeration Control - A Review." *Water Science and Technology* 67 (11): 2374–98.

Amaral, Andreia, Oliver Schraa, Leiv Rieger, Sylvie Gillot, Yannick Fayolle, Giacomo Bellandi, Youri Amerlinck, et al. 2016. "Towards Advanced Aeration Modelling: From Blower to Bubbles to Bulk." *Water Science & Technology* 75 (3–4): 507–17. https://doi.org/10.2166/wst.2016.365.

Amerlinck, Y, G Bellandi, A Amaral, S Weijers, and I Nopens. 2016. "Detailed Off-Gas Measurements for Improved Modelling of the Aeration Performance at the WWTP of Eindhoven." *Water Science and Technology* 74 (1): 203–11. https://doi.org/10.2166/wst.2016.200.

Banerjee, Sudeshna, Vivien Foster, Yvonne Ying, Heather Skilling, and Quentin Wodon. 2010. "Cost Recovery, Equity, and Efficiency in Water Tariffs Evidence from African Utilities," no. July: 1–52. https://doi.org/http://www-wds.worldbank.org/servlet/WDSContentServer/WDSP/IB/2010/07/28/000158349_20100728131236/Rendered/PDF/WPS5384.pdf.

Cosgrove, William J, and Daniel P Loucks. 2015. "Water Resources Research," 4823–39. https://doi.org/10.1002/2014WR016869.Received.

Dinar, Ariel. 2003. *The Political Economy Context of Water-Pricing Reforms. The Economics of Water Management In Developing Countries: Problems, Principles and Policies*. https://doi.org/10.4337/9781781950517.00010.

Emami, Nasir, Reza Sobhani, and Diego Rosso. 2018. “Diurnal Variations of the Energy Intensity and Associated Greenhouse Gas Emissions for Activated Sludge Processes” 7. https://doi.org/10.2166/wst.2018.054.

Garrido-Baserba, M., F. Pasini, L.-M. Jiang, D. Nolasco, H. De Clippeleir, A. Al-Omari, S. Murthy, and D. Rosso. 2017. “Using Dynamic Alpha Factors for Oxygen Transfer Optimization in WRRFs.” In *Water Environment Federation Technical Exhibition and Conference 2017, WEFTEC 2017*. Vol. 8.

Gernaey, A. Krist, Britta Petersen, Jean Pierre Ottoy, and Peter Vanrolleghem. 2001. “Activated Sludge Monitoring with Combined Respirometric-Titrimetric Measurements.” *Water Research* 35 (5): 1280–94. https://doi.org/10.1016/S0043-1354(00)00366-3.

Gillot, Sylvie, and Alain Héduit. 2008. “Prediction of Alpha Factor Values for Fine Pore Aeration Systems.” *Water Science and Technology* 57 (8): 1265–69. https://doi.org/10.2166/wst.2008.222.

Ingildsen, Pernille, and Gustaf Olsson. 2015. *Smart Water Utilities : Complexity Made Simple*. IWA Publishing.

Lago, Manuel, and Jaroslav Mysiak. 2015. “Preface.” *Use of Economic Instruments in Water Policy: Insights from International Experience*, v–vi. https://doi.org/10.1007/978-3-319-18287-2.

Leu, Shao-yuan, Diego Rosso, Lory E Larson, and Michael K Stenstrom. 2009. “Real-Time Aeration Efficiency Monitoring in the Activated Sludge Process and Methods to Reduce Energy Consumption and Operating Costs.” *Water Environment Research* 81 (12): 2471–81. https://doi.org/10.2175/106143009x425906.

Marne, Paris Est-créteil Val De. 2013. “Dossier De Paiement” 13 (December): 75012. https://doi.org/10.1061/(ASCE)1076-0342(2007)13.

Pajares, Encarnación Moral, Leticia Gallego Valero, and Isabel María Román Sánchez. 2019. “Cost of Urban Wastewater Treatment and Ecotaxes: Evidence from Municipalities in Southern Europe.” *Water (Switzerland)* 11 (3): 1–13. https://doi.org/10.3390/w11030423.

Palensky, Peter, and Dietmar Dietrich. 2011. “Demand Side Management: Demand Response, Intelligent Energy Systems, and Smart Loads.” *IEEE Transactions on Industrial Informatics* 7 (3): 381–88. https://doi.org/10.1109/TII.2011.2158841.

Pittoors, Erika, Yaping Guo, and Stijn W.H. Van Hulle. 2014. “Modeling Dissolved Oxygen Concentration for Optimizing Aeration Systems and Reducing Oxygen Consumption in Activated Sludge Processes: A Review.” *Chemical Engineering Communications*. https://doi.org/10.1080/00986445.2014.883974.

Rosso, D., R. Iranpour, and M. K. Stenstrom. 2005. “Fifteen Years of Offgas Transfer Efficiency Measurements on Fine-Pore Aerators: Key Role of Sludge Age and Normalized Air Flux.” *Water Environment Research* 77 (3): 266–73. https://doi.org/10.2175/106143005x41843.

Rosso, Diego. 2018. *Aeration, Mixing, and Energy: Bubbles and Sparks | IWA Publishing*. Edited by Diego Rosso. Irvine, California: IWA publishing.

Rosso, Diego, and Michael Stenstrom. 2006. “Economic Implications of Fine-Pore Diffuser Aging.” *Water Environment Research : A Research Publication of the Water Environment Federation* 78 (8): 810–15.

Schuchardt, A, J A Libra, C Sahlmann, U Wiesmann, and R Gnirss. 2007. “Evaluation of

Oxygen Transfer Efficiency under Process Conditions Using the Dynamic Off-Gas Method." *Environmental Technology* 28 (5): 479–89. https://doi.org/10.1080/09593332808618812.

Sorrell, Steve. 2015. "Reducing Energy Demand: A Review of Issues, Challenges and Approaches." *Renewable and Sustainable Energy Reviews* 47: 74–82. https://doi.org/10.1016/j.rser.2015.03.002.

Spees, K, L Lave - The Energy Journal, and Undefined 2008. 2008. "Impacts of Responsive Load in PJM: Load Shifting and Real Time Pricing." *JSTOR*, 101–21.

Stenstrom, Michael K., and R. Gary Gilbert. 1981. "Effects of Alpha, Beta and Theta Factor upon the Design, Specification and Operation of Aeration Systems." *Water Research*. https://doi.org/10.1016/0043-1354(81)90156-1.

Thompson, Lisa, and Mary Ann Piette. 2009. "Opportunities for Energy Efficiency and Open Automated Demand Response in Wastewater Treatment Facilities in California – Phase I Report Alex Lekov One Cyclotron Road MS 90R4000 Berkeley , CA 94720," no. 500.

2. Oxygen transfer and plant-wide energy assessment of primary screening in WRRFs*

* A modified version of this chapter is published in the 91st Annual WEFTEC conference proceedings, New Orleans, Louisiana, USA, October 2018 and is in review on Water Environment Research.

2.1 Abstract

Primary screening is gaining interest as a method to minimize aeration requirements while maximizing carbon harvesting for biogas production. Aeration efficiency indicators in a pilot sequential batch reactor (SBR) and a full-scale water resource recovery facility (WRRF) were investigated after the implementation of rotating belt filters/screens (RBF). In order to compare the impact between screened (350 μm) and non-screened primary influent, two identical treatment lines were monitored using off-gas and respirometric measurements. The study provides the first result on improved oxygen transfer efficiency due to primary sieving. Consistent aeration efficiency improvements of 27% and 20% between filter and non-screened were obtained at pilot and full-scale, respectively. Changes in aeration efficiency and carbon redirection were integrated in a set of models to investigate the primary screening impact on the WRRF energy balance. While the plant-wide assessment for different scenarios improved the energy balance up to 15%, a detailed comparative analysis between different treatment schemes gained insight into the advantages and limitations of the energetic sustainability of primary screening.

2.2 Introduction

Enhanced primary treatment and carbon diversion plays a key role in emerging wastewater treatment schemes where energy optimization and carbon management are of concern (Gori et al. 2011; Ho et al. 2017). Several wastewater microscreen technologies offering a higher degree of primary treatment are gaining interest in water resource recovery facilities (WRRFs) as a method to minimize aeration requirements while maximizing carbon diversion ((Caliskaner et al. 2015); (Ruiken et al. 2013)). Enhanced removal of particulate and colloidal fractions by filtration or screen-based methods can result in operational savings in the downstream aerobic biological processes by increasing the oxygen transfer efficiency, while allowing the recovery of energy in the form of methane via anaerobic sludge treatment processes ((Franchi and Santoro 2015); (Ruiken et al. 2013)).

Primary filters (PF) and rotating belt filters/screens (RBF) are among those technologies using cake filtration or screens as a method to increase the capture of suspended solids and organics. Screening-based technologies usually combine the functions of particle removal as well as thickening and dewatering in one unit process and can occupy one-tenth of the footprint of a primary clarifier (Franchi and Santoro 2015). Due to the large pore size of the screens (usually larger than 100μm), they are not true filters and allow the passage of the smaller fraction of colloids. However, their expected operating pressure drop is lower due to the larger size of the pores and the consequent reduced hydrodynamic obstruction (Ruiken et al. 2013).

The main difference between PFs and RBFs is the medium pore size which will influence the treatment performance and overall operational costs. While PFs achieves higher COD and TSS removal by using a relatively small pore size (i.e., 5 to 10 micrometer), the RBF reaches lower treatment removal due to the much larger size of the mesh pores (i.e., 100-500 μm;). In both cases,

TSS removal efficiency is significantly higher than the typical TSS removal (50-60%) obtained with conventional primary clarifiers (Metcalf & Eddy 2014). PF achieves an overall 75-85% TSS and 45-60% COD reduction (Caliskaner et al. 2014; 2015), whereas RBF achieves reductions of 20-40% TSS and 30-40% COD ((Taboada-Santos, Lema, and Carballa 2019); (Ho et al. 2017)).

In micro screen technologies, particles larger than the selected pore openings are effectively separated, whereas smaller particles can also be retained as their effective pore size is reduced by the retained material (especially cellulose) assembling as cake on the screen during solid separation ((Tien 2012); (Degroot et al. 2015)). The removal of nutrients should be expected, with a reported < 20% of nitrogen diversion from the primary sludge (DeGroot et al, 2015). Nonetheless, chemical addition has the potential to double the performance of belt filters ((Taboada-Santos et al. 2019); (Daynouri-Pancino et al. 2018)).

2.2.1 Impact on biogas production

The enhanced primary settling provided by PF and RBF augments the quantity and quality of the sludge diverted to digestion due to the increase in its energy value (Behera et al. 2018). Harvesting higher COD content in primary sludge in comparison to waste activated sludge (WAS) enables significant energy savings via carbon redirection (Caliskaner et al., 2014; Gori et al., 2013; Gori et al, 2011). While the retention time in conventional clarifiers is reduced at peak loading rates due the increased flow (with the concurrent reduction of primary sludge yield), primary screening technologies increase the potential methane yield as their ability to separate solids is independent of flow given that the screen rotational velocity is proportional to the applied head, and hence, flow.

Micro screens, when compared to gravity separation, offer the added advantage of carbon management as they enable more flexible operations with influent variations. The capability to adjust the loading condition by controlling the degree of COD and TSS removal before the secondary treatment by primary screening is important to be able to address potential imbalances in the C:N ratio of nitrifying/denitrifying systems. Adjusting RBF to lower BOD removal can enhance process performance in carbon limited systems and reduce (or avoid) the use of an external carbon source, while higher removals can be maximized under favourable conditions (Rusten et al. 2016; Razafimanantsoa et al. 2014). The capability of introducing "on-demand" pre-treatment would ensure denitrification in pinpointed circumstances as daily peaks of ammonia return flow from dewatering, etc.

2.2.2 Impact on oxygen requirements

Aeration is an essential operation in water resource recovery facilities (WRRFs) and is the main contributor to plant power demand, dominating the process energy requirements with the exclusion of site-specific pumping (Diego Rosso and Stenstrom 2006; Manel Garrido-Baserba et al. 2017; WEF 2009; Diego Rosso and Shaw 2015). The oxygen transfer efficiency decreases from its clean water value (SOTE, %) to process conditions (αSOTE, %) because of the loading conditions, among other co-related factors (i.e., surfactants, process characteristics, etc.), and this decrease is quantified through the alpha-factor (US EPA, 1989; ASCE, 2007; Jiang et al., 2017; Metcalf & Eddy, 2014; Stenstrom and Gilbert, 1981). Any effort to divert load from the secondary treatment would result in the beneficial reduction of the plant energy usage (Rahman et al. 2017; Gori et al. 2013). The decrease in total organic load following primary treatment (through gravity or barrier separation) reduces the total amount of oxygen required for the treatment (Caliskaner et

al. 2015; Degroot et al. 2015; Ruiken et al. 2013). The expectation is that primary treatment via barrier separation would increase oxygen transfer efficiency during the aerobic phase due to the reduced organic load and selectively alter the organic load fraction by size exclusion independently of the hydraulic load. Both phenomena are expected to decrease the electricity demand for aeration in secondary treatment. On the other hand, the performance of primary settling depends on the hydraulic loading, which implies lower separation efficiency at times of peak loading, which tend to correspond to the highest peak power periods (Emami, Sobhani, and Rosso 2018).

Previous studies highlighted the potential of primary screening to increase the capture of the less biodegradable (particulate) fraction, especially improving the entrapment of cellulose-derived constituents (Paulsrud, Rusten, and Aas 2014; Ruiken et al. 2013). Altering the organics fractionation (i.e., particulate, colloidal and soluble) by the implementation of barrier separation technologies will impact the overall energy balance. A few studies estimate the increase in the particulate fraction from 40% to 65% (Gupta 2018; Ahmed et al. 2019; Honda et al. 2002; Hurwitz et al. 1961; Verachtert et al. 1982), potentially representing from 27% to 55% of the total COD influent load. The improved removal of the slowly biodegradable COD fraction obtained by primary barrier separation influences sludge production and characteristics (Ruiken et al. 2013; Ahmed et al. 2019), and can result in lower specific sludge yield as compared to primary gravity clarification (Ruiken et al. 2013).

Our study compared two parallel activated sludge treatment trains on pilot- and full- scale reactors using off-gas and respirometric measurements. Our analysis on primary sieving and oxygen transfer efficiency furthers our understanding of the role of primary treatment on plant-wide process energy and helps improve existing process models.

2.3 Materials and methods

2.3.1 Pilot-scale testing

Two identical sequencing batch reactors (SBR), with a total volume of 8.5 litres each and a feeding volume of 3 litres, were used to measure the impact of primary screening on oxygen transfer efficiency (Fig. 2.1). The two SBRs were fed with the activated sludge from WWRF1 (Southern California). Reactors were fully automated following a 6h treatment cycle designed to replicate the stages of pre-denitrification and nitrification in WRRF2 (Aarle-Rixtel, Netherlands) as well as maintain loading conditions (i.e., F/M ratio).

Screened line or barrier separation/sieving was performed with a 350 μm filter mesh modular system. The filter loading (l m^{-2} h^{-1}) was selected to replicate the same barrier separation performance installed at full-scale in WRRF2 (model SF200; Salsnes, Norway). Backwash was carried out after the sieving phase to prevent excessive solid cake formation and guarantee consistency in TSS and COD removal.

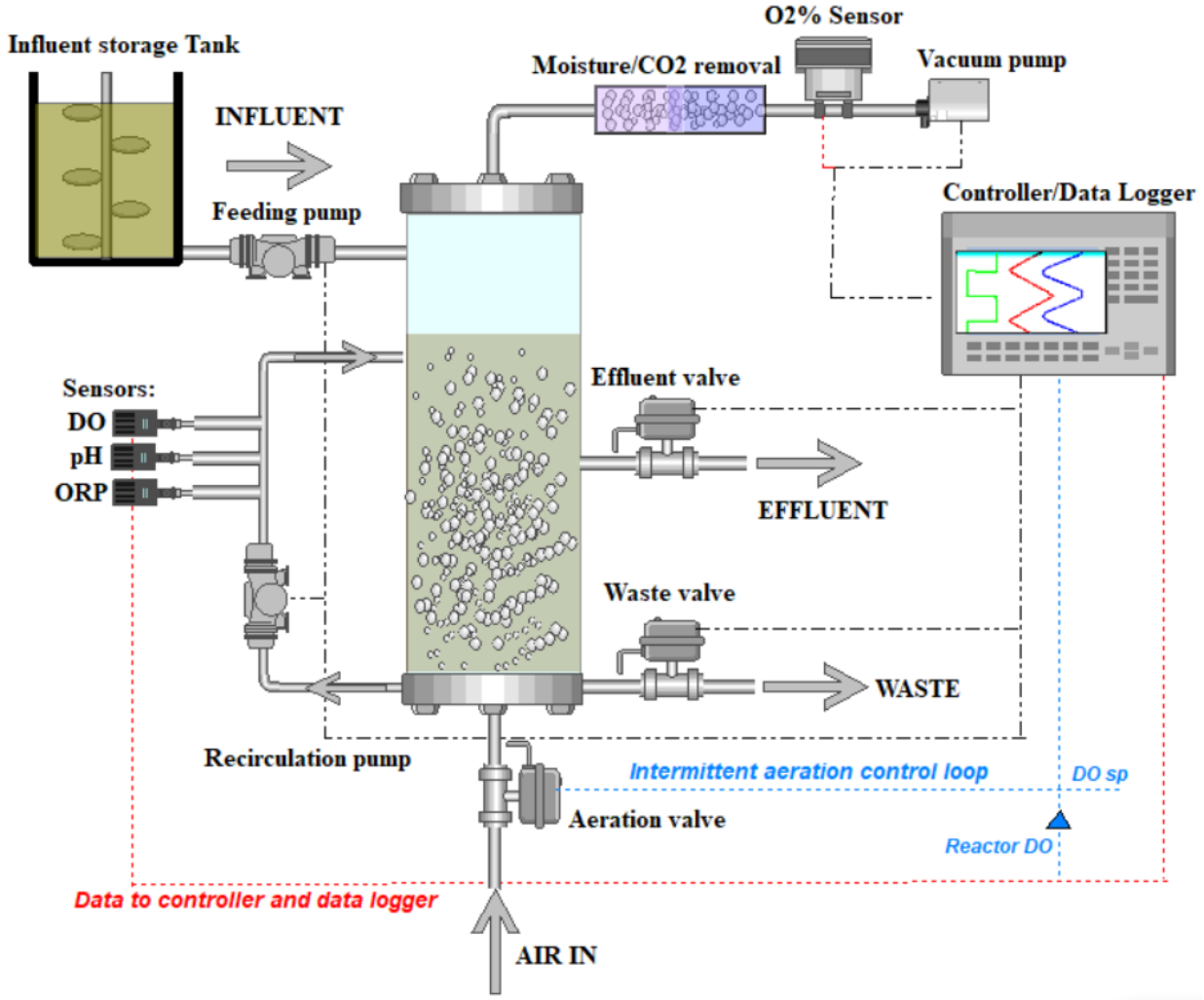

Figure 2.1 - Pilot-scale experimental layout (SBRs).

- *Feeding (< 5 min):* Each reactor was fed independently with municipal wastewater collected from WRRF1. An aliquot of the feed was screened at the plant site with a custom-built sieving system. The system was designed to simulate the removal performance offered by primary screening (specific area/volume influent ratio, cake formation, etc.).
- *Pre - Anoxic (60 min):* Once the reactors were filled to the desired level, complete mixing was provided by an external recirculation centrifugal pump. To prevent the process monitoring

and control sensors (T, pH, ORP, NH_4^+ and DO) from encumbering the reactor volume, they were installed on the external recirculation line.

- *Aerobic (100 min):* Air was delivered at a constant rate of 6 l min^{-1} through an automated control strategy. Fine bubbles were intermittently released by an EPDM membrane diffuser hosted in the bottom flange of each reactor to maintain an average dissolved oxygen concentration. All probes were connected to a controller that managed the data logging and implemented the aeration loop control based on dissolved oxygen low and high setpoint (i.e., IAP Intermittent Aeration Process). Fig. 2.2 shows the adopted control strategy which allowed tracking oxygen accumulation and uptake rate during the aerobic phase.
- *Post-Anoxic (60 min):* same as Pre-Anoxic.
- *Final Aerobic (30 min):* same as Aerobic.
- *Waste (5 – 10 seconds):* a pneumatic valve controlled by the PLC maintained the desired SRT. This step of the SBRs occurred once per day when the sum of mixed liquor volumes had to be removed from the reactor per each cycle. This was to ensure higher accuracy in the volume removed as time-constant for the opening/closing of the valves was negligible compared to the length of the operation (i.e, length of the mixed liquor withdrawal).
- *Settling (15 – 30 min).*
- *Effluent draw (1 – 2 min):* the supernatant was drawn through a pipe installed in the centre of the reactor. The drawing depth (about 2/3 of the total) was designed to collect a volume equivalent to the influent and maintain laminar conditions in the reactor to avoid biomass resuspension.
- *Idle (30 – 60 min).*

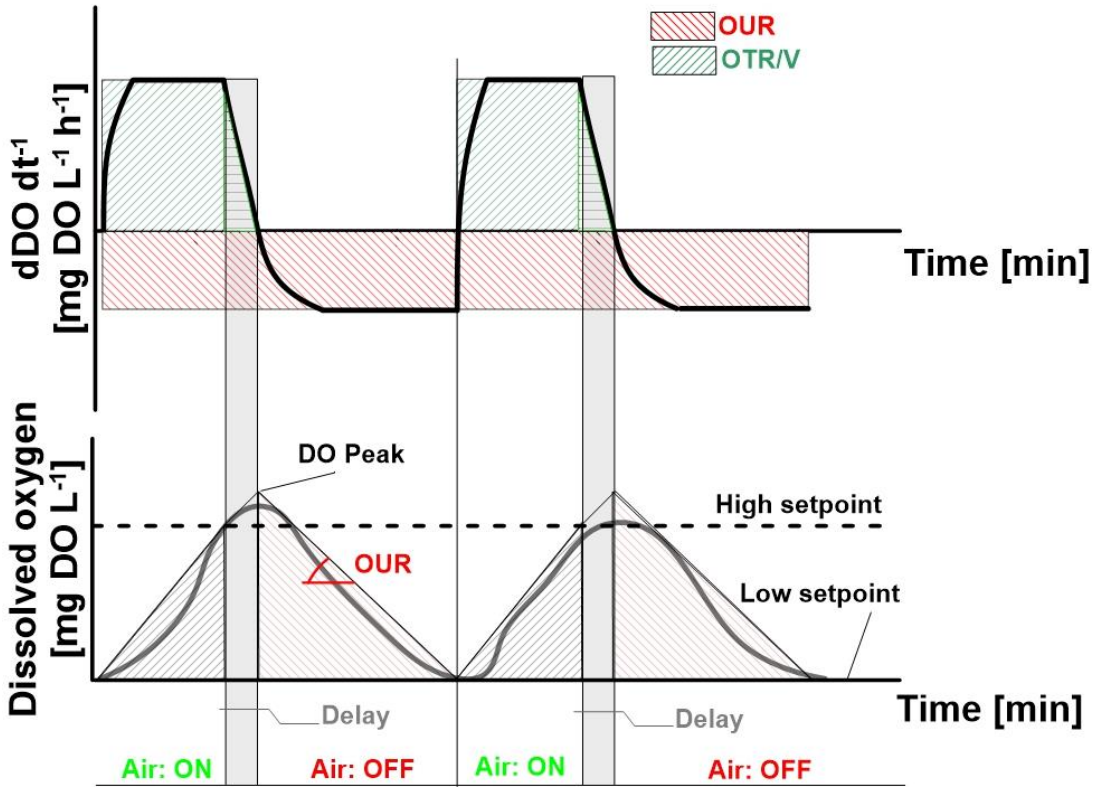

Figure 2.2 - Aeration control loop characteristics. The DO sensor was coupled with a PLC controller allowing to perform the corresponding measurements with shown respirometric pattern (accumulation, uptake).

2.3.2 Full-scale Water Resource Recovery Facilities

WRRF1 is located in Southern California and treats municipal wastewater for reclamation. It is designed for a maximum capacity of $3.4x10^3$ m^3 d^{-1} (9MGD) but is currently operated at approximately $1.9x10^3$ m^3 d^{-1} (5.1 MGD). The treatment process is composed of preliminary separation, primary clarification, secondary treatment, tertiary filtration, and disinfection.

Secondary treatment is operated in the Ludzack-Ettinger configuration with solids retention time of 5 to 8 days and nitrification/denitrification. The biosolids from primary and secondary treatment are dewatered and directed to anaerobic digestion.

WRRF2 is located in the southern region of the Netherlands and is designed for a peak capacity of $3.8x10^5$ m^3 d^{-1} (100 MGD) and an average flow of approximately $6x10^3$ m^3 d^{-1} (16MGD). Following preliminary separation, the flow was split between two lines, one with a primary screen (Salsnes Model #, 350 µm), and one fed unscreened influent. The secondary process has two identical lines following the Modified University of Cape Town (MUCT) configuration (Fig. 2.3). As shown in Fig. 2.3, the circular reactor consists of three zones: the central compartment is anaerobic ($3.5x10^3$ m^3), the middle is anoxic ($3.2x10^3$ m^3), and outer is aerobic ($1.3x10^4$ m^3). Wastewater enters the aeration compartment through low-level openings between the anoxic and aerobic zones, then transiting around the centre until reaching the outlet chamber level located at the outer side of the tank. The sludge lines from the two parallel trains are segregated, thereby making these two lines de facto independent treatment plants. Due to the elevated surface velocity and the impossibility of performing off-gas throughout the entire aerated surface, 17 sampling locations were selected for each treatment line, representing approximately 2% of the total aerated area.

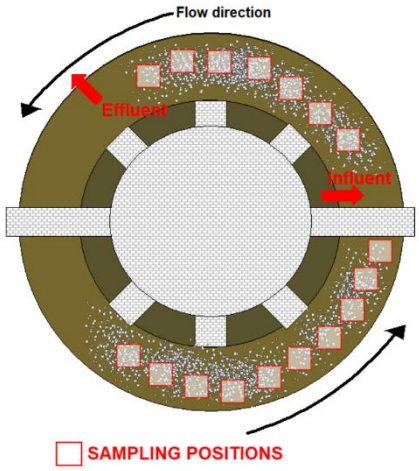

Figure 2.3 - On the left, an aerial view of the off-gas sampling positions along the aerated zones of WRRF2 secondary treatment tank is shown. On the right, it is shown a section of the tank with deployed off-gas test apparatus.

2.3.3 OUR calculations

Biomass activity or biomass volumetric oxygen consumption rate, related to the oxidation of organic matter, was estimated by the oxygen uptake rate (OUR). Two different approaches were adopted: OUR was derived from off-gas results following the standard ASCE method and independently measured by respirometric testing.

The OUR was calculated from the off-gas measurements following the standard ASCE method (ASCE 1997). The first method was applied to a completely mixed aeration tank and the dissolved oxygen mass balance was determined by the following equation:

$$\frac{dDO}{dt} = \left[\frac{\left(DO_{in} - DO\right)}{t^*}\right] + k_L a_f \left(DO^*_{\backsim 20} - DO\right) - OUR \qquad (1)$$

where t^* = detention time = V/Q and Q = total flow rate = Q_{inf} + Q_{rec}

By setting dc/dt equal to zero in Equation 1, the steady state solution relates the oxygen uptake rate (OUR) in the aeration tank, to the oxygen transfer coefficient and the steady state deficit:

$$\boldsymbol{OUR} = \frac{(\boldsymbol{C_{in}} - \boldsymbol{C})}{\boldsymbol{t^*}} + \boldsymbol{k_L a_f}\,(\boldsymbol{C^*_{20}} - \mathbf{C}) = \frac{(\boldsymbol{C_{in}} - \boldsymbol{C})}{\boldsymbol{t^*}} + \mathbf{OTR/V} \qquad (2)$$

where c = reactor concentration and dc/dt = 0

When DO does not change within the time window of the measurement, eq. 2 becomes an equality between OUR and the oxygen transfer per unit volume.

Oxygen Uptake Rate via respirometry was instead performed in absence of oxygen in the influent, where the equation (2) simplifies in:

$$\frac{\boldsymbol{dC}}{\boldsymbol{dt}} = -\boldsymbol{OUR} \qquad (3)$$

where t^* = Aeration TIME ON

2.3.4 Plant-wide evaluation framework for carbon diversion

To gain insight into the economic sustainability of deploying barrier separation technologies and to extend the analysis of primary treatment and carbon diversion to a plant-wide framework, four models representing the main primary treatment alternatives were developed. Two of the models represented the most traditional process flow diagrams (or layouts) in WRRFs and were used as benchmark baselines (Fig. 2.4). The first one followed the site-specific layout from the full-scale plant under study where no primary treatment was considered. This process flow diagram is often found in those scenarios with low TSS in the influent. To facilitate the comparison with other process flow diagrams, a conventional gravity primary clarifier was included in the second model. Two further models were developed to quantify and compare the energy requirements between primary treatment alternatives. One of the models considered the implementation of barrier separation technologies as primary treatment, while the other model considered a scenario where barrier and gravity separation were operated simultaneously. As barrier separation can modify its level of performance depending on the treatment goals, operations with solid removal ranging from 30% (low) to 60% (high) were investigated.

To replicate the WRRF2 full-scale layout, each scenario considered two treatment lines in parallel. The receiving influent was equally split between the two treatment lines composed of primary screening/clarification, secondary treatment, secondary clarification, and dewatering. For all the scenarios, primary and secondary sludge was directed to anaerobic digesters for energy recovery through combined heat and power (CHP) engines using anaerobically produced biogas. The energy recovery from CHP engines was assumed to be 33% of the process energy requirements (Reith, Mes, and Stams 2003).

Summary of models studied:

- Model #1 –Baseline: No clarifiers
- Model #2 –Baseline: Two primary gravity clarifiers
- Model #3: Two primary sieves
- Model #4: One primary sieve and one primary gravity clarifier

Two different flow rates were considered: medium $6x10^3$ m^3 d^{-1} (16 MGD) and large $3.8x10^5$ m^3 d^{-1} (100 MGD).

Model #4 represents the actual process flow diagram of WRRF2. To maximize the benefits of primary screening, three different operational strategies were evaluated: primary screening in continuous operation (24h), primary screening operating only during peak hours (8h), and primary screening operating during off-peak hours (16h). These results are investigated in §2.4.

These strategies were aimed at quantifying the potential of employing on-demand primary separation to abate organic load peaks in the influent ($Q_{in} = Q_{max}$) and during average loading conditions ($Q_{in} = Q_{avg}$). For each operational strategy, three levels of screening performance were assigned to barrier separation (20%, 40% and 60%), as dependency between the TSS% removal and TSS concentration in the influent was assessed by Franchi et al (2012). Thus, a range of TSS removal was preferred to a single value to better mimic different dilutions in TSS concentration during wet periods.

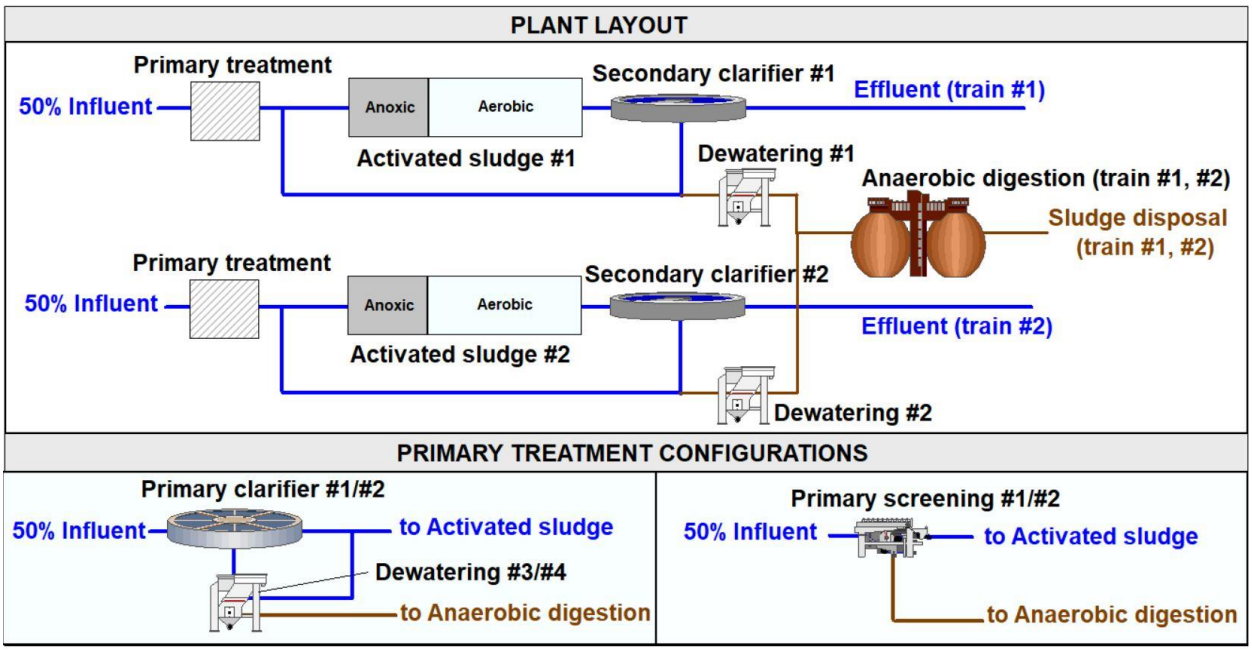

PRIMARY TREATMENT

MODEL #	TRAIN #1	TRAIN #2
1	None	None
2	Clarifier	Clarifier
3	Screen	Screen
4	Screen	Clarifier

Figure 2.4 - Model schematic with different primary treatment configurations. The plant composed by 2 treatment trains was modelled with 4 different layouts. Flow diagrams for primary clarification and screening are also shown.

2.3.5 Off-gas testing

An automated analyser sampled the off-gas leaving the liquid surface of the full-scale reactor and the SBR pilots, thereby calculating aeration efficiency indicators during the aerobic phase. The partial pressure of oxygen in the gas stream was measured by a ZrO_2 cell (Model 65, $AmiO_2$; Fountain Valley, CA). Oxygen transfer in process conditions was measured using the off-gas method following the ASCE testing protocol (ASCE, 1997). Off-gas analysis relies on a mass balance on the water column where the air flow is transiting, measuring both the oxygen partial pressure (pO_2, Pa or atm) and the air flux (Redmond et al. 1992; Schuchardt et al. 2007a). These two variables, together with the measurement of DO, salinity, total atmospheric pressure P, and temperature T, are used for the calculation of the standardized oxygen transfer efficiency at field conditions (αSOTE, %), the standardized oxygen transfer rate at field conditions (αSOTR, kg_{O2} h^{-1}), and the calculation of their respective air flow-weighted averages. The off-gas test assumes that nitrogen is conservative and requires either the measurement or removal of moisture and CO2 in the gas phase. Here we removed moisture and CO_2 with pellets of $CaSO_4$ (CAS No. 7778-18-9) and NaOH (CAS No. 1310-73-2). When clean water tests are available, α can be calculated a posteriori as the ratio of αSOTE and SOTE. SOTE values were obtained from the corresponding diffuser manufacturers.

2.3.6 Water quality

TSS was measured according to the standard methods (APHA 2005). COD was determined using Hach® kits (Loveland, CO).

2.3.7 Statistics

Statistical significance was determined with an unpaired t-test.

2.4 Results and discussion

The COD and TSS removal were measured both after the primary filtration/screening and after the secondary treatment (secondary effluent). After primary screening, COD and TSS removals by barrier separation equipment were 34.9±9% and 50±17%, respectively. Similar values were obtained at full-scale (30±4% and 42±9%, respectively; see supplementary information). These removals are in accordance with Franchi et al. (2012) who, after sampling more than 11 weeks of pilot-scale operations using primary barrier separation, reported TSS with a similar mesh (350 μm) removals ranging from 30 to 65%. As expected, after the secondary aeration treatment, COD and TSS removal efficiencies almost doubled (Figs.2.5a and 2.5b). The screened pilot scale SBR consistently showed higher COD and TSS removal (81±7.1% and 84±5.7%, respectively) in comparison to unscreened (58.7±6.1% and 65±7.4%, respectively), showing a relative improvement of 27.4% and 22.7%. Similar improvements in removal efficiency should be expected at full-scale, as similar removal percentages after the RBF were observed. However, at the time of testing, the two aeration tanks at the full-scale WRRF were operated differently as air flow rate requirements were calculated based on influent ammonia and phosphorous. Hence, the different aeration requirements satisfied by the different air flow rates supplied to the two tanks resulted in negligible differences in COD and TSS removal at the secondary effluent between screened (92±6.2% % and 96±4.8%, respectively) and non-screened (92.5±6.1% and 96.9±6.8%, respectively), hindering the comparison of the impact of the enhanced removal of COD and TSS between the screened and no-screened treatment line at full-scale.

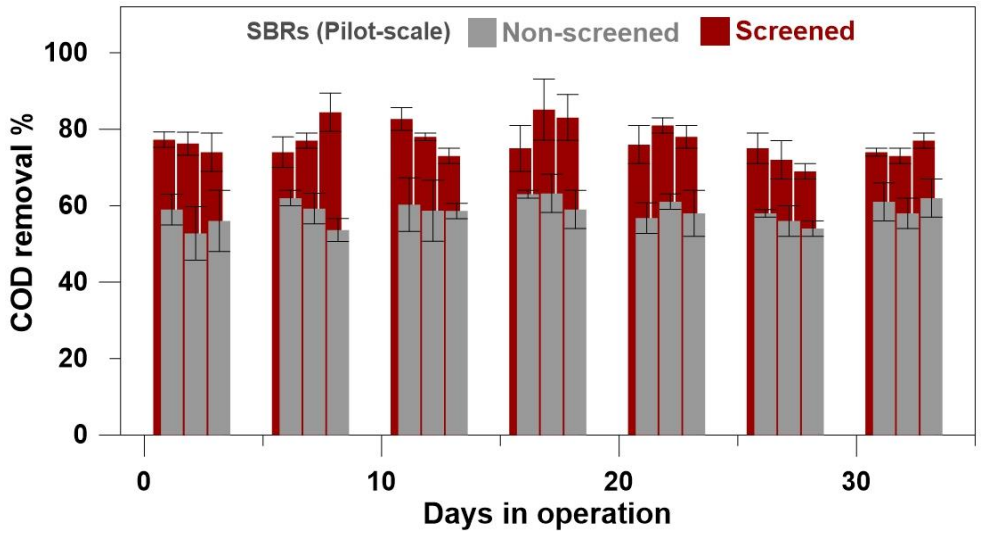

Figure 2.5a - COD removals after secondary treatment with an SBR, obtained after 30 days in operation for the process line with primary screening (red) and for the process line without primary treatment (grey).

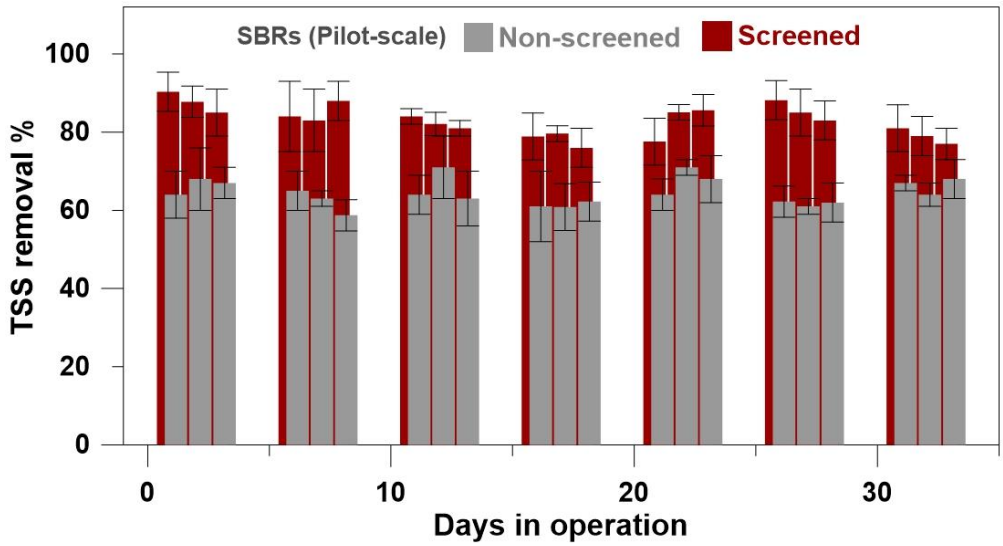

Figure 2.5b - TSS removals after secondary treatment with an SBR, obtained after 30 days in operation for the process line with primary screening (red) and for the process line without primary treatment (grey).

2.4.1 Impact of primary screening on oxygen requirements for aeration

The beneficial effect of primary screening on the reduction of aeration requirements was calculated for pilot and full-scale to quantify the net decrease in organic load to be oxidized in the aeration tank. Results confirmed that the oxygen requirements for the secondary treatment could be reduced in screened lines by almost 41% for the pilot reactor and by more than 32% for the full-scale. The daily oxygen demand over 30 days of operation for the pilot reactor is shown in Figs. 2.6a and 2.6b, where the reduction in oxygen requirements from 1.62±0.4 $Kg_{DO}\ d^{-1}$ for the non-screened line to 0.98±0.2 $Kg_{DO}\ d^{-1}$ for the screened line were estimated. Similarly, oxygen requirements at full scale were significantly reduced from the screened line (1108±143 $Kg_{DO}\ d^{-1}$) to the non-screened line (750±54 $Kg_{DO}\ d^{-1}$) in the first aerobic section of secondary tank.

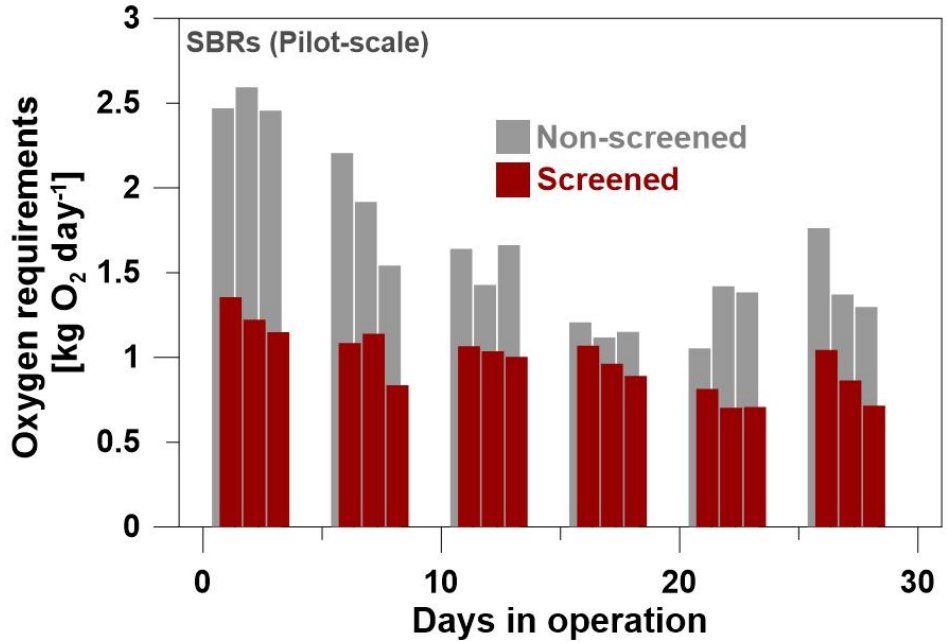

Figure 2.6a - Cumulative daily supplied oxygen for the sequential batch reactor, expressed in kg of oxygen supplied per day, for the 30 days in operation at pilot scale.

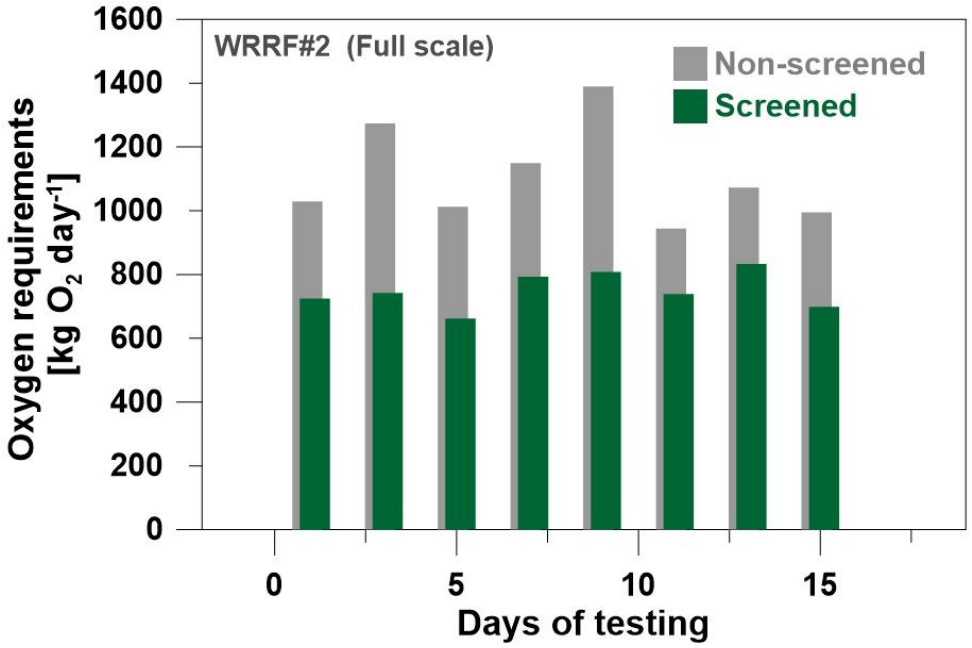

Figure 2.6b - Oxygen requirements for the first aerated section of the secondary treatment at WRRF#2, expressed in kg of oxygen supplied per day, for the 30 days in operation at pilot scale.

2.4.2 Impact of primary screening on oxygen uptake rate (OUR)

Respirometric studies were conducted to confirm the impact of carbon diversion on microbial activity after primary sieving. The OUR by the bacterial population was measured to investigate how the different loading conditions induced by primary screening influence bacterial activity. To enable the comparison between pilot and full-scale processes, the daily specific OUR over 30 days of operation is expressed per unit of MLSS. Figures 2.7a and 2.7b show a reduction in the oxygen uptake rate up to 35±8% and 44±6.2% for screened lines at pilot and full-scale, respectively. As expected, the lower loading conditions after primary screening decreased the activity of the microbial population. The pilot reactor experienced a reduction from 8.2±1.2 mg DO g $MLSS^{-1}$ h^{-1} (non-screened) to 5.3±1.4 mg DO g $MLSS^{-1}$ h^{-1} (screened). At full scale, a similar reduction was

observed with OUR decreasing from 13.1±3.1 mg DO g $MLSS^{-1}$ h^{-1} for non-screened line to 7.3±2.7 mg DO g $MLSS^{-1}$ h^{-1} for screened line.

Monitoring the OUR along the length of the aeration tank provided additional insights. While a decreasing OUR along the tanks is usually expected, as the organic load is being progressively metabolized by microbial biomass, the specific full-scale process characteristics resulted in an unusual increasing trend for both treatment lines in the first aerobic section of the secondary tank (Fig. 2.7b). Specific hydraulic conditions on reactors (circular geometry and high liquid velocity) and an unexpected spatial proximity between the influent and effluent points are considered the main reasons for this trend. Negligible differences in the second aerobic zone were found between the specific OUR for non-screened (10.5±3.3 mg DO g $MLSS^{-1}$ h^{-1}) and screened lines (9.6±1.7 mg DO g $MLSS^{-1}$ h^{-1}). A similar result was observed for oxygen transfer efficiency where 1.23±0.19 %/ft for non-screened and 1.26±0.35 %/ft for screened were measured. This confirmed the positive effect of the anoxic selector on oxygen transfer (Iranpour et al. 2000; Diego Rosso and Stenstrom 2007), resulting in more homogenous loading conditions between the screened and non-screened line in the second aerobic zone.

Recent studies have employed computational fluid dynamics (CFD) as a tool to investigate the uneven distribution of oxygen demand and air delivery (Amaral et al. 2019; Fayolle et al. 2007; Karpinska et al. 2016). Future studies, especially on circular tanks characterized by such high velocity gradients with their consequent effects on oxygen transfer should include CFD investigations to elucidate the effects of inlet and outlet placements on the oxygen demand patterns and on the layout of air supply (i.e., diffuser type and density).

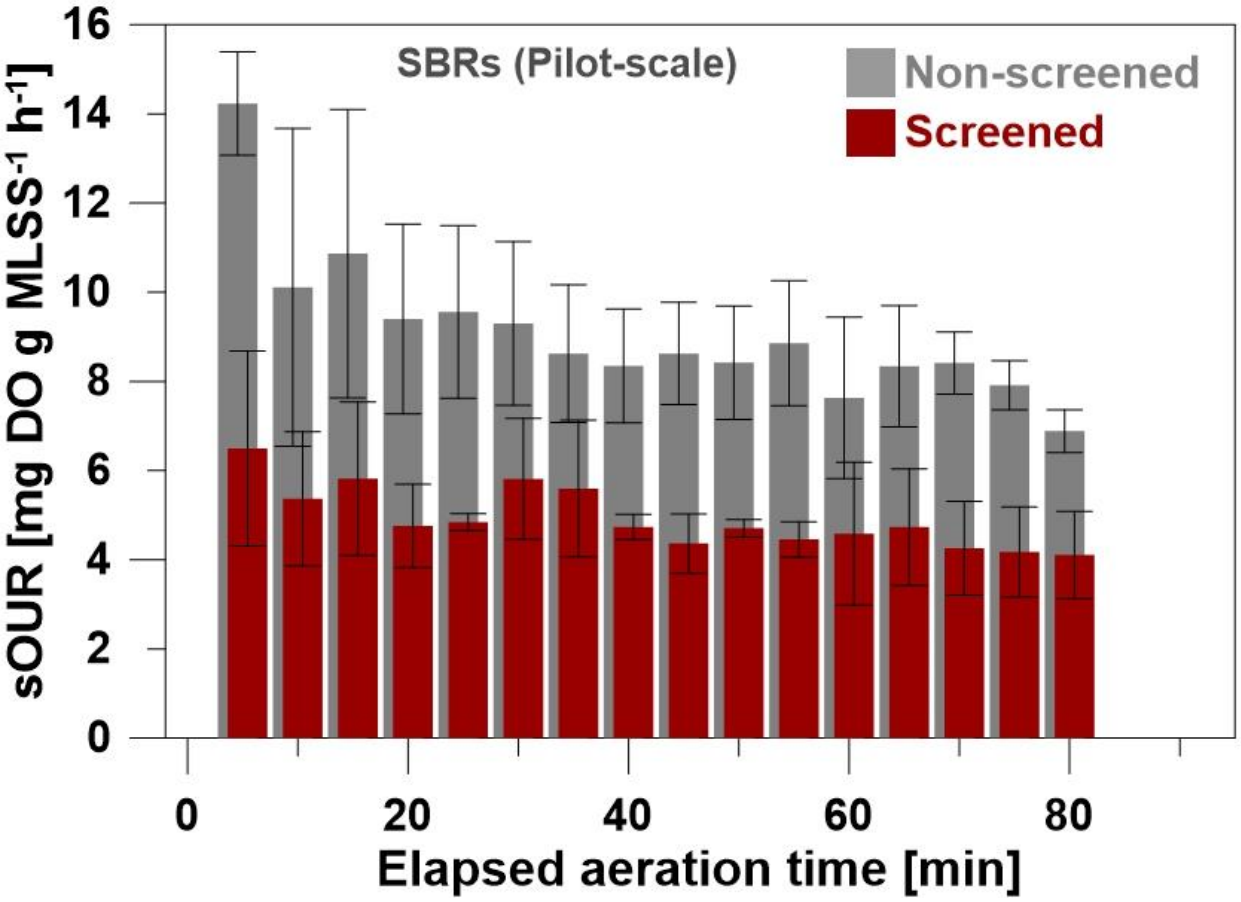

Figure 2.7a - Specific OUR Pilot-scale measurements during the aeration phase were averaged from 30 days in operations. The OUR (oxygen uptake rate) is expressed in mg dissolved oxygen per gram of mixed liqueur suspended solids per hour.

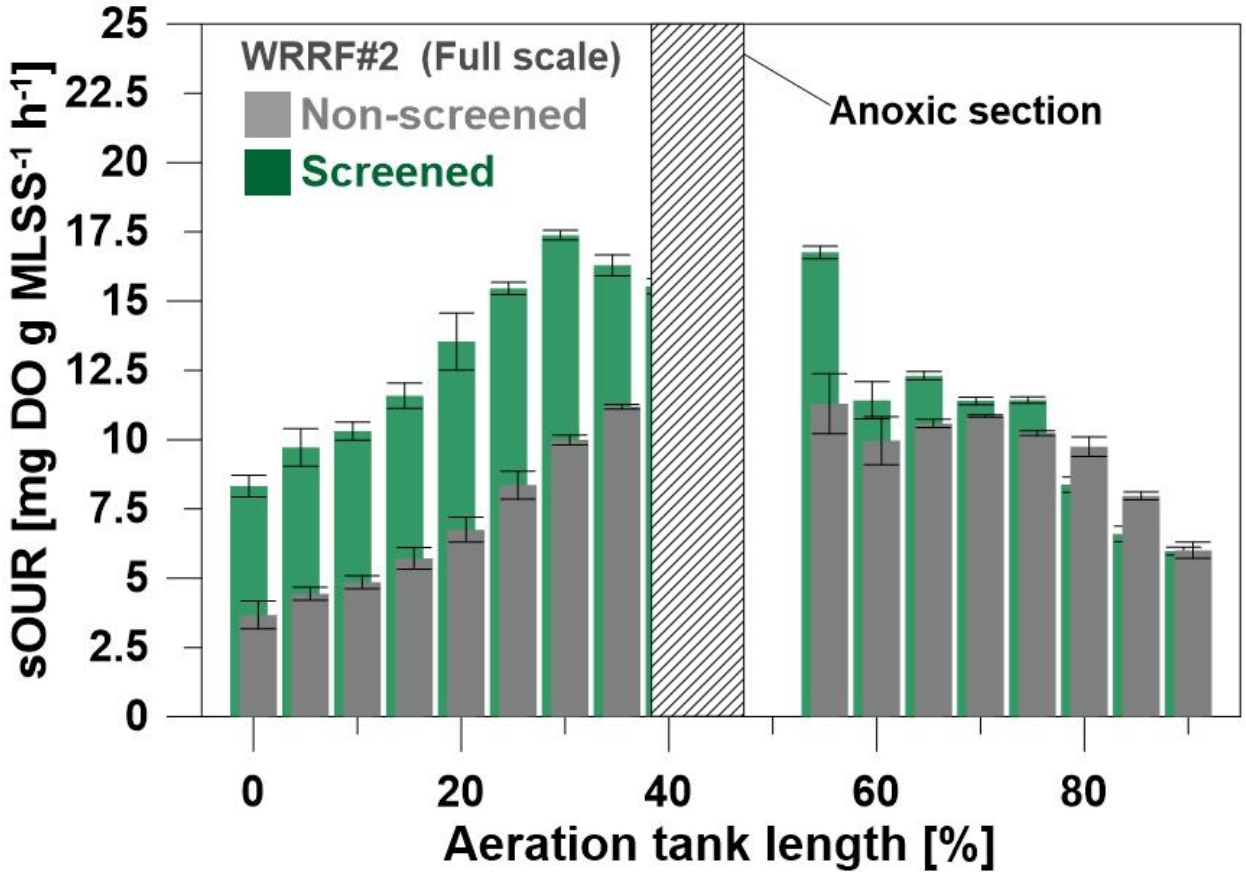

Figure 2.7b - Specific OUR along the full-scale aeration tank length is shown. The OUR (oxygen uptake rate) is expressed in mg dissolved oxygen per gram of mixed liqueur suspended solids per hour.

2.4.3 Impact of primary screening on oxygen transfer efficiency

The results from off-gas testing consistently showed an increase in oxygen transfer efficiency for screened lines (both pilot and full-scale) due to the lower loading conditions achieved after sieving (Fig. 2.8). The results are in agreement with previous studies (Leary et al.1968; Amaral, 2019). The screened line at the pilot reactor resulted in an oxygen transfer 40±3% higher (3.18 ±0.63 %/m) in relative comparison to the non-screened (2.27 ± 0.58 %/m). The

improvement in transfer efficiency could have been maximized due to the specific dimensions and layout of the pilot reactor. Full-scale results also produced an improved efficiency, although the complexity of hydraulics and other processes characteristics limited the improvement in αSOTE to 14±4%, in relative comparison between screened and non-screened. The screened line at full-scale reported an efficiency of 3.82±1.12 %/m for the first 60 meters in length (before the anoxic area) while than the non-screened was 4.26±0.95 %/m.

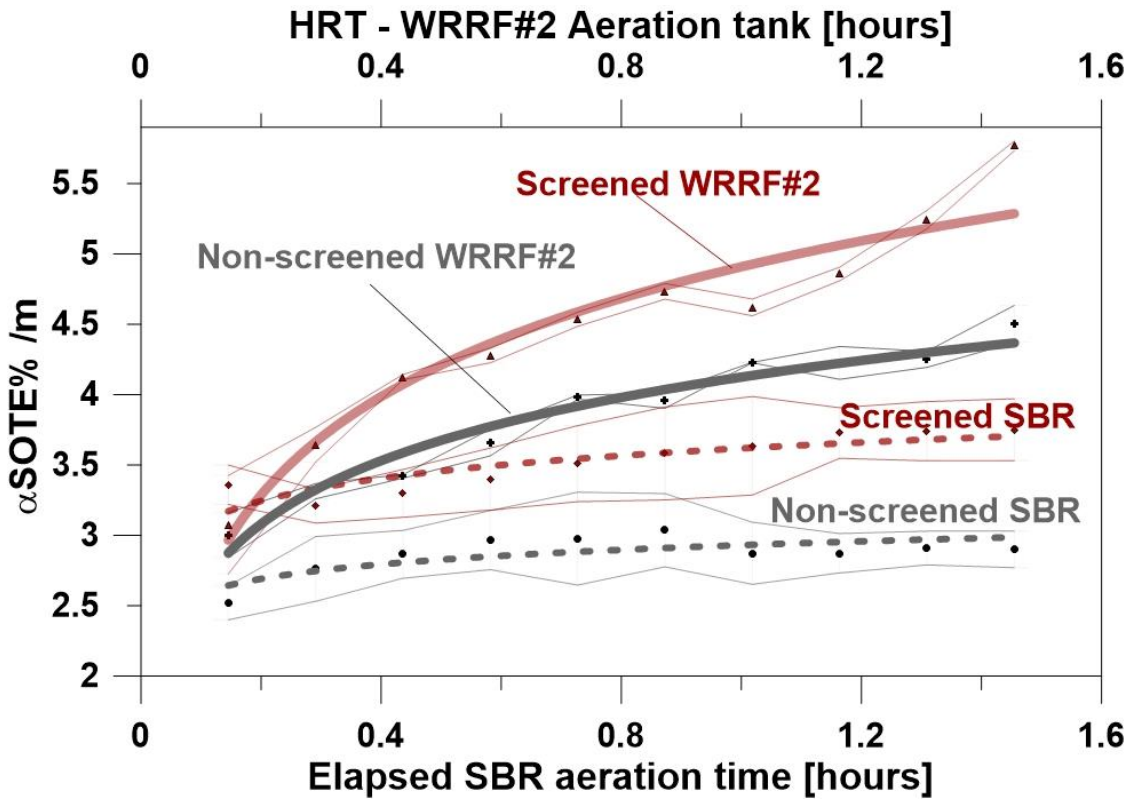

Figure 2.8 – Standard oxygen transfer efficiency in process water (αSOTE) for both screened and non-screened processes corresponding to pilot-scale (orange) and full-scale (blue) reactors. Pilot-scale measurements on SBRs are averages of 30 days of operation and are plotted against the time elapsed in the aeration cycle (bottom X axis). Measurements at full-scale are plotted against the top X axis, which represents the hydraulic retention time of the aeration tank.

2.4.4 Impact of primary screening on aeration efficiency

Aeration efficiency (AE) was also calculated to confirm the improvement in aeration efficiency indicators. This is defined as the ratio between Oxygen transfer rate (OTR, kg $O_{2transf}$ h^{-1}) and blower energy demand (kWh) derived from the adiabatic formula (Metcalf & Eddy 2014) and hence expressed in kilogram of oxygen supplied per kWh of energy required ($Kg_{O2supplied}$/kWh). As expected, screened treatment lines obtained higher AE values, increasing their efficiency in more than 27% in the case of pilot reactors and close to 20% within the first aerobic section at the full-scale (Figures 2.9a and 2.9b).

The daily aeration efficiency over 30 days of operation for the pilot reactor is shown in Fig. 2.9a, demonstrating an increase in the capacity to deliver higher amount of oxygen per kWh from 0.28±0.04 Kg_{DO} kWh^{-1} for the non-screened line to 0.22±0.05 Kg_{DO} kWh^{-1} for the screened line. Similarly, AE at full scale was significantly increased from the screened line (1.02±0.14 Kg_{DO} kWh^{-1}) to the non-screened line (1.23±0.11 Kg_{DO} kWh^{-1}), shown in Fig.2.9b. The results demonstrated the beneficial effect of primary screening on aeration efficiency during secondary aerobic treatment.

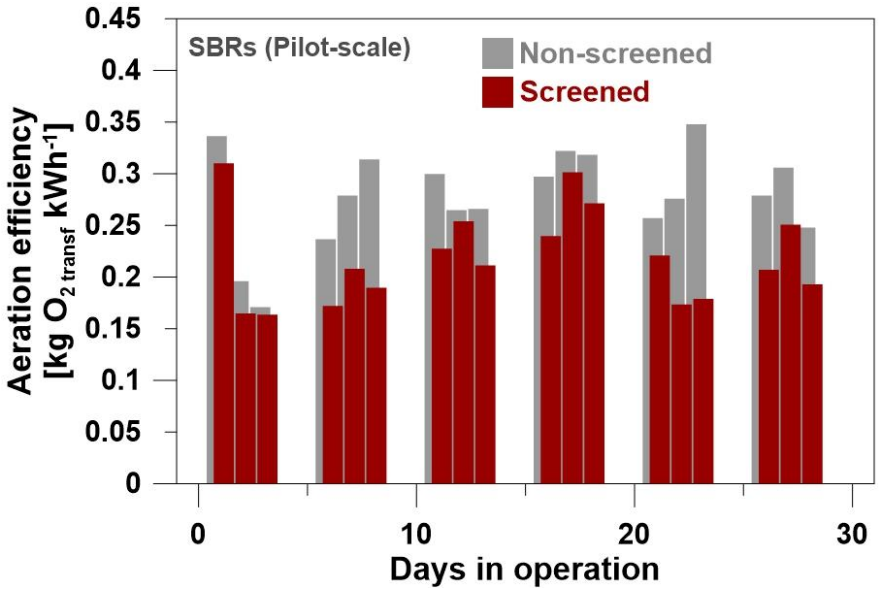

Figure 2.9a - Daily average aeration efficiency, expressed in kWh per kg of oxygen transferred, for the pilot-scale during 30 days in operation.

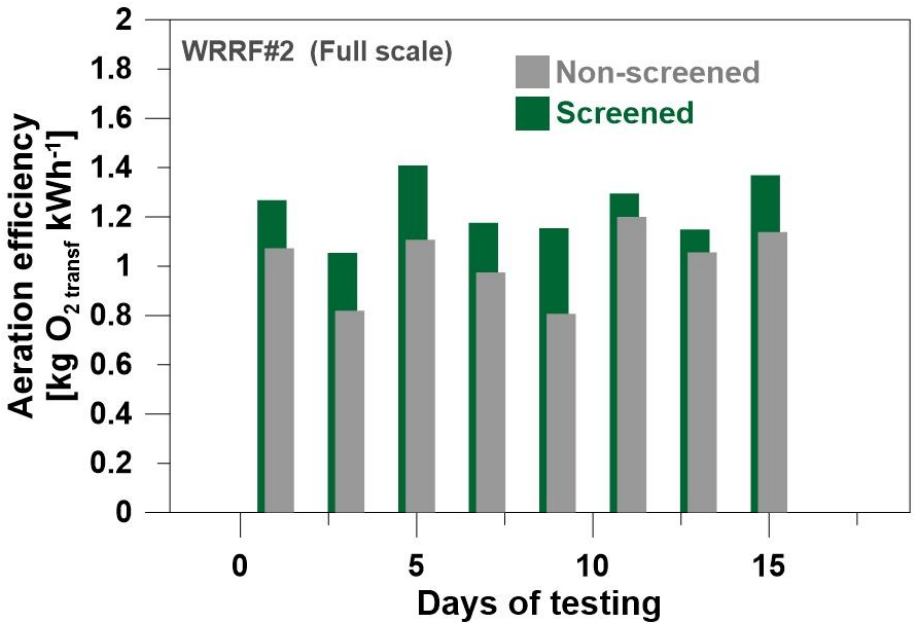

Figure 2.9b - Daily average aeration efficiency values during the 15 days full-scale testing, expressed in kWh per kg of oxygen transferred, are shown.

2.4.5 Plant-wide energy analysis: Operating Strategies for WRRF2

The results from the previous oxygen transfer efficiency characterization were used to improve the prediction capabilities of available models on wastewater treatment. The reported values from the carbon diversion and aeration efficiency achieved after primary screening (Table 1) were applied to a plant model developed in BioWin 5.2 (EnviroSim; Hamilton, ON) to determine the estimated impact on the energy balance and identify the most cost-effective operating scenario for WRRF2. In Figs. 2.10a and 2.10b, the baseline (unscreened column) represents WRRF2 having no primary treatment in either line, while for the other scenarios primary screening is implemented on only one line (with assumed TSS removals of 20%, 40% and 60%). The analysis regarding the impact of having both lines operated under barrier separation, gravity clarifiers, or a combination of both is explored in the following section (§2.4.8). The net energy demand was calculated considering the difference between produced energy through biogas generation and process energy demand, following the rational procedure from Gori et al (2011). We considered here the energy demand from primary, secondary, and sludge treatment, but not pumping which is the same for both lines and is heavily site-specific (not process specific).

Table 2.1 - Summary of results for pre-screened and non-screened treatment line.

	COD removal (%)	**TSS removal (%)**	**SOTE (%/ft)**	**AE (kg_{O2} kWh^{-1})**	**sOUR (mg_{O2} g_{MLSS}^{-1} h^{-1})**	**OTR (kg O_2 d^{-1})**
Pilot-scale SBR	+28.4	+22.7	+40	+27	-35	-40.1
Full-scale (only 1st aerobic section)	*nil*	*nil*	+15	+20	-44	-32.3
Full-scale (All tank)	*nil*	*nil*	+10	+10	-28	-21

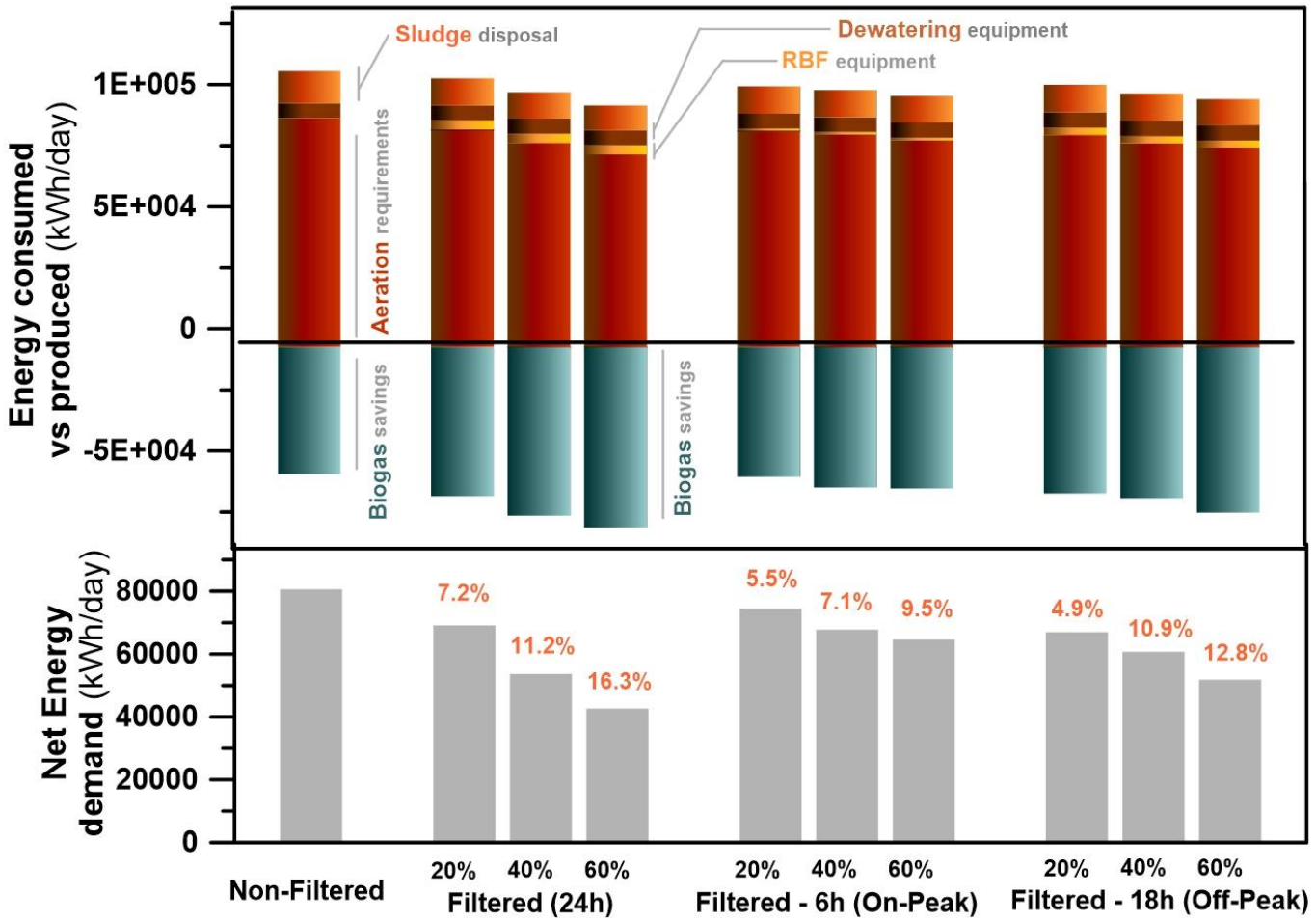

Figure 2.10a – Net power demand for the different operational strategies of primary treatment at the 38,00 m3/day (10MGD) WRRF. Power demand is the sum of secondary aeration requirements, RBF equipment, dewatering process and sludge disposal (i.e., xx and land application). Power production is estimated from the methane generation at the anaerobic digester.

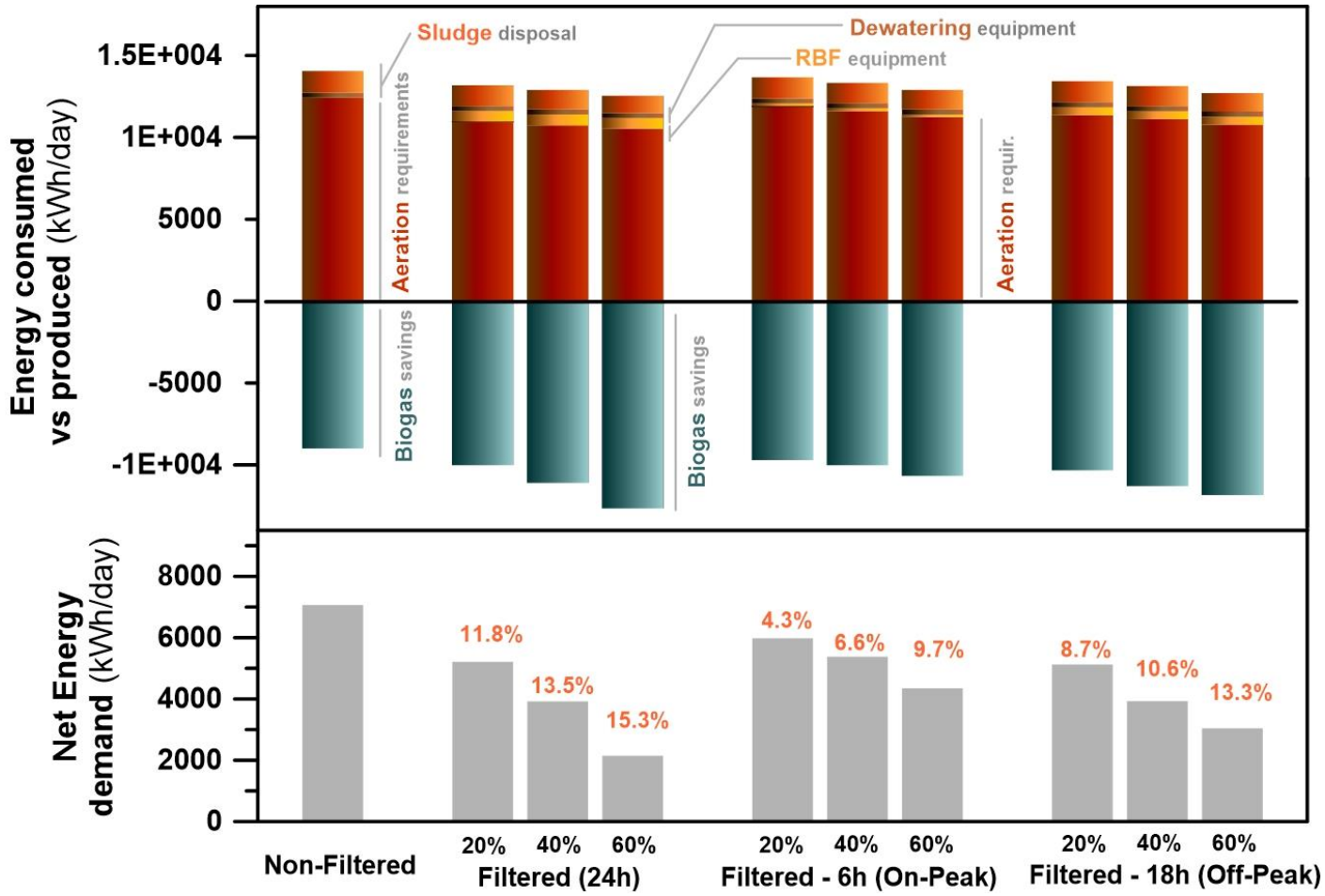

Figure 2.10b – Net power demand for the different operational strategies of primary treatment at the 380,000 m^3/day (100MGD) WRRF. Power demand is the sum of secondary aeration requirements, RBF equipment, dewatering process and sludge disposal (i.e., xx and land application). Power production is estimated from the methane generation at the anaerobic digester.

Primary clarifiers usually operate within a narrow removal range of BOD (35-42%) and TSS (60-65%), dictated by the HRT (Metcalf & Eddy, 2014). Barrier separation systems, on the other hand, can compensate the variations in flow by adjusting their rotational speed to achieve different levels of TSS and COD removals using proper control systems(Franchi and Santoro 2015). Avoiding excessive carbon diversion in primary separations is usually recommended when downstream biological processes are present (i.e., bio-P, N/DN) to prevent the excessive scalping of carbon substrates that otherwise results in a need for supplemental carbon (WRF et al. 2019). The opposite goal can be targeted when biogas production needs to be maximized (Gori et al, 2013; Razafimanantsoa et al., 2014; Rusten et al., 2016). Taking into account the capability to adjust the removal efficiency in RBFs systems, three different scenarios representing three potential desired objectives for operations were considered (20%, 40% and 60% TSS removal). Figure 10 shows that aeration is the highest contributor in the overall energy demand, representing around 70-75% of the total energy requirements, which is in accordance to existing knowledge (Reardon, 1995; Rosso et al., 2005; WEF, 2009).

Energy requirements for aeration decrease as the established percentage of removal in the RBF increases (from 20 to 60% scenarios), confirming the modelling results by Gori et al (2011; 2013). The organics that otherwise would be oxidized by costly aeration are now being redirected to the anaerobic digester, benefiting the plant's energy balance. The organic-rich primary sludge diversion to the anaerobic digester had twofold benefits: increasing the amount of primary sludge to energy recovery processes (anaerobic digester), which can yield 30-50% more methane than secondary sludge (Appels et al., 2008; Zhou et al., 2013; Takacs and Vanrolleghem, 2006; Gori et al, 2011), and also increasing the aeration efficiency during the secondary treatment, improving the oxygen mass transfer indicator (α) due to the lower organics concentrations (Jiang et al., 2017).

Solids disposal represents the second most energy demanding process (10% of the total energy requirements). Nevertheless, it has a limited role in the comparative scenario analysis as little variability between scenarios is observed. Although the sludge characteristics varies significantly along the different scenarios, as increasing the fraction of primary sludge by enhanced removal from barrier separation impacts sludge characteristics (e.g., biodegradability and methane potential), little impact is expected regarding the total volume of biosolids. The increase in harvested primary sludge by primary screening is balanced by the concurrent decrease in secondary sludge, as biomass growth is being limited. Also, the increased methane yield of primary sludge further reduced the VSS in the biosolids.

Barrier separation equipment is associated with energy requirements almost ten times higher than traditional clarifiers (Caliskaner et al. 2015; 2014; Franchi and Santoro 2015). However, although primary screening equipment is the third main contributor to the plant's energy demand, especially for those scenarios with longer operation times (i.e., continuous: 24h; Off-peak:18h and On-peak:6h), the overall costs never exceeded 5%, having limited impact on the overall energy balance. Note that in this analysis we do not include capital cost which would tip the balance against clarifiers if they had to be built anew. The existence of clarifiers already constructed and operational, on the other hand, would pose a constraint in the life-cycle cost analysis of these alternatives. Therefore, a thorough analysis for engineering projects involving these alternatives for primary separation should also include capital costs.

Also, the relatively high operational costs in comparison to gravity clarifiers are further compensated by the enhanced production of biogas. Dewatering presents the lowest energy requirements among the considered processes, ranging from 2% to 6%. Similar to the sludge

disposal process, the minor changes in total sludge volume do not vary the contributor weight along scenarios.

Figures 10a and 10b show that the highest reduction in net energy demand was obtained for those scenarios with higher TSS removal by the RBF. Independently of the established percentage of removal in screening, the use of a fine-mesh improved the net energy demand in all scenarios, confirming that barrier separation is a cost-effective approach for these scenarios.

The duty cycle of screens is key to the overall energy balance for the different operating strategies under study. The continuous operating strategy of screens (24h/d) resulted in the lowest net energy demand alternative, reducing energy footprint of 14%, 33% 47% for the established TSS removal ratios of 20, 40 and 60% in relative comparison to the non-primary scenario. The effect of harvesting the peak load for a 6h/d period, which was expected to reduce circadian amplification of energy cost discussed by Emami et al (2017), did not compensate the longer period of 18h established for the Off-peak operating strategy.

2.4.6 Plant-wide energy analysis: Screens vs Clarifiers (and combined option)

The assessment of plant-wide energy was carried out by comparing four treatment schemes: 1) No primary treatment (*baseline used in the previous section*); 2) Use of gravity clarifiers (*new baseline*); 3) Combination of primary clarifiers with screens; 4) Screens as sole primary treatment. The influence of plant size on the analysis was quantified by replicating the assessment with a ten-fold increase in design flow.

As previously discussed, the capability to adjust the loading conditions before the secondary treatment by barrier separation technologies is important to address potential imbalances in the

C:N ratio of nitrifying/denitrifying systems. If the maximization of carbon diversion from primary to sludge processing is prioritized (i.e. high TSS removal from screening), the suppression of denitrification in secondary treatment can occur if carbon is limiting substrate. Conversely, reducing screening separation to decrease the BOD removal (i.e. low TSS removal) can enhance denitrification in carbon-limited systems and reduce (or avoid) the use of supplemental carbon in secondary treatment. Additionally, whereas wet periods lead to a dilution effect of the influent, lower TSS removal may be achieved from primary screening as solids are insufficient for the creation of cake on the filter mesh (Santoro et al. 2015). Thus, for the plant-wide energy analysis, we considered the technical and economic feasibility of using barrier separation at two different TSS removal rates of 30% and 60%.

The comparison between the scenario without any type of primary treatment and primary barrier separation operated at 30% and 60% decreased energy demand by 44% and 73%, and the aeration operational costs by 22% and 36%. These results are similar to previous studies where RBF operated to remove 50% of the incoming TSS reported a decrease in power consumption ranging from 22 to 28% when compared to a no primary treatment scenario (Franchi and Santoro 2015). Similar results were found by Ruiken et al. (2013) who stated that the energy usage of a WRRF could be decreased by at least 40% using primary sieving/screening. Figures 2.11a and 2.11b yielded similar trends between the studied scenarios. For the case of large treatment plants ($3.8x10^5$ m^3 d^{-1}; Fig. 2.11b), the implementation of primary screening resulted in significantly higher savings on the net energy demand in relative comparison to the medium-scale plant ($3.8x10^3$ m^3 d^{-1}). While medium plant size with full and partial screening implementation (at 60% TSS removal) improved the plant-wide net energy demand in comparison to primary clarifiers by 8% and 1%, respectively, the larger plant scenario increased this difference to 11% and 6%

respectively. The large plant scenario also showed the most significant improvements when compared to the non-primary treatment option which results from the favourable economy of scale, especially in anaerobic digestion (M. Garrido-Baserba et al. 2015).

Figures 2.11a and 2.11b demonstrate that using screening as sole primary separation is considered the less energy-demanding alternative throughout the range of targeted TSS removal. The combination of clarifiers and RBF technology did not yield noteworthy higher savings in the high TSS removal scenario in comparison to primary clarifiers. Nevertheless, the application of site-specific operational strategies taking advantage of the potential to bypass organic loads during peak hours by shaving the concurrent cost due to circadian amplification may potentially decrease aeration costs.

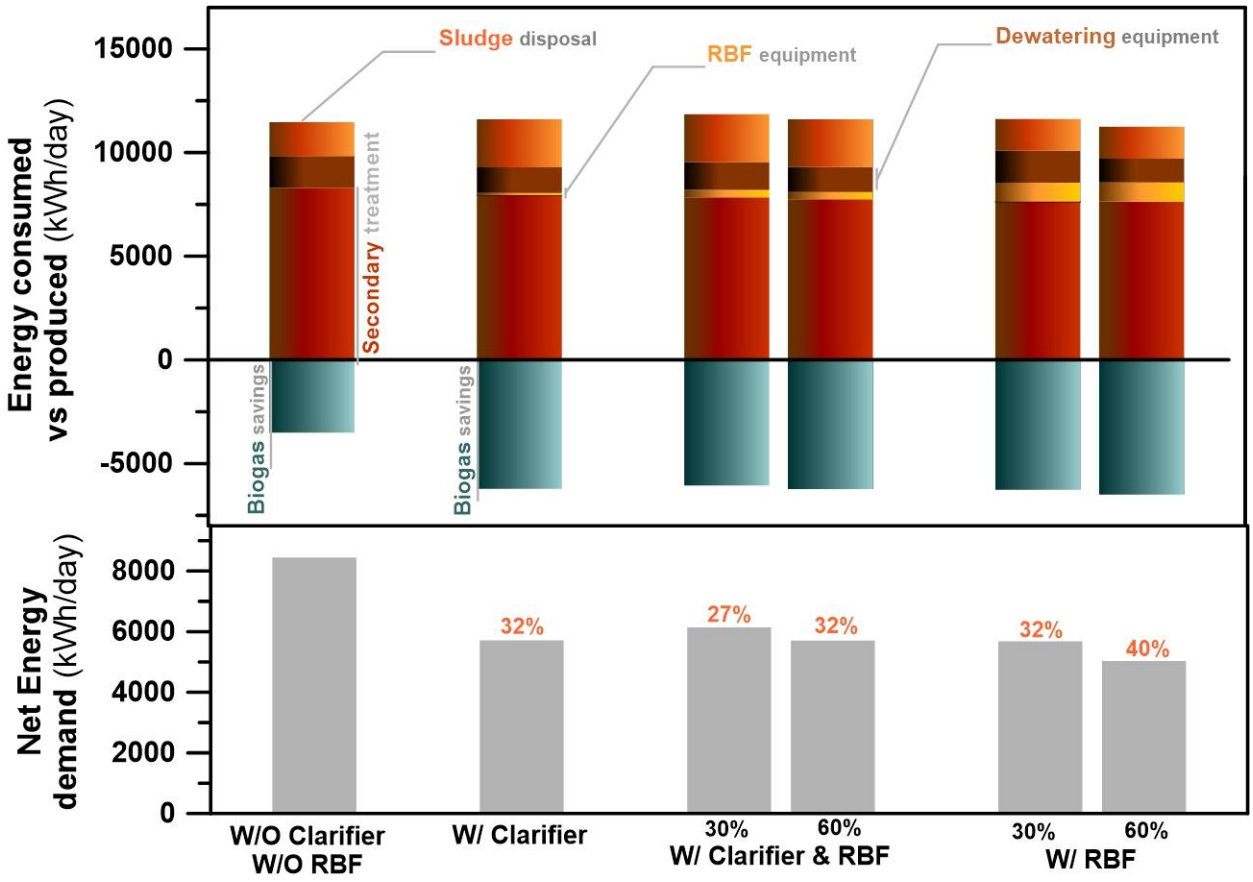

Figure 2.11a - Power demand and power production for different types of primary treatment schemes in a 38,000 m^3/day (10MGD) WRRF. Power demand is the sum of secondary aeration requirements, RBF equipment, dewatering process and sludge disposal. Power production is estimated from the methane generation at the anaerobic digester.

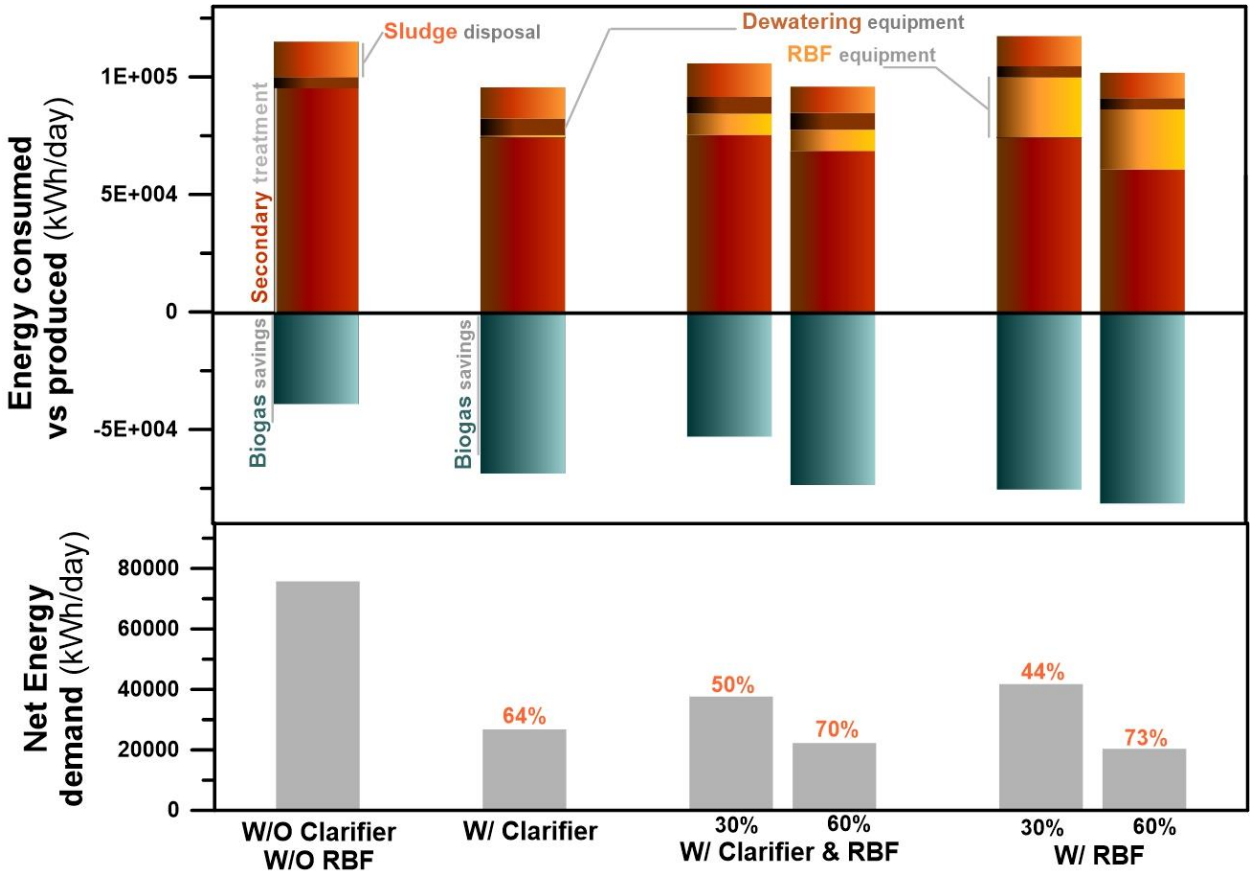

Figure 2.11b - Power demand and power production for different types of primary treatment schemes in a 380,000 m^3/day (100MGD) WRRF. Power demand is the sum of secondary aeration requirements, RBF equipment, dewatering process and sludge disposal. Power production is estimated from the methane generation at the anaerobic digester.

2.5 Summary and conclusions

Off-gas and respirometric measurement were performed in two parallel and identical aerobic biological treatments: one pilot and one at full-scale to study the impact of primary screening on the subsequent secondary operations on plant-wide energy balance. For both cases of pilot and full-scale, one line was fed with screened influent and the other with unscreened raw influent to investigate the difference in oxygen demand and transfer efficiency due to selective removal of a solid fraction of the influent organics. From our results it can be concluded that the screening of the influent by barrier separation not only decreases the overall organic load to be oxidized by the secondary biomass, but also positively influences oxygen transfer with benefits for the overall WRRF energy balance. Our study is the first independent report on the effects of oxygen transfer efficiency through primary screening. Consistent aeration efficiency improvements between filter and non-screened of 27% and 20% were obtained at pilot- and full-scale, respectively. Changes in aeration efficiency and carbon redirection were embedded in process models to investigate the primary screening impact on the WRRF energy balance. While the plant-wide assessment for different scenarios improved the energy balance up to 15%, a detailed comparative analysis between different treatment schemes gained insight into the advantages and limitations of the energetic sustainability of the use of primary screening. Future studies should consider a cost-benefit analysis of the potential for excessive carbon redirection on the need for supplemental carbon in denitrification. Also, the effect of capital cost on the overall life-cycle cost of these comparative scenarios should be included in future analyses.

References

Ahmed, A., Bahreini, G., Ho, D., Sirdhar, G., Gupta, M., Wessels, C., Marcelis, P., Elbeshbishy, E., Rosso, D., Santoro, D., Nakhla, G., 2019. Fate of Cellulose In Primary And Secondary Treatment Fate of cellulose in primary and secondary treatment at municipal water resource recovery facilities. Water Environ. Res.

Amaral, A., Schraa, O., Rieger, L., Gillot, S., Fayolle, Y., Bellandi, G., Amerlinck, Y., Mortier, S.T.F.C., Gori, R., Neves, R., Nopens, I., 2016. Towards advanced aeration modelling: from blower to bubbles to bulk. Water Sci. Technol. 75, 507–517. https://doi.org/10.2166/wst.2016.365

APHA, 2005. Standard methods for the examination of the water and wastewater.

Appels, L., Baeyens, J., Degrève, J., Dewil, R., 2008. Principles and potential of the anaerobic digestion of waste-activated sludge. Prog. Energy Combust. Sci. https://doi.org/10.1016/j.pecs.2008.06.002

ASCE, 2007. Measurement of Oxygen Transfer in Clean Water [WWW Document]. URL http://www.asce.org/templates/publications-book-detail.aspx?id=8108 (accessed 2.25.15).

Behera, C.R., Santoro, D., Gernaey, K. V., Sin, G., 2018. Organic carbon recovery modeling for a rotating belt filter and its impact assessment on a plant-wide scale. Chem. Eng. J. 334, 1965–1976. https://doi.org/10.1016/J.CEJ.2017.11.091

Caliskaner, O., Tchobanoglous, G., Reid, T., Kunzman, B., Young, R., Ramos, N., 2015. Evaluation and Demonstration of Five Different Filtration Technologies as an Advanced

Primary Treatment Method for Carbon Diversion. Proc. Water Environ. Fed. 2015, 795–818.

Caliskaner, O., Tchobanoglous, G., Young, R., Laybourne, S., 2014. Demonstration of Primary Effluent Filtration for Carbon Diversion to Save Energy and Increase Plant Capacity. Proc. Water Environ. Fed. 2014, 2911–2939.

Degroot, C., Sheikholeslamzadeh, E., Soleymani, A., Santoro, D., Batstone, D.J., Rosso, D., 2015. Modelling Rotating Belt Filter Performance and Nutrient Diversion Potential Using Computational Fluid Dynamics, in: WA Specialist Conference on Nutrient Removal and Recovery. Gdansk, Poland.

Franchi, A., Santoro, D., 2015. Current status of the rotating belt filtration (RBF) technology for municipal wastewater treatment. Water Pract. Technol. 10, 319–327. https://doi.org/10.2166/wpt.2015.038

Garrido-Baserba, M., Molinos-Senante, M., Abelleira-Pereira, J.M., Fdez-Güelfo, L.A., Poch, M., Hernández-Sancho, F., 2015. Selecting sewage sludge treatment alternatives in modern wastewater treatment plants using environmental decision support systems. J. Clean. Prod. 107. https://doi.org/10.1016/j.jclepro.2014.11.021

Garrido-Baserba, M., Sobhani, R., Asvapathanagul, P., McCarthy, G.W., Olson, B.H., Odize, V., Al-Omari, A., Murthy, S., Nifong, A., Godwin, J., Bott, C.B., Stenstrom, M.K., Shaw, A.R., Rosso, D., 2017. Modelling the link amongst fine-pore diffuser fouling, oxygen transfer efficiency, and aeration energy intensity. Water Res. 111, 127–139.

Gori, R., Giaccherini, F., Jiang, L.-M., Sobhani, R., Rosso, D., 2013. Role of primary sedimentation on plant-wide energy recovery and carbon footprint. Water Sci. Technol. 68, 870–878.

Gori, R., Jiang, L.-M., Sobhani, R., Rosso, D., 2011. Effects of soluble and particulate substrate on the carbon and energy footprint of wastewater treatment processes. Water Res. 45, 5858–5872.

Ho, D., Santoro, D., Sarathy, S., Scott, Z., 2017. Enhanced primary treatment, in: Lema, J., Suarez Martinez, S. (Eds.), Innovative Wastewater Treatment & Resource Recovery Technologies: Impacts on Energy, Economy and Environment IWA publishing, p. 690.

Honda, S., Miyata, N., Waste, K.I.-J. of M.C. 2002. Recovery of biomass cellulose from waste sewage sludge. J. Mater. Cycles Waste 4, 46–50.

Hurwitz, E., Beck, A., Sakellariou, E., Control, M.K.-J. (Water P, 1961. Degradation of cellulose by activated sludge treatment. JSTOR 33, 1070–1075.

Jiang, L.M., Garrido-Baserba, M., Nolasco, D., Al-Omari, A., DeClippeleir, H., Murthy, S., Rosso, D., 2017. Modelling oxygen transfer using dynamic alpha factors. Water Res. 124, 139–148.

Metcalf & Eddy, 2014. Wastewater Engineering: Treatment and Resource Recovery, 5th editio. ed. McGraw-Hill Education.

Paulsrud, B., Rusten, B., Aas, B., 2014. Increasing the sludge energy potential of wastewater treatment plants by introducing fine mesh sieves for primary treatment. Water Sci. Technol. 69, 560–565.

Razafimanantsoa, V.A., Ydstebø, L., Bilstad, T., Sahu, A.K., Rusten, B., 2014. Effect of selective organic fractions on denitrification rates using Salsnes Filter as primary treatment. Water Sci. Technol. 69, 1942–1948.

Rosso, D., Iranpour, R., Stenstrom, M.K., 2005. Fifteen years of offgas transfer efficiency

measurements on fine-pore aerators: key role of sludge age and normalized air flux. Water Environ. Res. 77, 266–273. https://doi.org/10.2175/106143005X41843

Rosso, D., Shaw, A.R., 2015. Framework for Energy Neutral Treatment for the 21st Century through Energy Efficient Aeration. Water Environ. Res. Found. (Project INFR2R12).

Rosso, D., Stenstrom, M., 2006. Economic implications of fine-pore diffuser aging. Water Environ. Res. 78, 810–815.

Ruiken, C.J., Breuer, G., Klaversma, E., Santiago, T., van Loosdrecht, M.C.M., 2013. Sieving wastewater – Cellulose recovery, economic and energy evaluation. Water Res. 47, 43–48.

Rusten, B., Razafimanantsoa, V.A., Andriamiarinjaka, M.A., Otis, C.L., Sahu, A.K., Bilstad, T., 2016. Impact of fine mesh sieve primary treatment on nitrogen removal in moving bed biofilm reactors. Water Sci. Technol. 73, 337–344.

Stenstrom, M.K., Gilbert, R.G., 1981. Effects of alpha, beta and theta factor upon the design, specification and operation of aeration systems. Water Res. 15, 643–654. https://doi.org/10.1016/0043-1354(81)90156-1

Taboada-Santos, A., Lema, J., Carballa, M., 2019. Opportunities for rotating belt filters in novel wastewater treatment plant configurations. Environ. Sci. Water Res. Technology. .

Tien, C., 2012. Principles of filtration. Elsevier, Oxford, UK.

Verachtert, H., Ramasamy, K., Meyers, M., Bevers, J., 1982. Investigations on cellulose biodegradation in activated sludge plants. J. Appl. Bacteriol. 52, 185–190.

WEF, 2009. Energy Conservation in Water and Wastewater Treatment Facilities, WEF Manual of Practice [WWW Document]. WEF Man. Pract. McGraw-Hill, Inc., New York, NY. URL

http://www.amazon.com/Energy-Conservation-Water-Wastewater-Facilities/dp/0071667946 (accessed 2.25.15).

Zhou, Y., Zhang, D.Q., Le, M.T., Puah, A.N., Ng, W.J., 2013. Energy utilization in sewage treatment - A review with comparisons. J. Water Clim. Chang. 4. https://doi.org/10.2166/wcc.2013.117

3. Quantification of energy and cost reduction from decreasing DO levels in full-scale WRRFs*

* A modified version of this chapter is published in the 92nd Annual WEFTEC conference proceedings, Chicago, Illinois, USA, October 2019 and is in review on Environmental Science and Technology.

3.1 Abstract

Water sanitation is transitioning from mere treatment to more sustainable approaches based on resource recovery and aiming to energy neutrality. Activated sludge (AS) processes are commonly adopted by Water Resource Recovery Facilities (WRRFs) to perform the treatment and comply to discharge limits. Generally, dated plant design and equipment result in limited operational elasticity to respond to varying loading conditions, ultimately increasing cost of treatment and GHG emissions. Despite energy optimization measures have been largely evaluated for AS processes through static and dynamic simulations, few are the full-scale applications reported in literature. Hence, the goal of the study is to quantify the energy savings associated with DO reduction at full-scale and demonstrate the importance of incorporating site-specific constrains to enhance model accuracy.

A yearlong characterization of aeration dynamics at full-scale WRRF enabled to quantify the effect of process fluctuations and evaluate optimization strategies, showing potential savings for cost of aeration up to 20% could be achieved ensuring effluent quality. A full-scale validation confirmed the predicted savings, demonstrating the beneficial effect of DO reduction on cost for aeration and the strong influence of operative choices and site-specific conditions (control strategy, loading conditions, influent flow variability, etc) on energy efficiency for aeration.

3.2 Introduction

Conventional wastewater treatment plants are transitioning towards water resource recovery facilities (WRRFs). The technification of the century-old process of activated sludge (AS) is required to enhance the sustainability of WRRFs operations and shift from an often-regarded inefficient use of resources and energy into a key element in the future of water management, seeking to close the water cycle by an efficient use of resources such as water, energy, and chemicals (Grant et al. 2012; van Loosdrecht and Brdjanovic 2014; Sedlak 2014). In WRRFs, aeration is a necessary operation and its efficiency in providing the required level of dissolved oxygen determines the WRRF economic and environmental sustainability (Rosso 2018). The energy demand required to ensure the process oxygen requirements often exceeds half of the total process energy demand ((Reardon 1995); (Rosso, Larson, and Stenstrom 2008)). In this context, the optimization of the aeration process has gained a lot of attention given its potential to reduce the process energy demand (Åmand et al., 2013; Ingildsen and Olsson, 2015). Technological developments since the 1970s and advances on modelling have played a key role on the optimization of the energy use by AS processes, allowing the improvement of aeration system design and operation. The ability to minimize peak power demand would ensure higher stability to the electrical grid, reduce operational costs, and abate energy footprint and GHG emissions (Olsson, 2015). A study concluded that a 1% shift in peak power demand would result in savings of 3.9% (billions of dollars at the system level (Spees, 2008). The local power company tariff structure prices can be almost 25% higher depending on the time of use in a plant with a ratio of 4.2-fold (for air flow rate and energy consumption) from peak to minimum (Emami, 2018). Nevertheless, many of the existing aeration systems lack the operational elasticity to efficiently respond to diurnal variations of oxygen requirements due to dated design approaches and

inadequate equipment. Historically, many WRRFs suffered from unnecessarily high air flows and dissolved oxygen (DO) concentrations, which have been deemed detrimental from the point of view of aeration efficiency (Åmand, Olsson, and Carlsson 2013) and ability to denitrify (Hodgson et al. 2019). Commonly, during periods of higher organic loadings, the oxygen transfer efficiency is not only decreased by the effects of the contaminants hindering the mass transfer from gas to liquid phase, but also the combined net effect of air flow rate increase resulting in 1) formation of larger bubbles, reduction of the surface to volume ratio; and 2) increased bubble rise velocity, reducing the contact time for oxygen transfer. (Rosso 2018)

Several are the factors limiting the integration of new techniques to the operation of existing plants. Above all, process stability to ensure effluent quality is prioritized over cost for treatment. Hence, changes to existing process conditions are usually undesirable by plant operators and over-aeration is usually selected to avoid non-compliance with effluent quality requirements. Secondly, incorrectly designed or tuned automated controls embed the potential risk of detrimental effects on the efficiency and lifespan of the aeration equipment, which can result in excessive energy consumption and cost to start and stop the blower motors, as well as an increase in wear and tear on the blowers, valves, and actuators, due to the continuous adjustment of operative variables(Ogurek and Alex 2015) Third, scale-dependent capital investment is required to renew or build new WRRFs (Guo et al. 2014). Due to the site-specific nature of potential costs and benefits achievable through optimization strategies (equipment, treatment capacity, cost of energy and TOU tariff, etc.), the value of the required capital investment may be difficult to evaluate for a general case.

DO set-point optimization is still a very active topic and many approaches have been suggested in recent years, from combinations of feedforward-feedback strategies to fuzzy control

and model-based control methods ((Chotkowski, Brdys, and Konarczak 2005); (Baroni et al. 2006); (Yinl and and Michael K. Stenstrom 1996); (Regmi et al. 2014)). This resulted in theoretical energy savings and improved stability of the system and consequently increased operational life of the aeration equipment and effluent quality (Pittoors, Guo, and W. H. Van Hulle 2014; Åmand, Olsson, and Carlsson 2013). The majority of these studies are performed with the help of the Benchmark Simulation Model, which proved to be a valuable tool to standardize and compare results from different studies (Åmand, Olsson, and Carlsson 2013).

The bulk of modelling efforts in the past decades has focused on biokinetics (e.g., the ASM family, beginning with (Henze 1987), while the inclusion of aeration dynamics has been overlooked until recently ((Jiang et al. 2017)). The integration of oxygen transfer dynamics can provide several advantages ranging from improved performance diagnostics (i.e., deficient valves, over-aeration, imbalanced flows, etc.) to enhanced capability to predict the response of process state variables to operational variations ((Jiang et al. 2017), (Schraa, Rieger, and Alex 2017)). Moreover, as cost for energy can vary significantly (depending on plant size, location, time of the day, season, etc.), a detailed description of the tariff-structures is fundamental to achieve accuracy for process performances and economic evaluations ((Pittoors, Guo, and Van Hulle 2014), (Aymerich et al. 2015)). However, the reliability of the models and predictions is yet to be improved as site-specific operative and technological conditions may strongly affect process dynamics, de facto decoupling the model mathematical description of process conditions from the real case of study.

One way to reduce the discrepancy between outcome of the model and full-scale implementation is by increasing process dynamics characterization, which was demonstrated to be

a key factor to maximize the reliability of plant's performance modelling and prediction ((Aymerich et al. 2015), (Pittoors, Guo, and W. H. Van Hulle 2014)).

Continuous monitoring, modelling, prediction, and ultimately control of aeration system based on oxygen transfer efficiency (OTE%) historical and real-time data are therefore needed to optimize and reduce the aeration energy demand ((Amaral et al. 2016); (Gernaey et al. 2001)). Despite successful examples of real-time monitoring of aeration efficiency indicators for optimization and process control were implemented at full-scale (Jenkins et al. 2008); (Schuchardt et al. 2007); (Amerlinck et al. 2016)), those are yet exceptions to the most common practice.

The goal of this work is to quantify the energy reduction associated with decreasing DO while imposing effluent quality as constraint and to ultimately quantify the yearly economic benefits. Long-term characterization of the aeration system dynamics via off-gas test allowed to track the variability of operating conditions adopted by the WRRF (DO, air flow rate) and evaluate the consequent oxygen transfer efficiency at field conditions (αSOTE%). Three sequential steps (i.e., year-round data data-collection, modelling based on field results, and full-scale experimental data validation) were performed in order to minimize the uncertainty between the modelling results and the full-scale implementation of the DO reduction. The implementation in the simulation platform of the seasonal and daily dynamics, together with the corresponding tariff structures, which are also seasonal and daily dependent, enabled the calculation of cost savings per each different season and also per daily time fraction (depending on the strategy). The study considered four different time periods daily to better understand the process dynamics and improve the diagnosis of future actions or strategies. The predicted reduction for cost of aeration when the DO setpoint was reduced from 1.9 to 1.7 mg l^{-1} was validated at full-scale. The continuous monitoring

of the dynamics of the aeration system demonstrated to be a valuable tool to improve process characterization, modelling accuracy and evaluate optimization strategies.

3.3 Material and methods:

3.3.1 WRRF#1 and WRRF#2:

The investigated facilities are located in Southern California (Regional Plants #4 and #5, Inland Empire Utilities Agency) and treated municipal wastewater for reclamation and reuse. WRRF#1 is designed for a maximum capacity of $6.3x10^3$ m^3 d^{-1} (14MGD) and operated at approximately $4.6x10^3$ m^3 d^{-1} (10 MGD). WRRF#2 is designed for a maximum capacity of $7.4x10^3$ m^3 d^{-1} (16.3 MGD) and is currently operated at approximately $4.1x10^3$ m3 d^{-1} (9 MGD). The liquid treatment section for both facilities consists of preliminary screening and grit removal, primary clarification, secondary treatment by aeration basins and clarification. Secondary treatment is operated with pre-anoxic reactors for nutrient removal, with an annual average solids retention time of 18 days. The secondary tank total volume of is divided in 3 anoxic and 3 aerobic sections. Air is supplied to the aeration tank by two equal blowers (370kW or 500HP) with 60%, 35% and 5% air distribution for the first, second and third section respectively. The solids removed from WRRF#1 and WRRF#2 were directed to a different facility for thickening, anaerobic digestion and energy recovery through a combination of a biogas powered microturbine, solar panels, and battery energy storage.

3.3.2 Telemetric off-gas analyser:

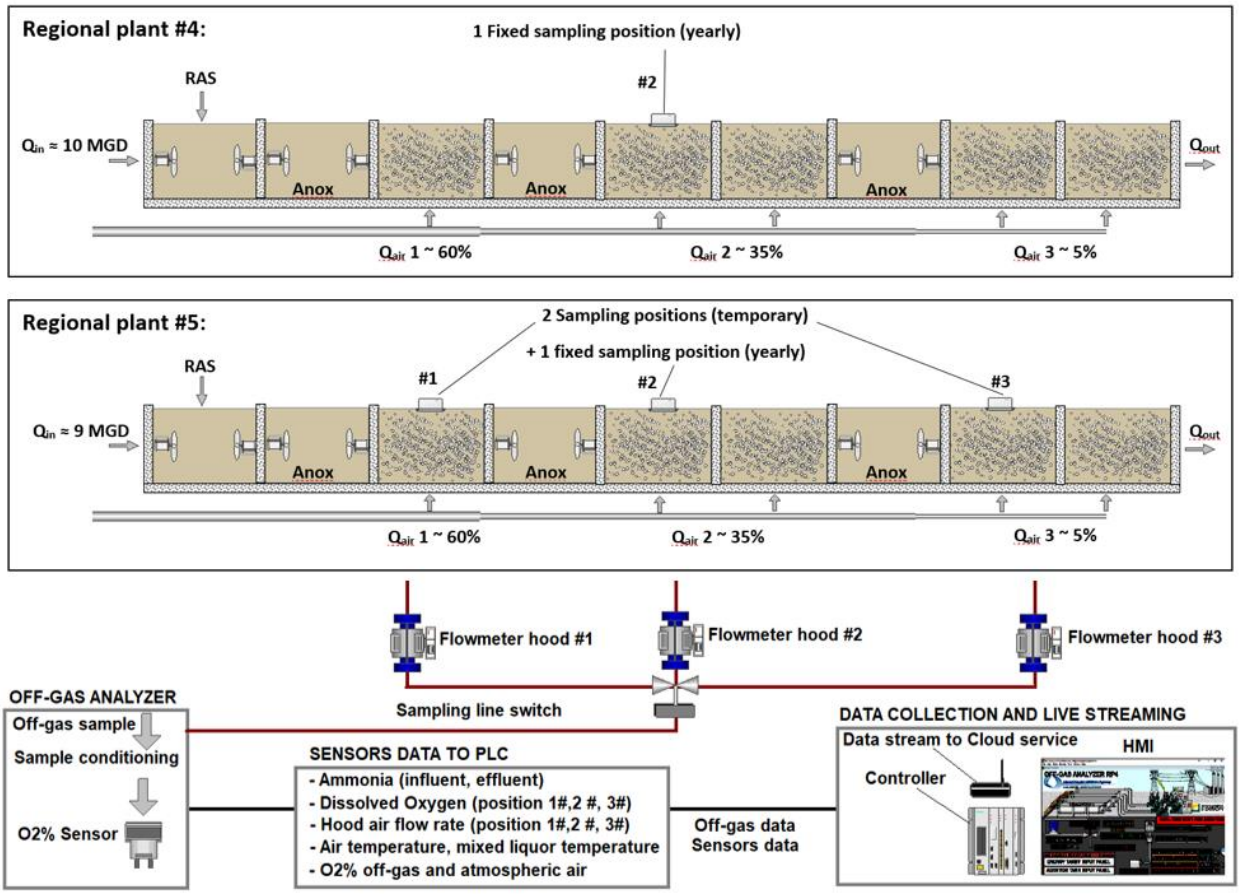

Figure 3 - The schematic secondary treatment tank layout for WRRFs #1 and #2 is shown. Position #2 (mid-section) was monitored for WRRF#1 during the long-term monitoring campaign while all three positions (influent, mid-section and effluent) were monitored during the validation at full-scale of modelling results at WRRF#2.

In traditional off-gas analysis, the off-gas is collected by a mobile hood and is conveyed through a flexible hose to the analyser. The data collection occurs by measuring the oxygen partial pressure and the flow rate of the off-gas using an analyser, which records the readouts from the sensors. This process is repeated as necessary at various locations along the aeration basin by

moving the floating hood. This methodology is generally time-consuming and labour-intensive as the hood is moved through various locations along the tank length. To obviate this shortcoming, two fully automated off-gas analysers were built and installed at WRRFs #1 and #2 with permanent hood stations. The permanent hood position was determined during a preliminary full off-gas mapping (performed according to the ASCE, 1997 method) to ensure the collection of representative results over the whole tank.

The analyser measured the off-gas flow and temperature while an off-gas aliquot was sampled every 15 minutes to measure oxygen, moisture, and carbon dioxide content in the gas phase. Additionally, the dissolved oxygen and water temperature were measured under the off-gas hood. The instruments output the oxygen transfer efficiency, alpha factor, air flow rate and dissolved oxygen, as well as blower power demand for aeration. The instrument additionally calculated the daily real-time aeration efficiency and cost for aeration using the Time-of-Use (TOU) tariff under contract between the wastewater treatment and power utilities. Real-time telemetry (Fig.3.1) enabled remote access to monitor the status of the instrument and schedule maintenance requirements. The instrument systematically collected data to characterize seasonal, monthly, and daily variations. Verification of the plausibility of the retrieved raw data and the detection of potential outliers was conducted by calculating the coefficient of variation (CV) and the use of traditional data reconciliation techniques. Averaged values from every set of representative data were calculated to show the main differences between winter, fall, spring, and summer.

Similarly, continuous hourly measurements enabled the calculation of the hourly average per each day to obtain 24-hour profiles. The data collected includes the: oxygen transfer efficiency

(OTE%), hood air flow rate (m^3 min^{-1} or SCFM); dissolved oxygen (DO, mg l^{-1}); alpha factor (dimensionless); and the influent flow rate variation (m^3 d^{-1} or MGD).

3.3.3 Operating scenarios simulation:

A multi-parameter study was performed to highlight and quantify potential benefits in short- and long-term through a variety of scenarios. For this purpose, a set of models was run with several scheduled data sets and different operating conditions based on the daily and seasonal dynamics collected during the year-long characterization. The WRRF model was developed with 9 CSTR in series in A/O/A/O/A/O configuration using a commercial simulator (Biowin ver. 5, Envirosim, Hamilton, ON). The geometry and diffuser characteristics were carefully implemented to replicate WRRF#1 plant condition. Steady-state and dynamic modelling were conducted for a range of DO setpoints to predict the potential cost savings associated to DO reduction. In particular, the approach presented in this study aimed at confirming the plausibility of reducing the current DO setpoint of 1.9 mg l^{-1} (in the first aerobic section) without producing a lower quality effluent. Different DO setpoints ranging from 2.5 to 1.5 mg l^{-1} were investigated, at an interval of +/- 0.2 mg l^{-1}. Additionally, the simulation of DO reduction was implemented at different times of the day to investigate the effect of variable loading conditions (hydraulic, organic) and cost of energy during diurnal operations. For this, the following time periods were considered: 00:09 – 15:00; 15:00 – 21:00; 21:00 – 03:00; 03:00 – 09:00, for each season.

3.3.4 Full-scale data validation:

Following the results obtained after the data collection and modelling phases, a careful attempt to reduce DO setpoint at full-scale was performed at WRRF#2. The setpoint was reduced by 0.2 mg l^{-1} (i.e., from 1.9 to 1.7 mg l^{-1}) in the first section of secondary tank composed by three-aerated sections with a similar configuration to the WRRF#1 (A/O-A/O), where the data-collection was conducted. Aeration efficiency indicators (αSOTE; air flow rate; dissolved oxygen) and process conditions (MLSS; sCOD) were monitored during 30 days of operations in 3 different sampling positions with a sampling frequency of 15 minutes (first, second, and third aerobic sections, as shown in Fig.1). Oxygen uptake rate (OUR, mg O_2 $(l\ h)^{-1}$) was measured with a frequency of 15-20 mins in the first and third aerobic sections via respirometric method (i.e, oxygen depletion in batch reactor), while ammonia concentrations, dissolved oxygen and air flow rate were continuously monitored in the same sections and averaged for every off-gas and respirometric data-point over the sampling period. Settling characteristics were measured hourly via SVI test (Sludge Volume Index, ml g $MLSS^{-1}$). A series of on-line alarms was implemented to ensure effluent quality and notify the facility employees to interrupt the test in case of ammonia breakthrough or significant decrease in biomass activity.

3.3.5 Power demand calculations:

Power demand was both measured at full-scale and derived from the off-gas measurements. Measured values were retrieved from the power meter of each blower during the preliminary phase of data collection and during the validation phase of the test. Estimated values for power demand for aeration were derived from off-gas measurements through the estimation of mechanical power demand (i.e., brake horsepower) from the adiabatic formula (Metcalf & Eddy, 2014; eq.1):

$$P_w = \frac{wRT}{29.7ne}\left[\left(\frac{p_2}{p_1}\right)^{0.283} - 1\right] \quad (1)$$

where: Pw = power required for each blower (kW)

w = ponderal air flow (kg s^{-1})

R = universal gas constant for air (8.314 kJ mol^{-1} K^{-1})

T = inlet temperature (K)

p_1 = inlet pressure (Pa)

p_2 = discharge pressure (Pa)

n = 0.283 for air (-)

e = blower efficiency (-)

Power demand calculations from off-gas measurements were calibrated comparing the observed results with the values from collected from power metering during the first month of data collection. The power demand in eq.1 is a function of the air flow and OTE, inlet and outlet flow pressure, air temperature and blower efficiency. Hence, a function describing the variation of discharge pressure and mechanical efficiency of the blowers would be required to for real-time calculations of power demand based on off-gas calculations. However, since the blower discharge pressure is dominated by the hydrostatic head, the variation in head loss and dynamic wet pressure (DWP) due to air flow variations can be considered negligible, allowing to adopt a constant value for inlet and outlet pressure (i.e, head loss, DWP). Thus, the continuous off-gas monitoring coupled with power metering would allow to highlight variations in the blower mechanical efficiency: whereas every other variable in eq.1 is accounted for, any discrepancy between the power demand

estimated and directly measured can be addressed to under/over estimation of the average blower efficiency during dynamic conditions.

3.3.6 Energy TOU tariff:

In the area where the treatment facilities are located, power demand and energy consumption are priced following a set of structures established to promote rational use of the existing infrastructure. The application of different energy pricing structures (e.g., time-of-use rates) and charges (e.g., energy usage, peak power demand charges) in the different billing terms results in very different operational costs depending on when the energy is used (hour, day, month, and season). WRRFs typically receive the highest loading flow rate (to be treated) when the cost of energy is also the highest. The consequent overlap between the receiving influent peak and the most expensive energy price exacerbates both the cost of treatment and the concurrent GHG emissions. Even small shifts in peak demand have a significant effect on savings to consumers and avoided costs for additional peak capacity.

Therefore, it is of the utmost importance to consider the tariff structure when assessing the cost savings from aeration optimization strategies. The software was equipped with an energy input panel, where details of the Time-Of-Use tariff were entered. The tariff structure is described in Tab. 1, where “live, fixed and penalty” costs are reported. In particular, “fixed” costs are expressed in USD per kW and rates are assigned to the user (in this case, the WRRF utility) depending on the monthly or seasonal highest power demand peak sustained; similarly, a fixed cost (DWR, state taxes) is added to the live cost of energy consumption and expressed in USD per kWh. For “live” cost, rates are variable depending on the Time of Use, where highest rates often correspond to periods of highest demand, expressed in USD per kWh. Finally, a “penalty” cost is

added, expressed in USD per kVAR, whereas inefficient equipment results in undesirable effect on the electrical grid (i.e, power factor adjustment).

Table 3.1 - Energy tariff for WRRFs #1 and #2

	FIXED COSTS		TOU RATES			POWER FACTOR ADJ
			On-peak	Mid-peak	Off-peak	
	Rate	Rate	Rate	Rate	Rate	Rate
	(USD/kW)	(USD/kWh)	(USD/kWh)	(USD/kWh)	(USD/kWh)	(USD/kVar)
WINTER (NOV TO MAY)	18.0	0.005	-	0.016	0.016	0.6
SUMMER (JUNE TO OCT)	18.3	0.005	0.018	0.018	0.018	0.6

3.4 Results and discussion:

3.4.1 Data-collection via off-gas monitoring and optimization strategies modelling

Data collected over 12 months of continuous monitoring of the mid-section of the aeration tank of WRRF#1 are shown in Figs. 3.1a - 3.1c. The effect of wastewater contaminants and hydraulic loading on oxygen transfer efficiency can be observed as OTE fluctuated through daily cycles at WRRF#1, reporting the lowest value for the peak in hydraulic and organic loading. Warmer temperatures confirmed the beneficial effect on transfer efficiency, as lower viscosity is expected, concurrently with higher biological kinetic, hence providing a faster removal of contaminants suppressing oxygen transfer (US-EPA 1987). This is confirmed by the difference measured between the daily average OTE for warm (spring and summer) and cold periods (fall, winter), which was 11±2% and 5.8±1.8% respectively.

Figures 3.1b and 3.1c show the effect of the circadian amplification of air flow during daily hydraulic peak, where the increase in air flow to satisfy the DO requirements during the peak loading periods can be observed. At these times, lowest OTE were measured for the concurrent detrimental effect of high load of contaminants and high air flow rate delivered to the tank. When seasonal process conditions are considered, it can be observed how the measured air flow was within the same order of magnitude throughout different seasons. Similar magnitude was unexpected considering the previously observed variations in transfer efficiency, which can be halved during winter months. Therefore, air flow measurements seemed to indicate that the same air flow was being delivered year- round. Minor differences were instead measured for DO over the seasons, except for fall, when possibly a different setpoint was implemented by the WRRF.

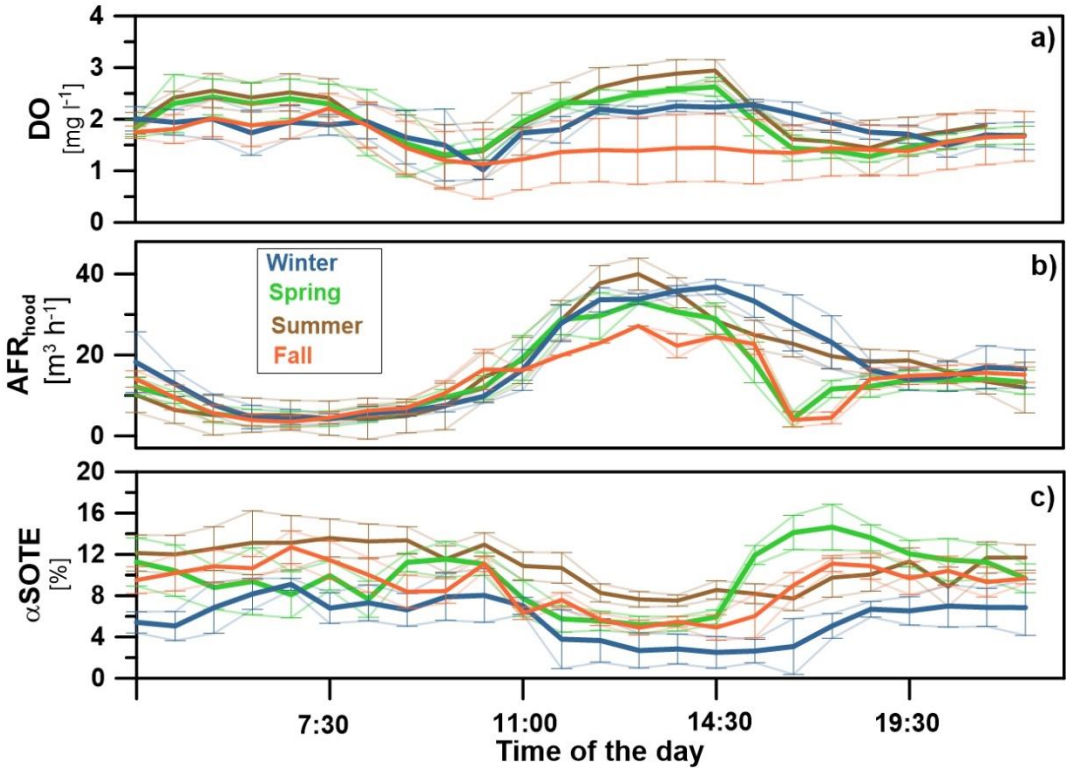

Figures 3.1a – 3.1c: Daily profiles (calculated as average of 200 days for one year) of OTE (a), DO (b), and air flow rate (c) in the mid-section of the aeration tank of WRRF#1.

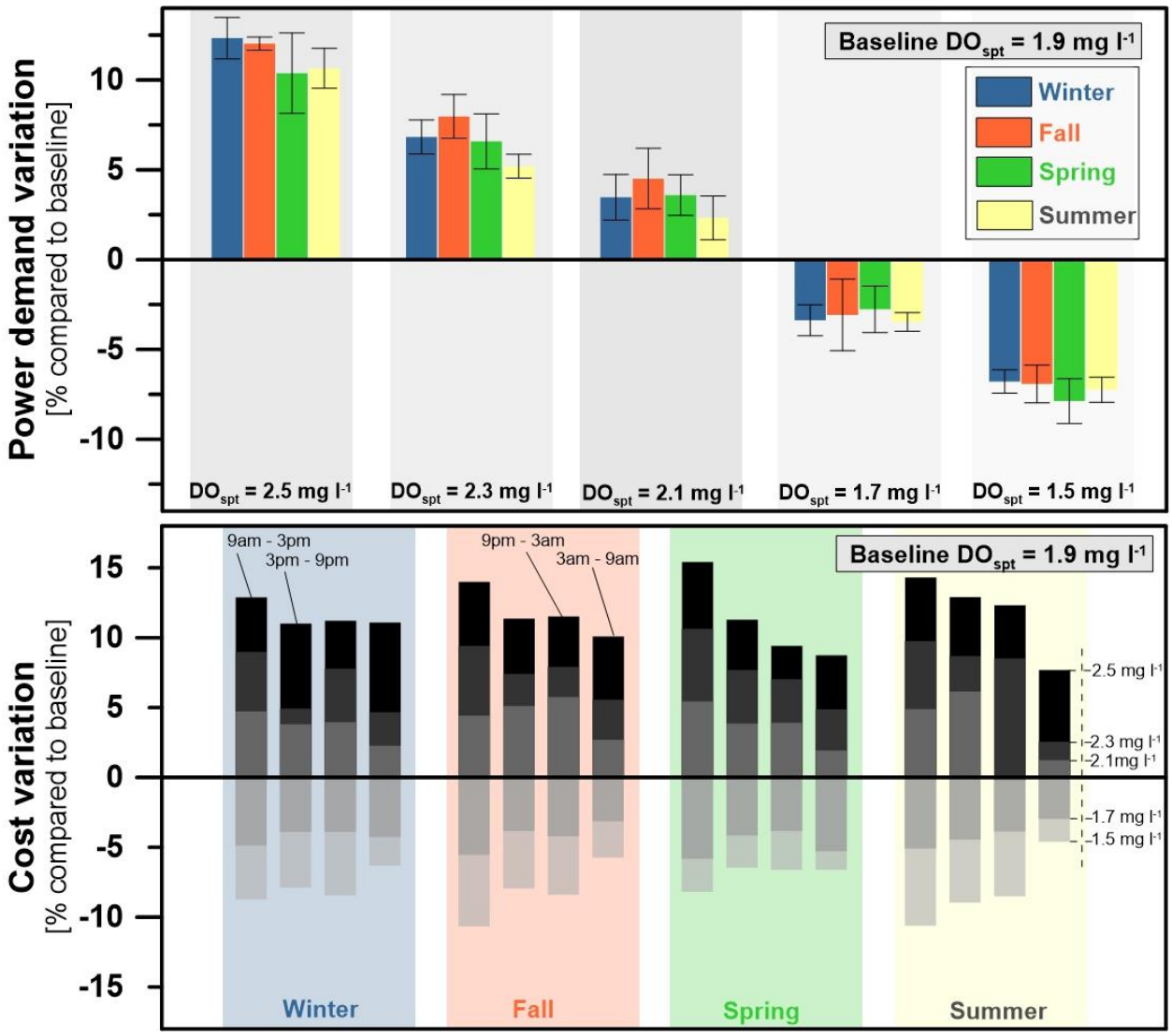

Figures 3.2 – 3.3: The results from modelling of DO setpoint reduction for WRRF#1 are reported. In Fig.3.2 (left) the savings in power demand for aeration are expressed in % compared to the baseline condition (no setpoint decrease) for the different seasons. Cost increase projections for the different seasons and time frames under study is shown in Fig.3.3 expressed in $ per hour saved compared to the baseline condition for the different seasons. Lower bar (light grey) corresponds to operational costs of using a setpoint of 1.5 mg l^{-1}. As the setpoint increases the costs expressed in $/hour increase also (darker grey, light blue).

The adoption of operational changes aimed to reduce energy footprint in secondary treatment was simulated using a commercially available software to quantify potential savings for cost of energy (Biowin ver. 5, Envirosim, Hamilton, ON). The model was designed to reproduce in detail the investigated facility to maximize the accuracy of the projected energy reduction. The implementation of the setpoint reduction in the model was simulated for different periods of the day (influent peak, influent off-peak) to investigate the effect of diurnal overlap of hydraulic and loading conditions with variable cost of energy.

The results reported in Fig. 3.2 and Fig. 3.3 showed the reduction for power demand and for the cost of aeration when the DO setpoint was decreased by 0.2 mg l^{-1} (i.e., to 1.7 mg l^{-1}). The set of modelled optimization strategies showed that increasing the DO setpoint from 1.9 to 2.5 mg l^{-1} would increase power demand for aeration up to 14% and cost for aeration up to 15%, depending on the season, resulting in comparable effluent quality. Contrarily, reducing the DO setpoint to 1.5 mg l^{-1} would result in the reduction of power demand up to 7% and cost for aeration up to 10%, maintain effluent quality within expected limits. The variable distribution of cost savings potentially achievable reducing DO setpoints is consistent with what was observed during the off-gas monitoring phase. The circadian amplification of air supplied to the tank on peak-hours (Fig. 3.1b) results in the consequent increase in cost for aeration (Figs. 3.2- 3.3), as confirmed by the highest savings for power demand and for cost of energy predicted for DO reduction during influent peak conditions. Additionally, it is observed how higher reductions in power demand were obtained for colder periods (when oxygen transfer efficiency was lower and air flow rate the higher) while comparable cost savings were achieved over the year as effect of variable cost of energy.

Full-scale validation of the DO setpoint reduction:

3.4.2.1 Effect on power demand for aeration

The effect of DO decrease on power demand for aeration was analysed. When only the average power demand is considered, the decrease by 0.1 mg l^{-1} in the DO setpoint resulted in an average reduction in power demand by 2% (from 423±77 kW to 415±39 kW). However, if the daily spectrum of operating conditions is analysed through the normalization of power demand over the influent flow, it can be observed how this yielded to significantly higher values. The daily profile of metered power demand from the two blowers over 30 days of experiment (15 days before and 15 after the DO setpoint decrease) is shown in Fig. 3.4, normalized as kW per m^3 of influent to the tank. The average power demand for aeration in the selected tank over the testing period decreased by 15.8% on average, from 12.7±3.5 to 10.4±1.9 W per m^3 (respectively before and after the change in the DO setpoint for the selected tank). As air flow rate to the tank was supplied by two blowers, this resulted in an average decrease of 10.5% (6.9 to 6.1 W per m^3) for the first and by 22.1% (5.7 to 4.3 W per m^3) for the second blower after the setpoint reduction.

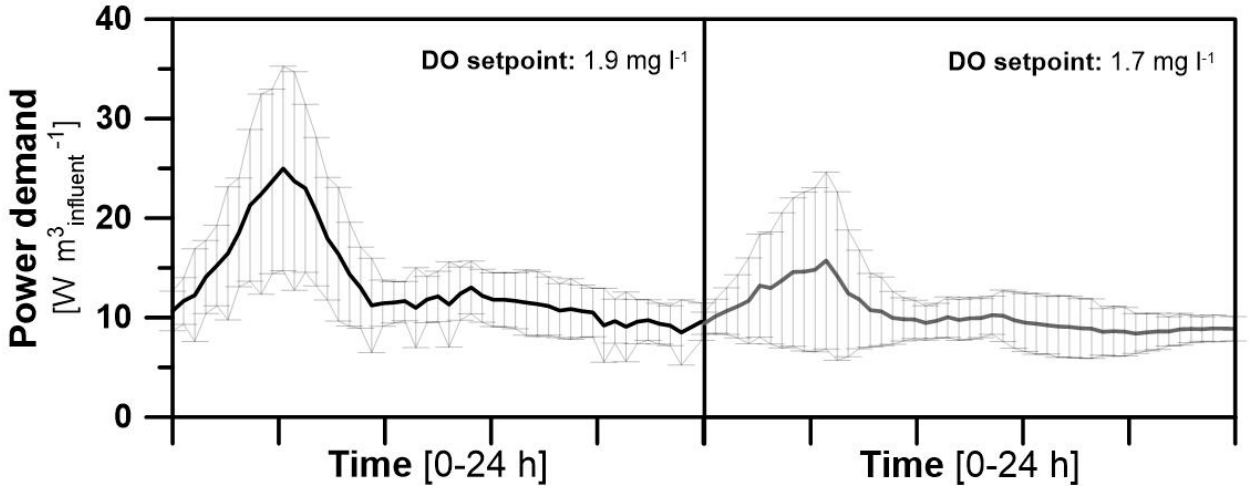

Figure 3.4 - The daily average profiles of power demand for aeration during 30 days of continuous monitoring are reported before and after the DO setpoint reduction. Power demand was normalized by the influent volume during the two consecutive testing periods.

Power demand reduction resulted from the decrease in delivered air flow and was enhanced by the improvement in αSOTE, since smaller and slower bubbles are released at lower air flows (USEPA 1989; Libra et al, 2002, 2005; Rosso et al, 2005; Gillot and Héduit, 2008). As shown in Tables 3.2 and 3.3, the DO reduction affected differently the three aerobic sections, where different operating conditions were observed due to the decreasing severity of loading conditions along the tank. Variations in energy savings during the day were due the concurrence of circadian variations in organic loading (i.e., oxygen demand), consequent OTE variations, and air flow rate supplied to the tank. The amplification of the energy curve over the circadian cycle confirms the findings by (Emami, Sobhani, and Rosso 2018) who concluded that a small number of hours during the electrical peak would cost the same or more than the rest of the day altogether. The reduction in DO had a positive effect on blower's operations, as it can be induced observing the values of standard deviation measured for power demand over the diurnal cycle, which was ±77 kW when the setpoint was 1.9 mg DO l^{-1} and decreased to ±39 kW (18% to 9.4% of the total demand), when

the setpoint was reduced to 1.7 mg DO l^{-1}. This suggests that higher mechanical efficiency from the blowers was obtained, as the frequency of adjustments from the aeration control system to provide stability for air flow rate, air pressure and dissolved oxygen (Franklin et al. 1994).

Table 3.2 - Variation of process conditions after DO reduction for each aerobic section.

Aerobic section			**Aerobic section**			**Aerobic section**			**Aerobic section**		
1st	**2nd**	**3rd**	**1st**	**2nd**	**3rd**	**1st**	**2nd**	**3rd**	**1st**	**2nd**	**3rd**
OTR [kg $O_{2\ transf}$ h^{-1}]			**Air flow rate** [m^3 h^{-1}]			**Dissolved oxygen** [mg DO l^{-1}]			**αSOTE** [%]		
DO set point: 1.9 mg l^{-1}											
209±13	204±74	58±1	3407±102	2190±641	342±5	1.9±0.1	1.5±0.3	0.6±0.0	7.9±0.6	11.8±1.4	21.5±1.8
DO set point: 1.7 mg l^{-1}											
255±13	152±54	45±6	3143±145	1603±415	318±3	1.7±0.1	1.6±0.3	0.5±0.0	10.5±1.6	11.9±1.5	18±2.3

Table 3.3 - Variation of process conditions after DO reduction, expressed in %.

AFR distribution [%]	65	35	5
Variations [%]	**First aerobic section (influent)**	**Mid aerobic section**	**Final aerobic section (effluent)**
AFR after DO drop (section average)	**-7.7**	**-26.7**	**-7**
AFR after DO drop (tank weighted average)	**-4.8**	**-8**	**-**
On-peak	-4.8	-10.1	-
Off-peak	-4.8	-6.9	-
OTR after DO drop (section average)	**22.1**	**-25.6**	**-22.4**
OTE after DO drop (section average)	**24.8**	**-**	**-16.3**
On-peak	30	-	-19.5
Off-peak	18	-	-11.5
Reduction in power demand for aeration [%]	**Blower 1**	**Blower 2**	
On-peak	11.6	19	
Off-peak	9.8	23.4	

** - = no effect*

****:** variations in process conditions and oxygen transfer are shown for each section before and after the setpoint reduction expressed in % for each section and for loading conditions. The reduction of air flow rate is expressed on average for each section and on weighted average over the tank for each section and loading conditions. The reduction in power demand for aeration for blower 1 and 2 and the overall savings are expressed for different loading condition.

3.4.2.2 Effect of on oxygen transfer

The daily profiles of the oxygen transfer efficiency for the three aerated sections are reported in Fig. 3.5. An improvement in αSOTE was measured in the first section (where 60% of the total air was fed), where the average transfer efficiency increased from 7.9±0.6% to 10.5±1.6%. Minor variations compared to the baseline conditions were observed for the mid-section (where 35% of the total air was fed), as the average αSOTE was 11.8±1.4% and 11.9±1.4% before and after the change, respectively. A negative effect was measured in correspondence of the effluent section where αSOTE decreased from 21.5±1.8% to 18±2.3% before and after the change, respectively. However, as only a marginal percentage of air was delivered to this section (5% of the total), this effect contributed negligibly to the overall energy footprint.

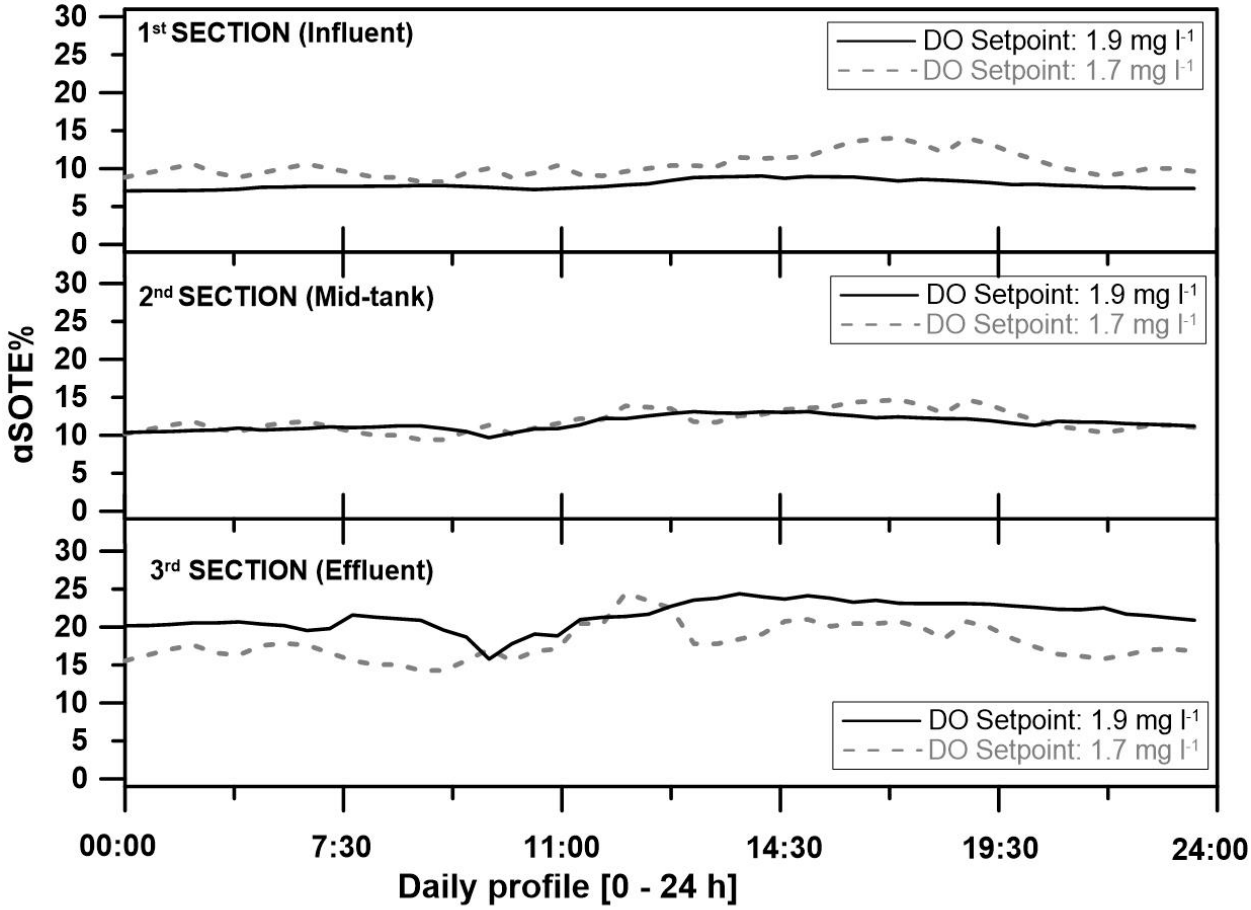

Figure 3.5 - The daily average profiles of αSOTE% during 30 days of continuous monitoring are reported for each aerobic section, before and after the DO setpoint reduction.

To evaluate the concurrent effect of reduced air flow and enhanced αSOTE, oxygen transfer rate profiles were analysed along the tank before and after the DO reduction. The set point decrease adopted in the first section induced a spatial modification of loading conditions over the remaining sections of the tank compared to the baseline conditions. Similar results were presented by (Schuchardt et al. 2007) and (Fan et al. 2017), who highlighted the influence of DO setpoints to strategically target optimal conditions for carbon oxidation and nitrification. While the average OTR over the whole aeration tank was comparable before and after the set point reduction (153±21

kgO_2 transferred per hour), the reduction in air flow rate resulted in the redistribution of OTR along the tank. In the second section, where αSOTE was not significantly affected by the setpoint variation applied in the previous (first) section, the OTR reduction was almost proportional to the air flow reduction (-26% for air flow, -25% for OTR). Contrarily, despite less air flow rate was supplied in the first section, higher OTR was observed in this section compared to the previous DO setpoint, due to the higher αSOTE. The effective treatment capacity of each aerated section (expressed in % over the tank OTR) was shifted from 43/41/16% to 56/34/10% for first, second, and third section respectively. The air supplied to the aeration tank was transferred 15% more efficiently in the first section as over-aeration was reduced. Since 60% of the total air flow was targeted during process design, the OTR redistribution seem to better satisfy the optimal operating conditions and load distribution along the tank length. Data collected in the first (influent) and second (mid-section) aerobic sections of WRRF#2 for the two consecutive periods operated at different DO setpoints are shown in Fig.3.5. The variation in air flow rate and OTR is expressed in % and compares the two periods of testing. When the DO setpoint was decreased in the first section of the aeration tank from the resulted air flow rate reduction affected both first and mid-section of the tank. Two different correlations between air flow rate reduction and OTR variation can be observed for the two sections. Shown in Fig. 3.6, a linear decrease ($R^2 = 0.73$) between air flow rate and OTR was observed in the mid-section, where OTE% variations between the two operating DO setpoints were negligible despite 26.5% air flux reduction (from 2190±641 to 1603±415 $m^3 h^{-1}$). Hence, as the range of operating conditions adopted for this section before and after the DO setpoint reduction ensured comparable transfer efficiency, the observed linear correlation between air flow reduction and OTR quantifies the rate of mass transfer reduction as the transfer efficiency is reduced. A non-linear variation was instead observed for the first section,

where the setpoint reduction was implemented. As the setpoint was reduced from 1.9 to 1.7 mg l^{-1}, dissolved oxygen effectively decreased by 7.6% in this section (from 1.88±0.12 mg l^{-1} to 1.69±0.16 mg l^{-1}) resulting in 7% reduction of air fed from the blowers to this section (4.8% over the total tank, from 3407±102 to 3143±145 m^3 h^{-1}). Contrarily to the mid-section, the reduction of air supplied in the first section resulted in a beneficial effect on OTR, which increased as the air flow rate was lowered. An exponential fit (R^2 = 0.49) allowed describing the variable effect of air flow rate reduction on OTR for optimal and over-aerated conditions, when all data from first and mid-section are considered. A similar non-linear behaviour was previously described by (Iranpour and Stenstrom 2001), who quantified the loss of efficiency in oxygen transfer due to excessive air flow. Finally, a minor variation was measured for the third section, where dissolved oxygen was comparable before and after the DO reduction and equal to 0.55 mg l^{-1}, while air flow rate decreased 7%, from 342±5 to 318±3 m^3 h^{-e1}, with no significant influence over the process performance.

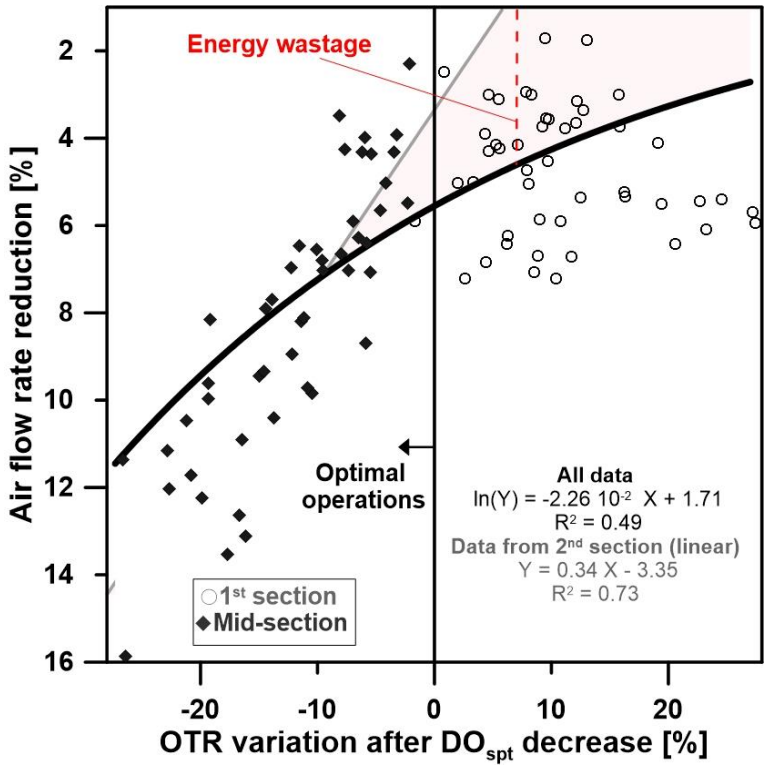

Figure 3.6 – The difference between air flow rate and oxygen transfer rate (OTR) expressed in % between two operating conditions at WRRF#2 is shown. The datasets for first and mid-sections show the difference behaviour between the two sections when the DO setpoint was reduced from 1.9 to 1.7 mg DO l^{-1}.

3.4.2.3 Effect of DO setpoint reduction on blower operations

The daily profile of power distribution between the two blowers is reported in Fig. 3.7, expressed in % of power demand from the main blower ($kW_{blower\#1}$) over the total blower capacity (i.e., $kW_{blower\#1}$+$kW_{blower\#2}$). The reduction in air flow rate targeted by the aeration control when the set point was decreased modified the blower turndown. The average power demand distribution between blower#1 and blower#2 was shifted from 56/44% (±12%) to 58/42% (±3%) when the DO was lowered. The effect of DO reduction was variable under influent peak and off-peak periods

due to the transient loading and operating conditions, as previously described. For high loading conditions (on-peak, 00:09 – 17:00), power demand was almost evenly distributed between the two blowers, on average. However, power demand from blower#1 showed higher variability as this blower was elected to provide the peak of air flow rate required to match the maximum oxygen demand. As shown in Fig. 3.8, when DO was reduced, power demand to operate blower#1 decreased by 11.6% compared to the previous conditions, while a 19% reduction was measured for blower#2. For low loading conditions (off-peak, 5 pm to 9 am), energy savings recorded for blower#1 were 9.8% while a 23.4% reduction was measured for blower#2, compared to the baseline. Thus, by quantifying the difference in the energy savings recorded for blower #1 and #1 during high and low loading conditions, it was possible to investigate the operating conditions resulting in the increased blower's efficiency. When the highest air flow rate was required by the process, the continuous flow adjustments required to maintain the required DO set point mainly affected blower#1, while blower#2 was operated at steady state. The DO reduction allowed to minimize the counter-productive "anti-windup" effect of blower#1, as suggested from the lower standard deviation measured for daily power demand, and the highest reduction of power demand observed for on-peak conditions (11.6% vs 9.8% obtained off-peak). A possible explanation of this can be provided assuming a reduction in the frequency of adjustments of the aeration control. The setpoint reduction resulted in a lower gap between tank DO (i.e, measured value) and the imposed setpoint (i.e, target value) decreasing the amplitude of disturbance in the PID aeration control, thus offering more favourable operating conditions for the blowers. Additionally, resulting from the DO setpoint and related air flow rate decrease, the aeration control elected the capacity of a single blower adequate to supply most the oxygen requirements, thus reducing the use of other blowers composing the blower-house. In our case, this can be observed during low loading

conditions, where higher energy reduction was measured for the blower#2 compared to high loading conditions (23.4% vs 19% obtained on-peak). Overall, savings for power demand during off-peak periods were more substantial as the DO setpoint decrease resulted in reduced over-aeration during low load. However, as cost for energy is generally time-based and peak of power demand often overlays with the higher cost for energy, the energy savings achieved during peak loading conditions can result in higher economic savings compared to off-peak.

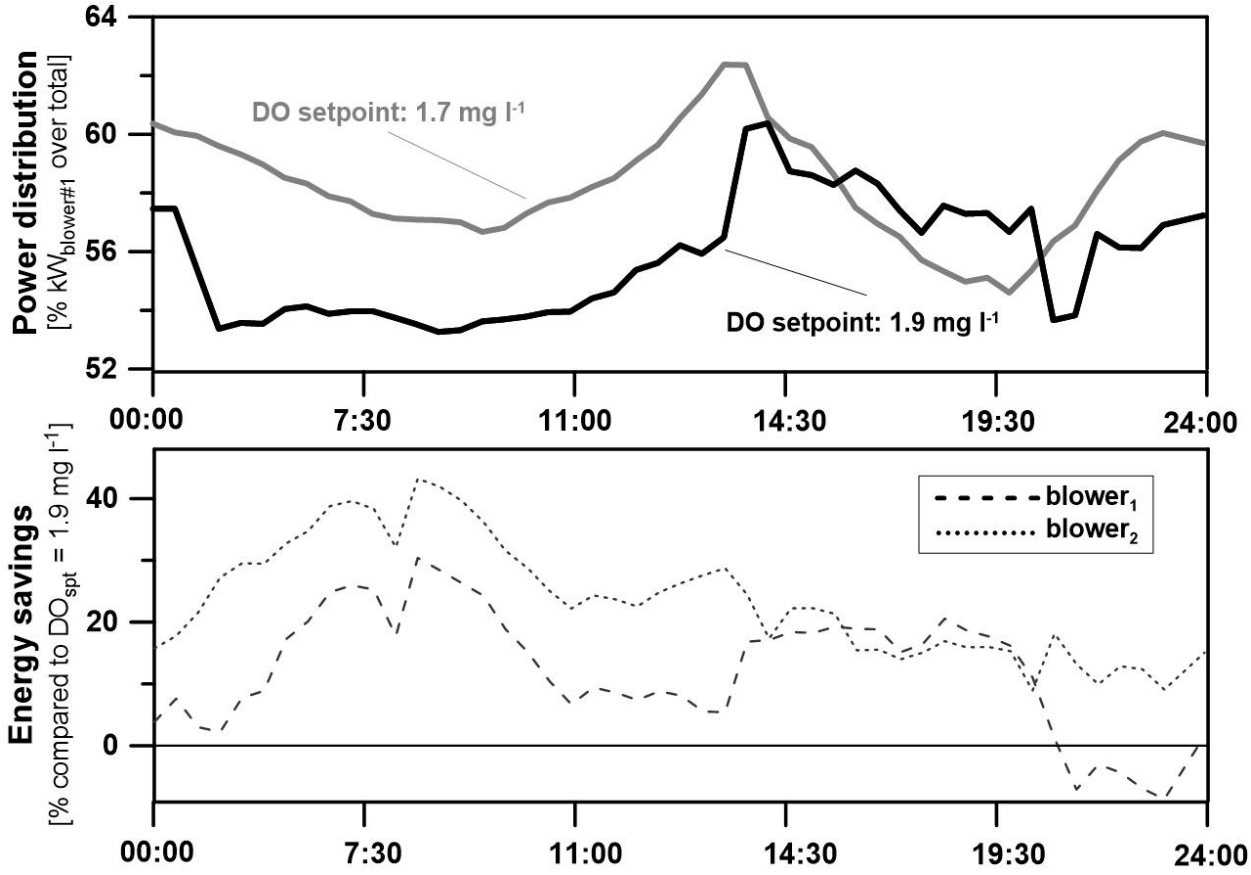

Figures 3.7 – 3.8: The daily average profiles of blower's power demand distribution during 30 days of continuous monitoring is reported, before and after the setpoint reduction, expressed in % over the total capacity is shown in Fig.3.7 (upper). The daily profile of savings for power demand expressed in % compared to the baseline conditions for blowers #1, #2 and total is shown in Fig.3.8.

3.5 Summary and conclusions

Continuous long-term monitoring of aeration and its efficiency allowed the characterization of daily and seasonal dynamics of process operations for secondary treatment in WRRFs. The collected profiles were implemented in a series of site-specific models to quantify energy footprint reduction associated with DO reduction imposing effluent quality as a constraint. The energy savings predicted from modelling were validated at full-scale with the implementation of a DO set point reduction from 1.9 to 1.7 mg l^{-1} in the first aerobic section of the secondary treatment tank of a WRRF. On average, our quantification indicates a 2% reduction in power demand for aeration resulted from 0.1 mg l^{-1} reduction of DO set point. However, when daily dynamics were considered, 17.6% reduction (on average) in specific power demand (W $m^3_{inf.}{}^{-1}$) for aeration was observed, while effluent quality and process stability were ensured. The spatial distribution of OTR over the tank length shifted from 43/41/16% to 56/34/10% for first, second and third aerobic sections, while the tank average was comparable before and after the DO variation.

The air flow decreased by 7.8%, 26.8% and 7.6% for first, second and third section, respectively, yielding to a 13% reduction in total air flow compared to the previous conditions and 25% increase in αSOTE in the first section, where 60% of the total air flow was supplied. The DO decrease implemented in the aeration control reduced the total power demand and modified it distribution among the two blowers which shifted from 56/44% to 58/42% for blower#1/blower#2, on average, as shown in Fig.3.7. Power demand reduction for blower#1 resulted from the minimization of over-aerated conditions and improved blower's stability during high loading

conditions, while the overall air flow rate reduction allowed to decrease blower #2 usage during low loading conditions (Fig. 3.8).

In conclusion, this study quantified the significant savings in power demand and energy costs associated with a moderate decrease in DO setpoint, while ensuring effluent quality. It was observed how a moderate modification of process conditions (0.2 mg l^{-1} DO reduction) yielded to a complex response of the aeration control system over the tank length. Hence, site-specific considerations are required to successfully evaluate and adopt the optimization strategy, as existing conditions may limit or even nullify the beneficial effect of process modifications.

References

Åmand, L., G. Olsson, and B. Carlsson. 2013. "Aeration Control - A Review." *Water Science and Technology* 67 (11): 2374–98.

Amaral, Andreia, Oliver Schraa, Leiv Rieger, Sylvie Gillot, Yannick Fayolle, Giacomo Bellandi, Youri Amerlinck, et al. 2016. "Towards Advanced Aeration Modelling: From Blower to Bubbles to Bulk." *Water Science & Technology* 75 (3–4): 507–17. https://doi.org/10.2166/wst.2016.365.

Amerlinck, Y, G Bellandi, A Amaral, S Weijers, and I Nopens. 2016. "Detailed Off-Gas Measurements for Improved Modelling of the Aeration Performance at the WWTP of Eindhoven." *Water Science and Technology* 74 (1): 203–11. https://doi.org/10.2166/wst.2016.200.

Aymerich, I, L Rieger, R Sobhani, D Rosso, and Ll Corominas. 2015. "The Difference between Energy Consumption and Energy Cost: Modelling Energy Tariff Structures for Water Resource Recovery Facilities." *Water Research* 81: 113–23. https://doi.org/10.1016/j.watres.2015.04.033.

Baroni, P, G Bertanza, C Collivignarelli, and V Zambarda. 2006. "Process Improvement and Energy Saving in a Full Scale Wastewater Treatment Plant: Air Supply Regulation by a Fuzzy Logic System." *Environmental Technology* 27 (7): 733–46. https://doi.org/10.1080/09593332708618689.

Chotkowski, W, M A Brdys, and K Konarczak. 2005. "Dissolved Oxygen Control for Activated Sludge Processes." *International Journal of Systems Science* 36 (12): 727–36.

https://doi.org/10.1080/00207720500218866.

Emami, Nasir, Reza Sobhani, and Diego Rosso. 2018. “Diurnal Variations of the Energy Intensity and Associated Greenhouse Gas Emissions for Activated Sludge Processes.” *Water Science and Technology* 77 (7): 1838–50.

Fan, Haitao, Lu Qi, Guoqiang Liu, Yuankai Zhang, Qiang Fan, and Hongchen Wang. 2017. “Aeration Optimization through Operation at Low Dissolved Oxygen Concentrations: Evaluation of Oxygen Mass Transfer Dynamics in Different Activated Sludge Systems.” *Journal of Environmental Sciences (China)* 55: 224–35. https://doi.org/10.1016/j.jes.2016.08.008.

Gernaey, A. Krist, Britta Petersen, Jean Pierre Ottoy, and Peter Vanrolleghem. 2001. “Activated Sludge Monitoring with Combined Respirometric-Titrimetric Measurements.” *Water Research* 35 (5): 1280–94. https://doi.org/10.1016/S0043-1354(00)00366-3.

Grant, S. B., J.-D. Saphores, D. L. Feldman, a. J. Hamilton, T. D. Fletcher, P. L. M. Cook, M. Stewardson, et al. 2012. “Taking the ‘Waste’ Out of ‘Wastewater’ for Human Water Security and Ecosystem Sustainability.” *Science* 337 (6095): 681–86. https://doi.org/10.1126/science.1216852.

Guo, Tianjiao, James Englehardt, and Tingting Wu. 2014. “Review of Cost versus Scale: Water and Wastewater Treatment and Reuse Processes.” *Water Science and Technology* 69 (2): 223–34. https://doi.org/10.2166/wst.2013.734.

Henze, Mogens. 2015. “Activated Sludge Model No 1,” no. 1.

Hodgson, B., R. Subramanian, B. Cavanaugh, D. Rosso, K. Brischke, and M. Garrido-Baserba.

2019. “Our Blowers Are Too Large! We’re Wasting Too Much Energy!....Hmmm..Maybe Not!” *WEFTEC 2019 - 92nd Annual Water Environment Federation’s Technical Exhibition and Conference*, 1415–35.

Ingildsen, Pernille, and Gustaf Olsson. 2015. *Smart Water Utilities : Complexity Made Simple.* IWA Publishing.

Iranpour, Reza, and Michael K. Stenstrom. 2001. “Relationship Between Oxygen Transfer Rate and Air flow for Fine-Pore Aeration Under Process Conditions.” *Water Environment Research* 73 (3): 266–75. https://doi.org/10.2175/106143001x139272.

Jiang, Lu Man, Manel Garrido-Baserba, Daniel Nolasco, Ahmed Al-Omari, Haydee DeClippeleir, Sudhir Murthy, and Diego Rosso. 2017. “Modelling Oxygen Transfer Using Dynamic Alpha Factors.” *Water Research* 124: 139–48. https://doi.org/10.1016/j.watres.2017.07.032.

Loosdrecht, Mark C. M. van, and Damir Brdjanovic. 2014. “Anticipating the next Century of Wastewater Treatment.” *Science* 344 (6191): 1452–53.

Ogurek, Michael, and Jens Alex. 2015. “A Novel Integrated Approach for Designing , Testing and Implementing WRRF Process Control Solutions.” In .

Pittoors, Erika, Yaping Guo, and Stijn W.H. Van Hulle. 2014. “Modeling Dissolved Oxygen Concentration for Optimizing Aeration Systems and Reducing Oxygen Consumption in Activated Sludge Processes: A Review.” *Chemical Engineering Communications*. https://doi.org/10.1080/00986445.2014.883974.

Pittoors, Erika, Yaping Guo, and Stijn W. H. Van Hulle. 2014. “MODELING DISSOLVED

OXYGEN CONCENTRATION FOR OPTIMIZING AERATION SYSTEMS AND REDUCING OXYGEN CONSUMPTION IN ACTIVATED SLUDGE PROCESSES: A REVIEW." *Chemical Engineering Communications* 201 (8): 983–1002. https://doi.org/10.1080/00986445.2014.883974.

Reardon, David J. 1995. "Turning down the Power." *Civil Engineering* 65 (8): 54–56.

Regmi, Pusker, Mark W Miller, Becky Holgate, Ryder Bunce, Hongkeun Park, Kartik Chandran, Bernhard Wett, Sudhir Murthy, and Charles B Bott. 2014. "Control of Aeration, Aerobic SRT and COD Input for Mainstream Nitritation/Denitritation." *Water Research* 57: 162–71. https://doi.org/10.1016/j.watres.2014.03.035.

Rosso, Diego. 2018. *Aeration, Mixing, and Energy: Bubbles and Sparks | IWA Publishing*. Edited by Diego Rosso. Irvine, California: IWA publishing.

Rosso, Diego, Lory E Larson, and Michael K Stenstrom. 2008. "Aeration of Large-Scale Municipal Wastewater Treatment Plants: State of the Art." *Water Science and Technology*. https://doi.org/10.2166/wst.2008.218.

Schraa, Oliver, Leiv Rieger, and Jens Alex. 2017. "Development of a Model for Activated Sludge Aeration Systems: Linking Air Supply, Distribution, and Demand." *Water Science and Technology* 75 (3): 552–60. https://doi.org/10.2166/wst.2016.481.

Schuchardt, A, J A Libra, C Sahlmann, U Wiesmann, and R Gnirss. 2007. "Evaluation of Oxygen Transfer Efficiency under Process Conditions Using the Dynamic Off-Gas Method." *Environmental Technology* 28 (5): 479–89. https://doi.org/10.1080/09593332808618812.

Sedlak, D. 2014. *Water 4.0: The Past, Present, and Future of the World's Most Vital Resource*.

Spees, K, L Lave - The Energy Journal, and Undefined 2008. 2008. "Impacts of Responsive Load in PJM: Load Shifting and Real Time Pricing." *JSTOR*, 101–21.

Yinl, Mark T., and and Michael K. Stenstrom. 1996. "HPO-AS PROCESS." *Journal of Environmental Engineering* 122 (6): 484–92.

4. Off-gas and respirometric measurements to optimize secondary treatment in WRRFs*

* A modified version of this chapter is published in the 91st Annual WEFTEC conference proceedings, New Orleans, Louisiana, USA, October 2018 and is in preparation for Water Research and the 93rd Annual WEFTEC conference, New Orleans, Louisiana, USA, October 2020.

4.1 Abstract

Aeration is one of the key steps of activated sludge (AS) treatment as well as one of the most energy intensive. The optimization of aeration systems can provide significant benefits varying from cost of treatment to improved stability of the electrical grid and GHG emissions reduction. Despite its importance, aeration systems in water resource recovery facilities (WRRFs) are often operated inefficiently whereas high air flow rates provided during peak of loading conditions to guarantee effluent quality often results in excessive aeration. Moreover, the time-based energy results in the amplification of cost for aeration during periods of lowest efficiency, exacerbating the negative effect of low operational efficiency.

Hence, the goal of this study is to develop a set of strategies to characterize process dynamics and highlight margin of improvements for energy efficiency and treatment capacity. Real-time monitoring of respirometric rates and aeration efficiency allowed to track strategic daily dynamics and provided correlations between oxygen requirements and biomass loading conditions, expressed by specific oxygen uptake rate (sOUR) and OTE%. The wide range of operating conditions covered by the experimental campaign allowed to investigate potential limitations of calculations from derived off-gas test, whenever geometric or hydraulic singularities are found (baffles, proximity to influent/effluent points, etc.).

The study confirmed the key role of a continuous process monitoring (off-gas test, respirometric test) to improve accuracy for process description, process control, process modelling and calibration.

4.2 Introduction

Water and resource recovery facilities (WRRFs) employ energy-intensive processes ((Marne 2013)). The energy consumption of a WRRF is defined by both operating and design parameters, including the technology used in the process, the size of the plant, the volume and the contaminant load of the influent (Metcalf & Eddy, 2014). Some of the characteristics mentioned above, such as the volume of the treated wastewater and its contaminant load, present daily or yearly fluctuations, with impacts on the operating conditions of the treatment process (Luccarini et al. 2010); (Campos and Von Sperling 1996)). Aeration is widely recognized as the core unit for wastewater treatment and a main component of the WRRF energy footprint. Alongside being a critical stage of treatment, aeration is one of the most energy intensive, frequently constituting 45 to 75% of the total energy cost for treatment ((Reardon 1995); (Rosso, Iranpour, and Stenstrom 2005)WEF, 2009).

Several studies have investigated the effect of environmental and operational conditions on oxygen transfer ((S. Gillot and Héduit 2000), Rosso and Stenstrom, 2006a, (Jimenez et al. 2014), (Karpinska, 2016), (Sommer et al. 2017)). Strong influence on oxygen transfer is exerted by multiple factors: flow regime resulting from air flow rate and type of diffusers (e.g., Rosso et al, 2005; (Sylvie Gillot and Héduit 2008) presence of surfactants (e.g., Zlokarnik, 1979; Rosso and Stenstrom, 2006b;) and rheological characteristics of the activated sludge (Gillot et al., 2005, (Germain et al. 2007), Fabiyi and Novak, 2008, Racault et al., 2011, Ratkovich et al., 2013, (Durán et al. 2016); (Jochen Henkel et al. 2009); Wagner et al, 2002). Moreover, the influence of the mean cell retention time (MCRT, d) was investigated extensively, showing that longer retention time is associated with better removal of surfactants from the water phase and consequently better oxygen

transfer (Rosso et al., 2009; (Krampe and Krauth 2003); (Germain et al. 2007); Henkel et al., 2009a, 2009b; (Fan et al. 2017a).

The dissolved oxygen (DO, mg l^{-1}) concentration is an indicator of the aerobic process condition: a minimum DO is necessary to guarantee that the oxygen requirements are met by the aeration system, and higher DO values are used to control the aeration system (Olsson 1999). In the ideal case, the oxygen transferred to the aeration tank equals the oxygen required from the biomass to oxidize the contaminants while providing adequate mixing to ensure solids suspension and maintaining residual DO concentration. Commonly, the DO is set at an approximate target of 2 mg l^{-1} at the exit of the aerobic tank, to prevent anoxic conditions in the secondary clarifiers (Metcalf & Eddy, 2014). Excessive air flow rates lead to unnecessarily elevated DO levels, which can be associated with hindered denitrification (due to the undesirable internal recirculation of DO) and challenges in secondary solid separation (Jenkins et at. 2003, Rosso, 2019; (Hodgson et al. 2019). Conversely, insufficient DO concentration resulting from inefficient aeration control may lead to lower effluent quality and reduced process stability, associated with filamentous bulking, poor settling, and microbial growth inhibition (Åmand, 2011).

Over the diurnal cycle, the DO concentration in all compartments of a secondary reactor tends to vary in response to process loading (Leu et al. 2009) and seasonal periods (Libra et al. 2005). As the process loading increases, the biomass oxygen uptake rate (OUR, mg l^{-1} h^{-1}) increases, for reactors that are not air limited. Respirometry is commonly adopted to measure OUR for a wide range of DO concentration. However, in the classic testing methodology, days are required to exhaust the organic load. This provides insightful results about the biomass's characteristic yet it offers partially spendable information for process control. Thus, continuous monitoring of OUR was introduced through off-line procedures based on steady-state calculations

(Beccari et al. 2002) as well as in-situ real-time measurements for process control ((Andreottola et al. 2007); (Baeza, Gabriel, and Lafuente 2002); (Sin and Vanrolleghem 2004)). Alternatively, off-gas analysis could be adopted to quantify OUR under varying conditions independently from DO concentration (ASCE 1996). This is achieved applying an oxygen mass balance to the control volume defined by the hood area times the tank depth, allowing to evaluate OUR despite the degree of loading conditions during the test.

Several options were developed to implement advanced DO control based on process state variables such as ammonia, combining feedback and feed-forward algorithms or using fuzzy logic ((Chotkowski, Brdys, and Konarczak 2005); (Baroni et al. 2006); (Yinl and and Michael K. Stenstrom 1996); (Regmi et al. 2014)). Ayesa (2006) highlighted the value of automated instrumentation and control at WRRFs to improve process design and operations. DO control strategies, which are typically associated with limited predictive capability, can be complemented with model-based prediction of DO, resulting in improved aeration efficiency, process stability and effluent quality, extending the operational life of the equipment and overall yielding to significant savings for cost of energy. ((Amand et al. 2011); (Rieger et al. 2012); (Pittoors, Guo, and Van Hulle 2014); (Aymerich et al. 2015)).

Trillo, Jenkins et al. (2004) developed a feedforward DO control strategy based on real-time off-gas analysis where the results were used to calculate the change in air flow. More, the profiles of oxygen demand for carbon and ammonia oxidization over the tank length were obtained by Schuchardt et al. (2007) through real-time off-gas analysis. (Amerlinck et al. 2016) applied off-gas monitoring to characterize process dynamics and applied the data to improve the aeration model accuracy for DO concentration. Sahlmann et al. (2004) and Thunberg, Sundin, and Carlsson (2009) investigated a cascade controller and a strategy to redistribute air flow by setpoint

differentiations to match oxygen demand and minimise sludge stabilization. Additional insights were offered by Yoo and Kim (2009) where auto-tuning PID controls for DO setpoints were implemented based on off-gas and respirometric measurements, showing potential energy savings and increased treatment stability.

Nonetheless, the risk-adverse nature of WRRF management to avoid liability for non-compliance to discharge limits is still hindering the application of advanced automated aeration control (Olsson, 2012), despite most aeration systems are currently unable to effectively adapt air supply to varying oxygen requirements (Pittoors, Guo, and Van Hulle 2014).

Thus, the extended investigation of the relationship between the oxygen transfer and demand from microorganisms would offer a representative description of the aeration process varying conditions. Time-series analysis of specific respirometric rates and biomass kinetic coefficients such as half-saturation constant and decay rate (Sin and Vanrolleghem 2006) can support process diagnostics, modelling and control allowing the quantification of optimized sludge recycle rates (Stenstrom and Andrews, 1979), of aerobic storage (Goel et al. 1999) of the rates of simultaneous uptake and growth of heterotrophic and autotrophic biomass (Beccari et al. 2002); (Marsili-Libelli and Tabani 2002)), nitrification ((Guisasola et al. 2005); (Puig et al. 2005)), of the rate of denitrification (Third, Burnett, and Cord-Ruwisch 2003) and of the rate of endogenous respiration (Koch et al. 2000).

Moreover, as the fractionation of organic load varies with time and position along the aeration tank, different contributions to the total oxygen uptake for carbon oxidation and nitrification are expected (Ohashi et al. 1995, Hu et al. 2009). Many authors have reported a wide range of half-saturation DO coefficients for Monod kinetic forms for AOB and NOB, yet the results were often dependent on the test conditions (pure or mixed cultures, pH, DO, ammonia

concentration, MCRT, etc.) ((Stenstrom and Poduska 1980); (HU et al. 2009)). Furthermore, the measurement of DO in water should be carefully scrutinized, since different DO sensors are associated with different time constants and error, especially at the lowest range ((Philichi and Stenstrom 1989); (Baquero-Rodríguez et al. 2018); (Y. Jiang et al. 2018)).

Recent studies showed how high nitrification rates could be achieved at low DO when the biomass MCRT is adequate to prevent nitifiers bacteria washout (Jubany et al. 2009)). Therefore, nitrification rate can be manipulated in case long MRCT and low DO are maintained for adequate time, the autotrophic yield would be higher than of heterotrophic, as faster substrate uptake and lower decay rate for autotrophic bacteria would be resulting (HU et al. 2009). Moreover, as oxygen uptake for nitrogen and carbon is spatially distributed inside the floc volume, low dissolved oxygen concentration would result in a concentration gradient decreasing towards the centre of the floc, where anoxic micro-zones are created (Stenstrom and Poduska 1980). Operating at such conditions may led to the successful development of SND processes or different pathways of nitrogen utilization (partial nitrification) ((Pochana, Keller, and Lant 1999); (Holman and Wareham 2005); (Fan et al. 2017b)).

In this study, two WWRFs with anoxic/aerobic secondary treatment layout and different loading conditions (single feed, step-feed) were investigated through automated real-time monitoring of respirometric rates for carbon oxidation and nitrification as well as aeration efficiency indicators. An automated apparatus allowed to perform a multi-parameter analysis of process and operating conditions to quantify time and space variability and highlight optimal conditions. A methodology to diagnostic criticalities and to evaluate optimization strategies in secondary treatment was developed. Finally, potential limitations or bias of the results collected during test are discussed.

4.3 Materials and methods

4.3.1 Oxygen requirements in secondary treatment

Oxygen requirements is secondary treatment were derived by stoichiometric calculations based on water quality (soluble COD, ammonia). Samples were collected for each aerobic section, thus the spatial mapping of contaminants concentration allowed to create a profile of oxygen requirements for carbon oxidation and nitrification along the tank length. The coefficient applied to quantify the fractionation of carbonaceous load were: 1 mg DO per mg $sCOD^{-1}$, 0.33 sCOD/bCOD, 0.45 rbCOD/sCOD. Oxygen requirements for nitrification was calculated adopting the following coefficients: 4.57 mg DO per mg NH_3-N^{-1}.

4.3.2 Power demand calculation:

The blowers operating conditions were analysed to quantify the variations in power demand and highlight optimal process conditions (i.e., max aeration efficiency). Power demand for aeration was derived from off-gas measurements for WRRF#1 and #2 and additionally measured via power metering at WRRF#2. The mechanical power (break horsepower) demand was derived from the adiabatic formula shown in (eq.1) based on off-gas test results.

$$P_w = \frac{wRT_1}{29.7\ n\ e}\left[\left(\frac{p_2}{p_1}\right)^{0.283} - 1\right] \qquad \text{(Eq. 1)}$$

Where:

P_w is the power required for each blower (kW);

w is the weight of air flow expressed in kg O_2/h (kg/s);

R is gas constant for air (8.314 kJ/k mol K);

T_1 is the absolute inlet temperature;

p_1 is absolute inlet pressure, p_2 is absolute outlet pressure, depending on aeration system and diffusers submergence;

n is a constant equal to 0.283 for air;

e is the blower mechanical efficiency (<1).

Shown in eq.1 it is possible to highlight how temperature, mass of oxygen transferred, pressure and mechanical efficiency are the variables affecting the continuous calculation of power demand from off-gas measurements. Whereas pressure for inlet and outlet can be assumed constant for the tested conditions and the effect of temperature is partially accounted for by the standardization of off-gas results (i.e, OTE% vs αSOTE%), little attention is generally dedicated to the understanding variation of mechanical efficiency. Because many blowers are operated at constant pressure, variations in the air flow rate for daily load fluctuations are adjusted through variations in the rotation and/or the adjustment of the air inlet/outlet section. This may likely result in variable efficiency over the day, whereas constant mechanical efficiency is generally considered in the calculations. Hence, the data series obtained from power metering were used to calibrate the adiabatic formula and evaluate optimal operating conditions for the blowers.

4.3.3 Test conduct:

Two different facilities treating municipal wastewater were investigated in Southern California. Large and medium plant sizes as well as different plant configuration were selected to cover a wide range of operating conditions and investigate criticalities/singularities due to the conduct of the test at site-specific conditions.

WRRF#1 served a population of approximately 1 million people treating an average influent flow rate of $3.8x10^5$ m^3 d^{-1} (100MGD). The secondary treatment was divided in 5 parallel aeration tanks, while every unit was operated as a 4-pass step-feed where 50%,30% and 20% of influent were distributed along passes 1 – 3. Each pass was divided with alternating anoxic and aerobic zones (Fig. 4.1a) and biomass was operated with MCRT an average of 16 days. The density of fine bubbles diffusers in each section decreased along the tank, while air was delivered from the same group of blowers for both headers pipe to the tested tank, controlled with a scheduled air flow rate control. WRRF#2 is designed for a maximum capacity of $6.1x10^3$ m^3 d^{-1} (16.3MGD) but currently operated at approximately $3.4x10^3$ m3 d^{-1} (9 MGD). The liquid treatment section consisted of preliminary screening and grit removal, primary clarification, secondary treatment by aeration basins and clarification. Secondary treatment is operated in the pre-denitrification – nitrification configuration for nutrient removal with a MCRT of 18 days. Secondary tank total volume of is divided in 3 anoxic and 3 aerobic sections. Air is supplied to the aeration tank by the equal blowers (500HP) with 60%, 35% and 5% air distribution for the first, second and third section respectively. The solids removed were directed to a different facility for thickening, anaerobic digestion, and dewatering. The utility recovers energy through a combination of a biogas powered microturbine, solar panels, and battery energy storage.

4.3.4 Experimental setup:

The experimental setup consisted of off-gas test apparatus and respirometer. A system of valves allowed to capture samples from multiple points with a single set of sensors. Two hoods were deployed at different points of the aeration tank to capture off-gas for a minimum of 8 hours of sampling periods. The hoods were equipped with dissolved oxygen sensor and piping system to sample mixed liquor at the depth of about 1 meter below the off-gas sampling point. While off-gas was collected from the hoods, mixed liquor was sampled to fill a batch reactor where respirometric test were performed. The sampling system was fully automatic and data was logged on-site and sent to a cloud based databased through the PLC controller. Following is a detailed description of the components and methodologies adopted.

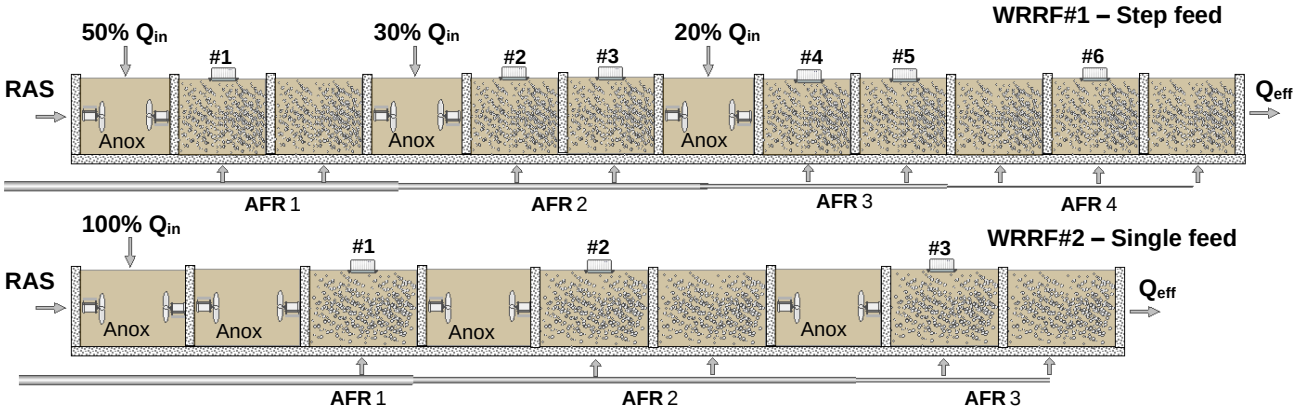

Figure 4.1a – Secondary tanks layout for WRRF#1 and WRRF#2. Sampling positions for off-gas and respirometric measurements are numbered along the tank length highlighted in the box.

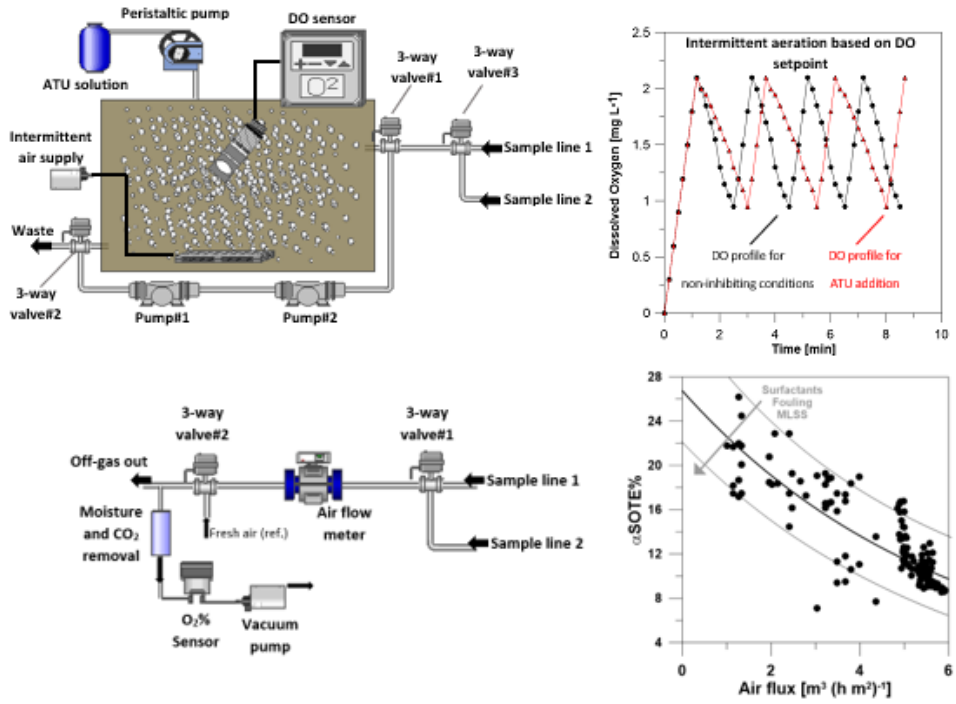

Figures 4.1b, 4.1c – (upper) Respirometer layout is shown. The batch of mixed liquor (2.2 l) was sampled and OUR calculations were performed by intermittent aeration provided by a DO setpoint control. OUR was measured for non-inhibited (carbon + ammonia) and inhibited conditions for nitrification by ATU addition (only carbon). (lower) Off-gas apparatus is shown, composed of air flow meter, O2% sensor, sample conditioning and valves system to select off-gas and fresh air.

4.3.5 Respirometer:

The respirometric equipment (Fig. 4.1b) was fully automated and the control strategy designed to minimize lag time between samples and ensure repeatability of the test (volume of the sample, mixing conditions, etc.). In particular, the procedure for each set of measurements was composed: mixed liquor sampling, alternating non-aerated mixing and aerated mixing, waste. A set of centrifugal pumps allowed to collect a volume of 2.2 liters of mixed liquor in correspondence to the off-gas sampling location. The consistent sampling volume was ensured by the control strategy based on a timer coupled with level sensor in the batch reactor and overflow system in case of overfilling. Once the batch reactor was filled to the design volume, the 3-way valves system was switched to create a closed loop with reactor and the centrifugal pumps, so to recirculate the sample. The inlet and outlet points of the recirculation line were designed to avoid turbulent surface conditions (not to favor oxygen transfer from atmospheric air) and mixing through recirculation was provided until the DO level reached the low setpoint (approximately 1 mg/l of DO). The dissolved oxygen was measured by a membrane DO sensor fixed in inclined position in the reactor to prevent bubbles build up on the membrane and situated to avoid dead mixing zones or flow shortcuts due to recirculation. At this point, the mixed liquor was aerated through a porous stone fed by a low flow rate air blower. As the DO concentration reach the high setpoint, the aeration was switched off by the controller. At this time, the decreasing slope of DO concentration (eq.4) was recorded until DO reached the low setpoint to measure oxygen demand for carbon and ammonia oxidation (OUR_{Tot}). The OUR measurement was performed for 3 cycles (cycle: air on, air off) providing triplicate calculations for averaging. A dedicated part of the control loop was here implemented to prevent over-aeration and minimize the length of the measurement cycle as

well as maintain the sample constantly within the low and high dissolved oxygen setpoint. The concomitant effect of the DO sensors technology, the mixing provided by the recirculation pumps and aeration control strategy allowed to track DO variations with adequate resolution. Once 3 valid values were recorded from the PLC, the valves system was switched, mixed liquor from the batch reactor was re-pumped into the tank and a new sampling phase started. A fresh sample from the same location was this time conditioned to measure the fractionation of oxygen demand. A solution of allylthiourea (ATU) was added by a peristaltic pump to the reactor before the mixed liquor was sampled to a concentration of 10-15 mg/liter to create inhibiting conditions for nitrification (Baquero-Rodríguez et al. 2018).This respirometric rate for carbon oxidation (OUR_C) was then calculated with the same method described above. Once OUR_{Tot} and OUR_C were measured for one position, the valves system was switch and a different location was selected to restart the test.

4.3.6 Off-gas test:

Likely to the respirometric equipment, the off-gas apparatus was fully automated (Fig. 4.1c). The control strategy allowed to perform and log measurements minimizing the lag-time between the results obtained at different locations for respirometric and off-gas tests. The gas leaving the hoods was directed to the instrument through PVC pipes and 3-way valves system, in order to selectively direct the flow incoming from the two sampling points to the instrument or to a release valve, respectively, and avoid pressure build-up in the system. The first section of the sampling line of the instrument hosted a mass flow meter (Kurz, 454FTB) to measure air flow rate. Length and diameter of the piping system were designed to avoid turbulence and favor laminar regime to ensure accuracy in the measurement. While the air flow rate and tank dissolved oxygen

were measured, a vacuum pump sampled the off-gas flowing in the PVC pipe, forcing it to a column containing salts (drierite, sodium hydroxide in pellets) to remove moisture and CO_2. The gas was then passing through a O_2% sensor (AMI, Model 65) to measure the O_2 content in the process air. The calculation of the OTE% was performed when atmospheric air was sampled by switching a 3-way valve upstream the sampling line, to measure the reference point of oxygen content in the influent air to the tank (O_2% in) and wash the sampling line. For every off-gas measurement (sampling frequency ~ 15 mins) a time-stamped result for OTR, OUR and blower's BHP was calculated and logged in real-time through the PLC controller. The adopted methodology did not fully conform to the standard (ASCE 1997), as the number and the position of the measurements were designed to track time-space variability of aeration efficiency rather than represent an average performance of the tank.

4.3.7 Oxygen Uptake Calculation:

A mass balance for oxygen within the volume of each completely mixed reactor is determined by the equation:

$$\boldsymbol{Q\left(DO_{\mathrm{in}}-DO\right)+k_La_f\left(DO^*_{20}-\mathrm{DO}\right)V=V\frac{\Delta DO}{\Delta t}} \quad \text{(Eq. 2)}$$

Dividing by V and letting Δ -> 0 yields the following differential equation:

$$\boldsymbol{\frac{dDO}{dt}=\left[\frac{\left(DO_{\mathrm{in}}-DO\right)}{t^*}\right]+=k_La_f\left(DO^*_{20}-\mathrm{DO}\right)-OUR} \quad \text{(Eq. 3)}$$

where t^* = detention time = V/Q and Q = total flow rate = Q_{inf} + Q_{rec}

By setting dC/dt equal to zero in Eq. 3, the steady state solution relates the oxygen uptake rate (OUR) in the aeration tank, to the oxygen transfer coefficient and the steady state deficit:

$$\boldsymbol{OUR = \frac{\left(DO_{in} - DO\right)}{t^*} + k_L a_f \left(DO^*_{\backsim 20} - DO\right)} \qquad \text{(Eq. 4)}$$

where DO = reactor concentration and dDO/dt = 0 (ASCE 1997)

4.3.8 Oxygen Uptake Rate via respirometry:

Biological oxygen demand through respirometric test is performed in absence of influent oxygen in batch reactor, where the equation to determine the oxygen uptake rate simplifies in:

$$\boldsymbol{\frac{dDO}{dt} = -OUR} \qquad \text{(Eq. 5)}$$

In this case, an automatic dissolved oxygen control based on minimum and maximum setpoints provided intermittent aeration to perform multiple respirations and average the slope of DO depletion.

4.3.9 Water quality:

TSS was measured according to the standard methods (APHA 2005). COD and Ammonia were determined using Hach® for low and high range kits (Loveland, CO).

4.4 Results and discussion

4.4.1 Analysis of respirometric OUR on-line monitoring

The effect of loading conditions on biomass oxygen demand is shown in Fig.4.2. Ammonia and soluble COD were adopted as indicators for organic load during the daily variability. Samples were collected hourly at each sampling point to track temporal and spatial influent variability. The average contaminants concentration in the aeration tank over the test period for WRRF#1 and WRRF#2 respectively was 69±43 mg l^{-1} and 87±60 mg l^{-1} for soluble COD while 18±13 mg l^{-1} and 5±5 mg l^{-1} was measured for ammonia. Overall, the highest average respiration rates resulted for carbon oxidation which was equal to 9.5±2.8 and 10.9 ± 8.8 mg DO per (g MLSS h)$^{-1}$ for WRRF#1 and WRRF#2, respectively, while for rates for nitrification were measured to be 3.2 ± 2.1 for WRRF#1 and 0.9 ± 0.4 mg DO per (g MLSS h)$^{-1}$ for WRRF#2, respectively. The concomitant oxygen demand of nitrification and carbon oxidation was differentiated to address the magnitude of the two processes on the biomass activity. The correlation observed between specific OUR and substrate concentration shown in Fig.4.2 corroborated the validity of the adopted methodology.

The relationship between specific OUR and oxygen requirements for soluble COD showed the expected semi-saturational kinetic form where respirometric rates tended to an asymptotic maximum for non-limiting and non-inhibiting substrate. The shaded area sitting on the fit for COD data represents different fractionation of carbonaceous substrate, as rbCOD decreased along the tank length. The semi-saturation coefficient for carbon was estimated around ks_{bCOD} ~ 50 mg bCOD l^{-1}, in accordance to what commonly presented in literature (Metcalf&Eddy). Similar

correlation between oxygen requirements and respiration rates was observed for nitrification, where the asymptotic maximum was reached for lower concentrations. In this case the semi-saturational constant was estimated around 10-15 mg NH_3-N l^{-1}.

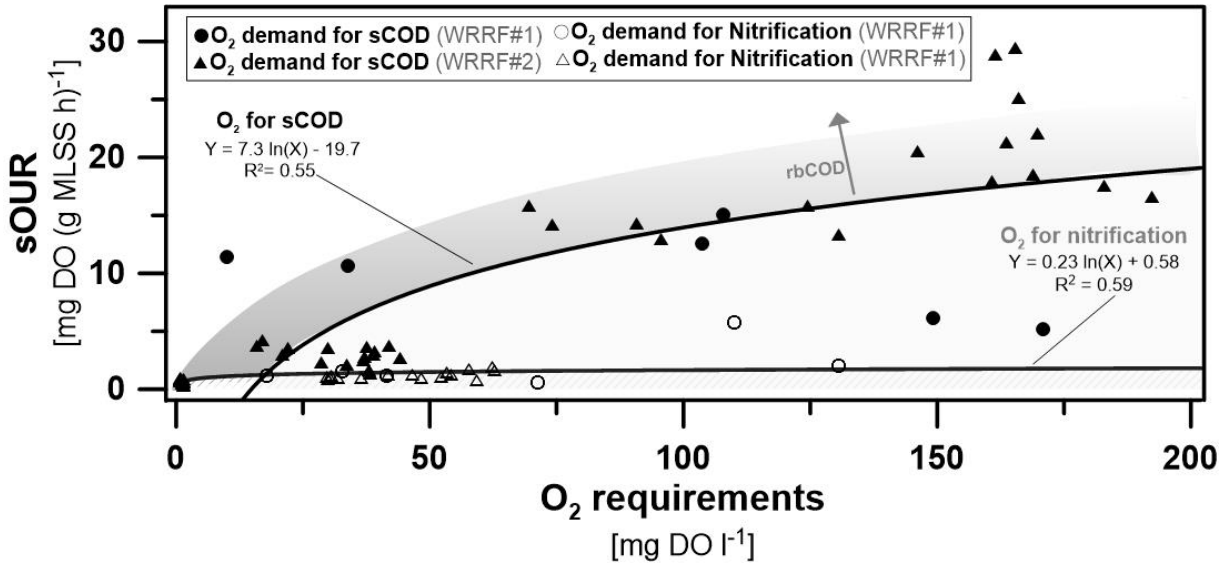

Figure 4.2 – The specific oxygen uptake rate and oxygen requirements for WRRF#1 and WRFF#2 are shown. Specific OUR is expressed in mg DO per g MLSS h^{-1} while oxygen requirements for sCOD and ammonia are derived water quality analysis and expressed in mg DO $l^{-1.}$

4.4.2 Effect of C:N ratio and operating conditions on nitrification

Shown in Fig. 4.3, the soluble C:N ratio was analyzed to investigate the influence on the competition for organic carbon and ammonium for nutrients and oxygen inside the biofilm (Satoh et al. 2000). The ratio between soluble carbonaceous substrate (sCOD) and ammonia was calculated from the water quality analysis and is shown on X axis, while specific OUR for nitrification from respirometric measurements is expressed in mg DO per g $MLSS^{-1}$ h^{-1}. The daily

averages resulting from each sampling point from two WRRFs (#1,#2) showed how nitrification rate was affected by organic substrate composition (sCOD, ammonia, DO): when easily biodegradable carbon was significantly higher than ammonium, heterotrophic activity was favored compared to nitrification. Lower oxygen demand for nitrification compared to carbon oxidation was observed within 15% of the aeration tank length for WRRFs #1 and #2.

The highest nitrification rates compared to oxygen uptake for carbon was measured within 30% of the tank length for single-feed while it was instead shifted towards the end of the tank for the step-feed configuration. A plug-flow behavior was observed for WRRF#2 (single-feed) where respirometric rates and organic load decreased along the tank length, whereas more homogenous conditions were observed for WRRF#1 due to the step-feed configuration, resulting in a narrower range of C:N ratio along the tank length. The critical ratio between carbonaceous and ammonia (C:N*) is highlighted in Fig. 4.3 to represent the threshold after which nitrification rates are independent from substrate concentration as heterotrophic respiration outcompete nitrifiers activity.

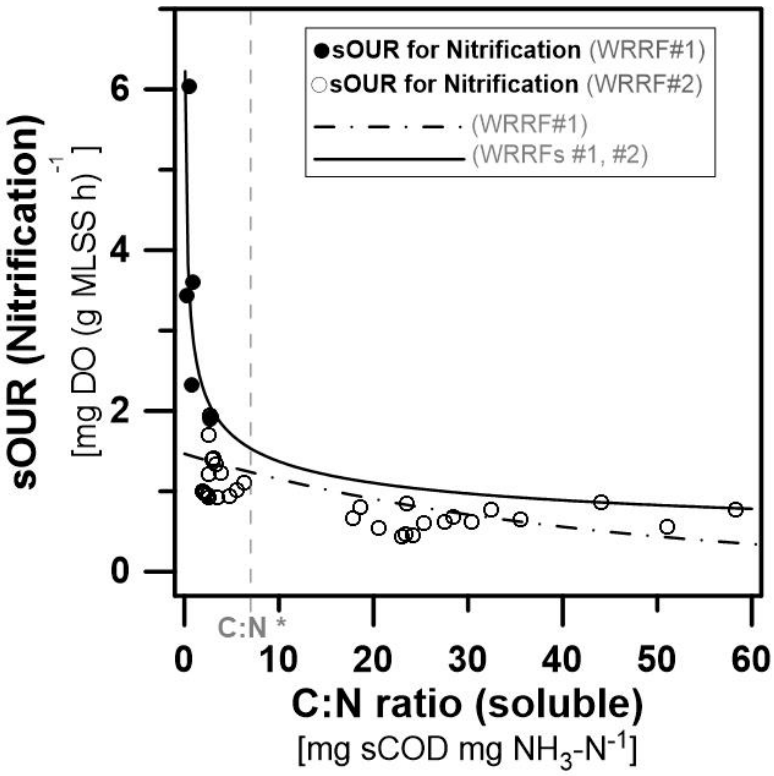

Figure 4.3 – The effect of sCOD:N ratio and dissolved oxygen on oxygen demand for nitrification are shown. The C:N ratio was derived from water quality (sCOD, ammonia); specific OUR for nitrification was measured from respirometric test and expressed in mg DO g MLSS h; dissolved oxygen is expressed in mg DO l^{-1}.

4.4.3 Effect of MLSS and contaminants concentration on oxygen transfer

The effect of contaminants concentration on biomass oxygen demand and transfer efficiency is shown in Fig. 4.4. Many authors engaged in the investigation of a surrogate indicator to describe the effect loading conditions on oxygen transfer. A correlation between COD and alpha factor was first highlighted by Steinmetz (1996) and extended by the results presented by Germain et al. (2007) and Leu et al. (2009). The data presented were able to correlate alpha factor and COD

concentration ($R^2 = 0.7$) despite results were obtained at different WRRFs operating with different aeration systems (fine bubbles, coarse bubbles).

Thus, extended monitoring of organic load allowed to predict the oxygen transfer efficiency independently from the aeration equipment adopted. More, as COD measurements are commonly adopted by most facilities to periodically define process performances, this was recognized to be a representative surrogate indicator. However, the continuous characterization of COD may fail to accurately track the variation of loading conditions and the effect on oxygen transfer. First, total COD measurements would not allow to define the organic load fractionation and introduce uncertainty about the biomass activity related to carbon or ammonia oxidation. Second, the variable concentration of surfactants cannot be defined as a solid correlation between COD measurements and surfactants is yet to be found.

Hence, the analysis of the effect of loading conditions on oxygen transfer was additionally investigated with the inclusion of MLSS characteristics through the definition of specific OUR, as the effect of MLVSS and MCRT on oxygen transfer is largely recognized ((Mena et al. 2005), (Raszka, Chorvatova, and Wanner 2006), (J. Henkel, Cornel, and Wagner 2011), Rosso et. al, Garrido et al.). Daily averaged results from multiple sampling points at WRRF#1 and WRRF#2 shown comparable average process conditions between the facilities, although higher variability in transfer efficiency and oxygen demand was measured for WRRF#2.

This difference between the WRRFs is attributable to the distribution of organic load: for WRRF#2, the single feed resulted in the expected decreasing trend along the tank length for sOUR and OTE%, thus assimilable to plug-flow reactor. Consequentially, wider differential of oxygen requirements between influent and effluent sections along the tank resulted in wider range of air flow rate supplied, hence the larger variability of transfer efficiency. For WRRF#1, less variability

was observed as the step-feed configurations resulted in more homogenous conditions over the tank. Correlation describing loading and oxygen transfer was observed when specific OUR was introduced in the quantification of loading conditions instead of COD concentration. When only the data collected at WRRF#2 were included the resulting R^2 for the fit was 0.85, which was reduced to 0.75 when all data (WRRF#1, WRRF#2) were considered, comparably to what previously observed by Garrido and Leu et al.

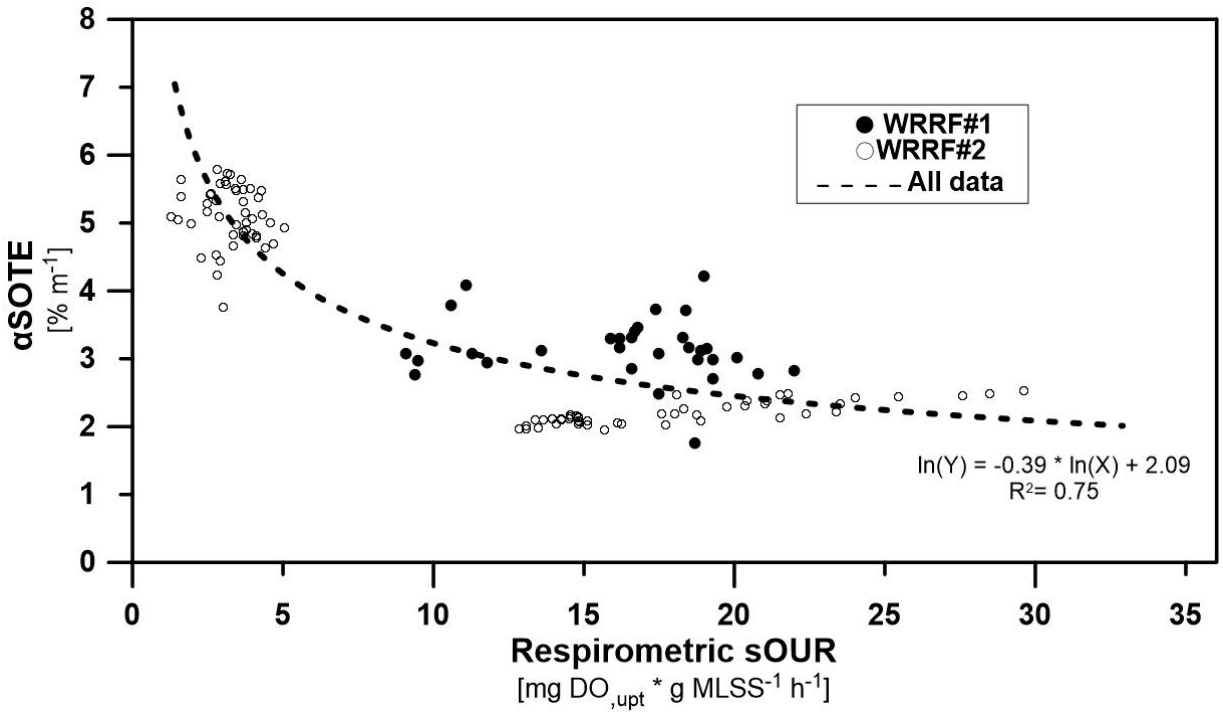

Figure 4.4 – The effect of loading conditions and MLSS concentration and MCRT on oxygen transfer is shown for WRRF#1 and #WRRF#2. Oxygen transfer is expressed by SOTE% per m^{-1} of depth and loading conditions and MLSS concentration are expressed in mg DO per g MLSS h^{-1} by respirometric measurements.

4.4.4 Effect of loading and operating conditions on aeration efficiency

The effect of the operating conditions on the cost of aeration along the tank length is shown in Figs.4.5a, 4.5b, 4.5c, 4.5d. The range of different air flow rates adopted during the day and along the tank length to ensure adequate air supply resulted in variable aeration efficiency (Tables 4.2, 4.3). Daily average data collected from multiple positions at WRRFs #1 and #2 allowed to map the variation of process state variables along the tank length. Biomass loading conditions for carbon oxidation and nitrification were quantified by the ratio between each reactor's oxygen demand and oxygen requirements (theoretical, calculated stoichiometrically from water quality analysis), expressed in mg O_2 of uptake per mg O_2 required (Fig. 4.5a).

The effect of operating conditions on sludge settleability and floc volume was expressed by the SVI in ml per g MLSS (Fig.4.5b). The efficiency of air supply for each operating condition was quantified through the calculation of aeration efficiency (SAE), expressed in kg O_2 transferred per kWh (Fig. 4.5c). To correlate process performances in terms of operative parameters, air flow rate and dissolved oxygen were also considered (Fig. 4.5d). Through the analysis of Figs.4.5a-4.5d, a comprehensive evaluation of optimization measures for both process performances and energy efficiency can be performed. Once the correlation between oxygen requirements and oxygen demand are known at any time and any given section of the tank, loading or biomass conditions can be modified to match the desired improvement. Viceversa, if increased aeration efficiency is targeted, the air flow rate reduction can be evaluated together with the process stability for oxygen demand and settling characteristics. In this study, lowest SAE values were observed on average within the first 30% of the aeration tank length, correspondent to highest air flow rate and dissolved oxygen (Fig. 4.5d). Highest SAE values were instead measured for the aerobic sections

closer to the tank effluent where load and air flow rate reached the lowest values, as expected. Nitrification decreased to its minimum while carbon oxidation approached its maximum as SAE increased.

Dissolved oxygen and air flow rate were progressively reduced. For this highest SAE range, the asymptotic correlation between aeration efficiency and tank length (Fig. 4.5c) represents the approach to a maximum aeration efficiency where the limit is set in function of the adopted aeration equipment (fine bubbles, coarse bubbles, diffusers density, blower's efficiency, etc.). Thus, by analyzing the variation of SAE and loading conditions, the optimal operating point maximizing treatment capacity and minimizing the counter-productive effect of excessive aeration on the cost of secondary treatment can be evaluated. If the optimal range of air flow rates is accurately evaluated for site-specific conditions, energy wastage for over-aeration can be minimized by a local reduction of the DO setpoint (Schuchardt et al. 2007).

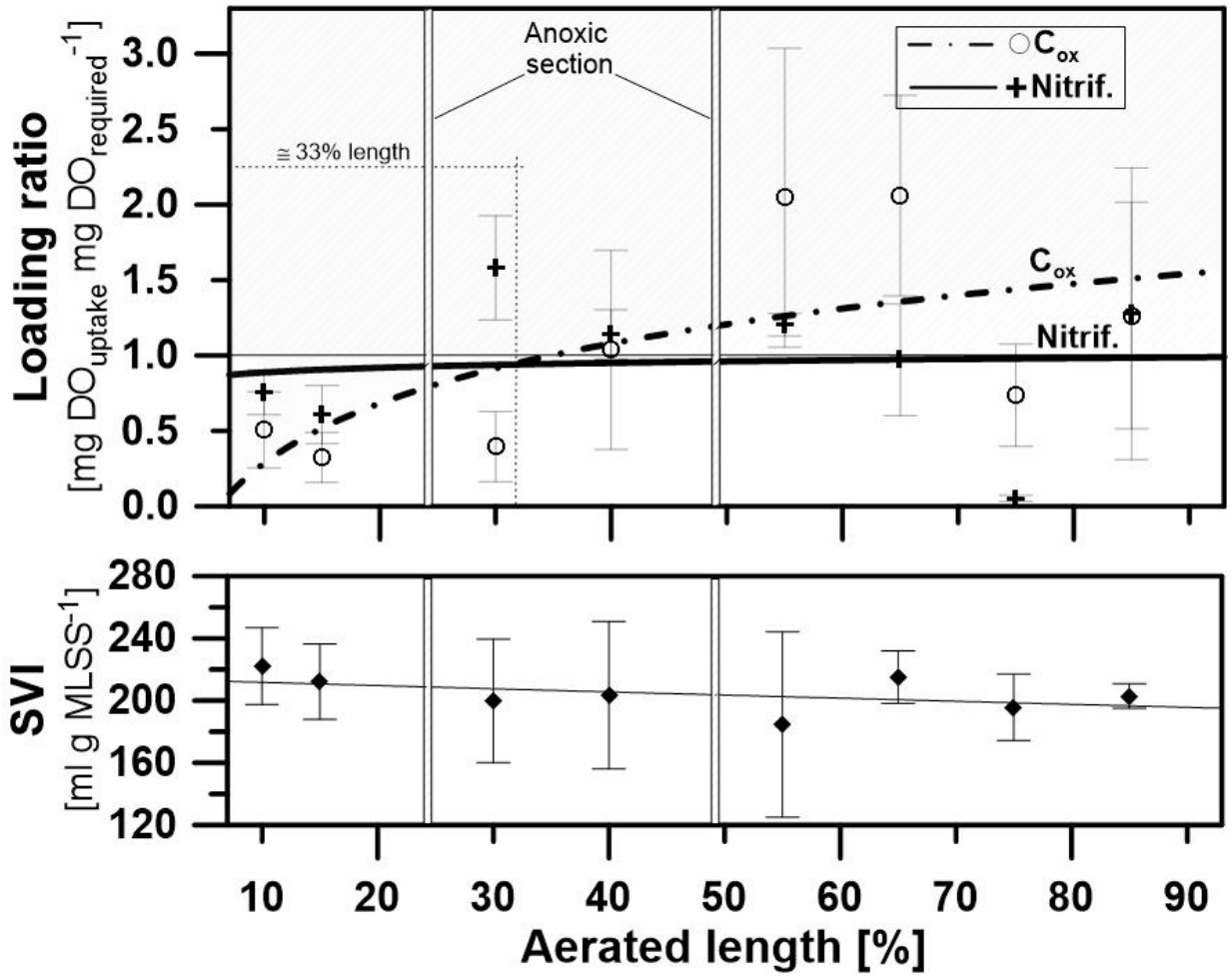

Figures 4.5a, 4.5b - Loading conditions expressed in mg O_2 of uptake per mg O_2 of required for carbon oxidation and nitrification are reported in Fig.4.5a (upper) along the tank length. Floc volume and settling characteristics are shown in Fig.4.5b expressed in ml per g of MLSS (lower).

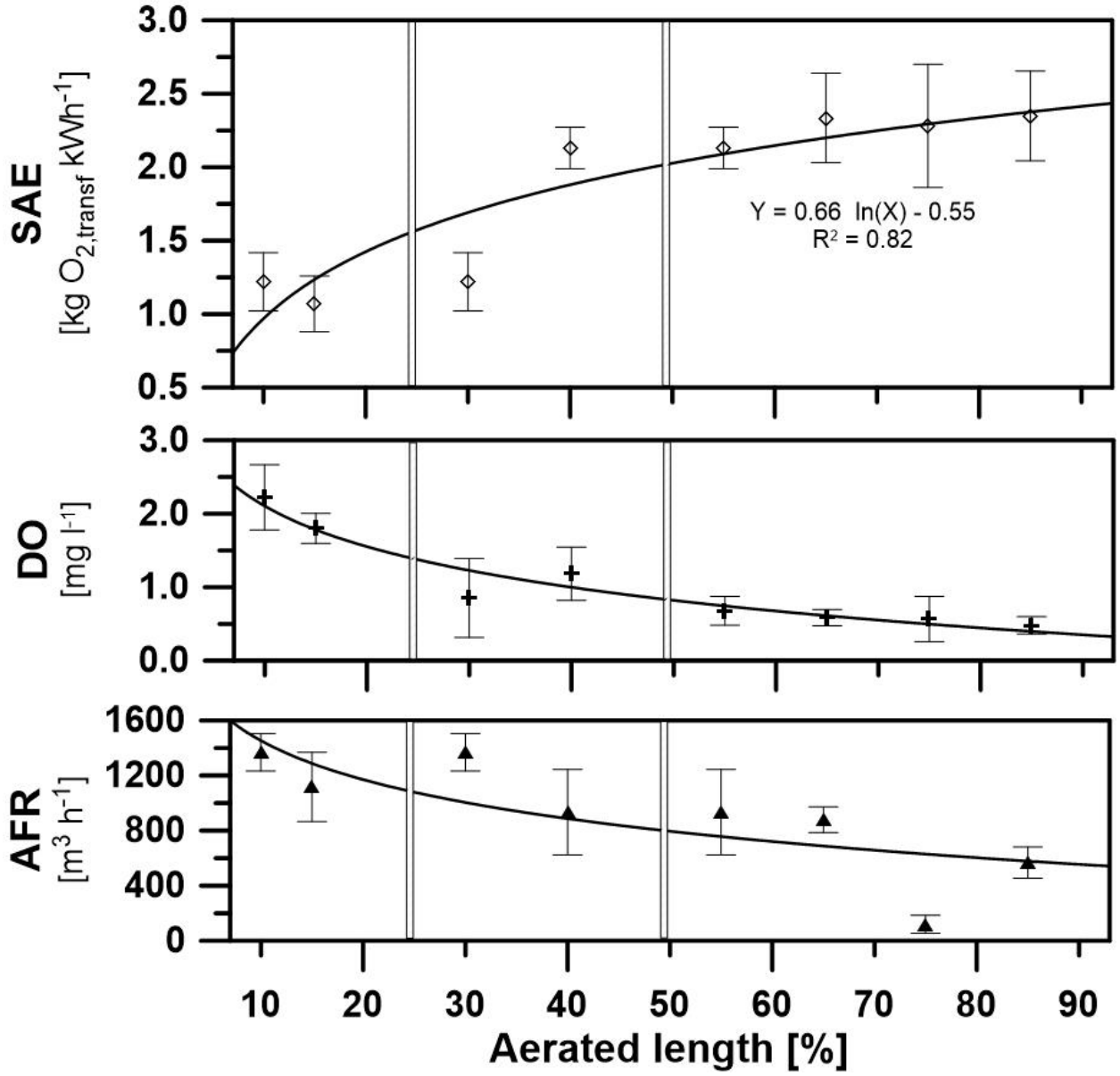

Figures 4.5c, 4.5d –The profile of aeration efficiency (SAE) along the tank is shown in Fig. 4.5c (mid-bottom) expressed in kg O_2 transferred per kWh. The effect of operating conditions is shown in Fig.4.5d (bottom) where DO concentration and air flow rate are reported.

Table 4.1 - Summary of average process conditions at WRRFs #1 and #2.

Parameter	WRRF#1	WRRF#2
Influent configuration	Step-feed	Single feed
Flow rate [MGD]	22.7	8.2
Flow rate [m^3 d^{-1}]	80,930	31,040
MLSS [mg l^{-1}]	5300	3300
MCRT [days]	16±3	18±2
BOD_5 [mg l^{-1}]$_{influent}$	204	300
TSS [mg l^{-1}]$_{influent}$	134	294
NH_3 [mg l^{-1}]$_{influent}$	33.7	43.2
NH_3 [mg l^{-1}]$_{effluent}$	0.6	0.1
Side water depth [m]	4.5	4.8
Diffusers submergence [m]	3.8	4.5

Table 4.2 - Summary of off-gas and respirometric results for WRRFs #1 and 2.

Process conditions	WRRF#1	WRRF#2
DO [mg l^{-1}]	1.1 ± 0.59	1.24 ± 0.63
AFR [SCFM]	1863 ± 379	1924 ± 1531
sOUR for C ox [mg DO (g MLSS h)$^{-1}$]	9.5 ± 2.8	10.9 ± 8.8
sOUR for Nitrif. [mg DO (g MLSS h)$^{-1}$]	3.2 ± 2.1	0.9 ± 0.4
αSOTE [% m of depth^{-1}]	3.2± 0.5	3.7± 1.5
SAE [kg $O_{2\ transf.}$ kWh^{-1}]	1.9± 0.5	1.6± 0.7

4.4.5 Limitations and advantages of off-gas test monitoring

In order to produce comparable results between different basins, the standard methodology (ASCE 1997) requires constant air flow rate and a minimum coverage of 2% of the basin surface area to consider the results representative. However, no specific indications about time of the day and the operating conditions are expressed. The effect of process variability may therefore be overlooked and yield to unsatisfactory conclusions, especially in the case aeration system is controlled based on influent organic load, resulting in large daily variability. More, the flow field in the mixed liquor is strongly affected by the turbulence provided by aeration and mixing system (Tchobanoglous et al. 2003, Gresch et al. 2011, Karpinska et al. 2015). Therefore, the spatial distribution and size of the air plume may be influenced by geometric and site-specific operating conditions, introducing potential sources of inconsistency in the measurements. The validity of the results produced from off-gas monitoring was evaluated in real-time by the independent calculation of OUR from respirometric measurements and by blower's power demand metering. As off-gas test results allow to derive biomass oxygen demand (eq. 4) and power demand for the blowers (eq. 1), the difference between the "standard" (OUR respirometric, kW from power metering) and "derived" value (OUR off-gas, kW off-gas) can be adopted as a quality control soft sensor and provide further insights about the limitations of off-gas test results.

For OUR, the calculation from off-gas test is obtained imposing a closed oxygen mass balance to tank volume underlying the sampling hoods surface. Thus, the oscillation and spatial variability of air plumes may limit the applicability of the methodology where geometric and hydraulic singularities are observed (i.e, baffles, high liquid air flow rate, proximity to point with recirculating flows, etc.). In this study, despite caution was used to ensure spatial proximity

between sampling points for mixed liquor and the hoods collecting off-gas as well as high frequency of measurements to avoid delays between the two datasets, different OUR resulted from the two methodologies.

The respirometric (OUR_{resp}) and off-gas (OUR_{og}) results are shown in Fig 4.6. As the "standard" value from respirometry (OUR_{resp}) was assumed to represent real-time tank loading conditions for carbon oxidation and ammonia nitrification, the quantification of the differential value between the methodologies would allow to highlight under- or over-aerated conditions. Specifically, if $OUR_{resp}>OUR_{og}$, this would represent lack of oxygen supplied to the tank and enable to calculate the required air flow rate to match the optimal demand by difference between the two. On the other hand, if $OUR_{resp}<OUR_{og}$, this quantifies the inaccuracy in the OTR estimation for non-representative air flux is sampled from the hoods, when higher air flow increases turbulence and induces plumes spatial modification. In case where OTE% is the lowest (i.e, high load, high air flow), the disparity between the values is additionally exacerbated by the non-linear trend between air low rate and OTR when over-aeration occurs, which amplifies the over-estimation of OUR as higher apparent oxygen transfer results from the calculations compared to the real values (Iranpour and Stenstrom 2001).

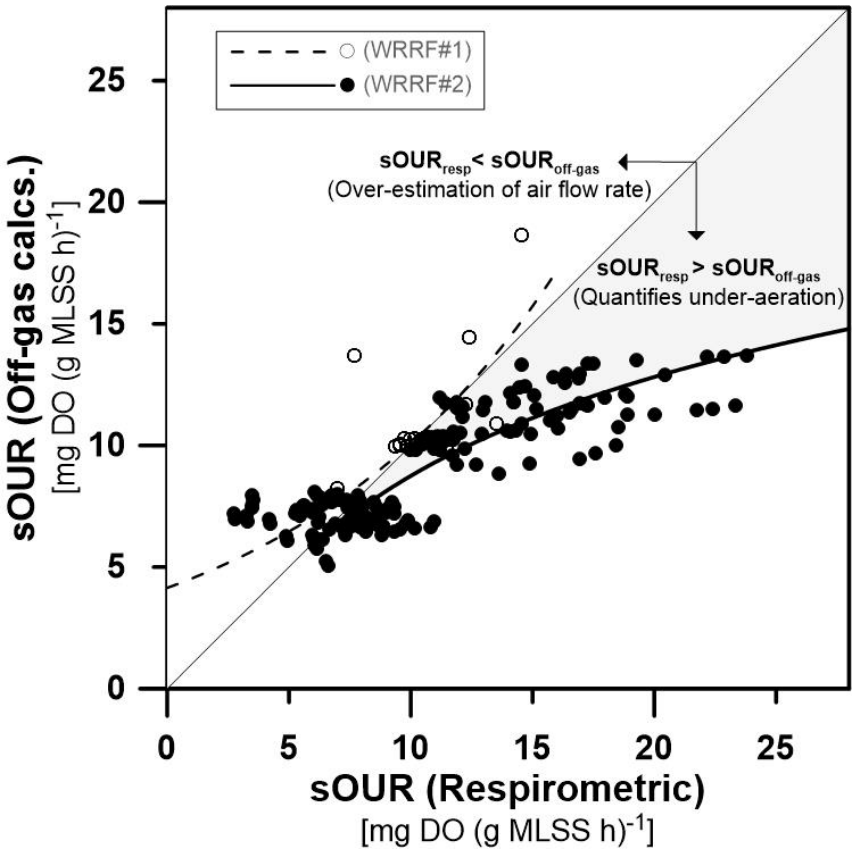

Figure 4.6 – The specific OUR measured from off-gas and respirometric methodology is shown. This is to investigate the validity of OUR measurements from off-gas test results and highlight sources of uncertainty in the measurements.

For blower power demand, the analysis of the differential value between metered ($kW_{metered}$) and off-gas calculation ($kW_{off\text{-}gas}$) can corroborate the analysis of OUR over-under estimation and ultimately allow to calibrate the adiabatic formula (eq.1) for site-specific conditions. Results collected at WRRF#2 during two consecutive testing periods operated at different DO are shown in Fig. 4.7 expressed in kW MG^{-1}, to overcome differences due to non-comparable loading conditions. Two separate linear trends can be highlighted for the datasets, where the DO modification resulted in higher slope observed for the linear fit of data collected at 1.7 mg l^{-1} compared to the previous condition (1.9 mg l^{-1}). Because the aeration system at WRRF#2 was operated at constant header pressure, only two variables comparing in eq.1 could embed the source of error: first, the under or over-estimation of the mass of oxygen transferred (W_{O2}); second, the incorrect estimation of blower efficiency due to a significant deviation from the assumed value. For the first case, the analysis of OUR results previously described would allow to highlight and exclude non-representative values. For the second case, the analysis of the differential value between the measured (metered) and estimated (off-gas) power demand would allow to quantify the variation in blower's efficiency and highlight optimal conditions, while constantly recalibrating the estimation to improve accuracy in the adoption of the adiabatic formula (eq.1).

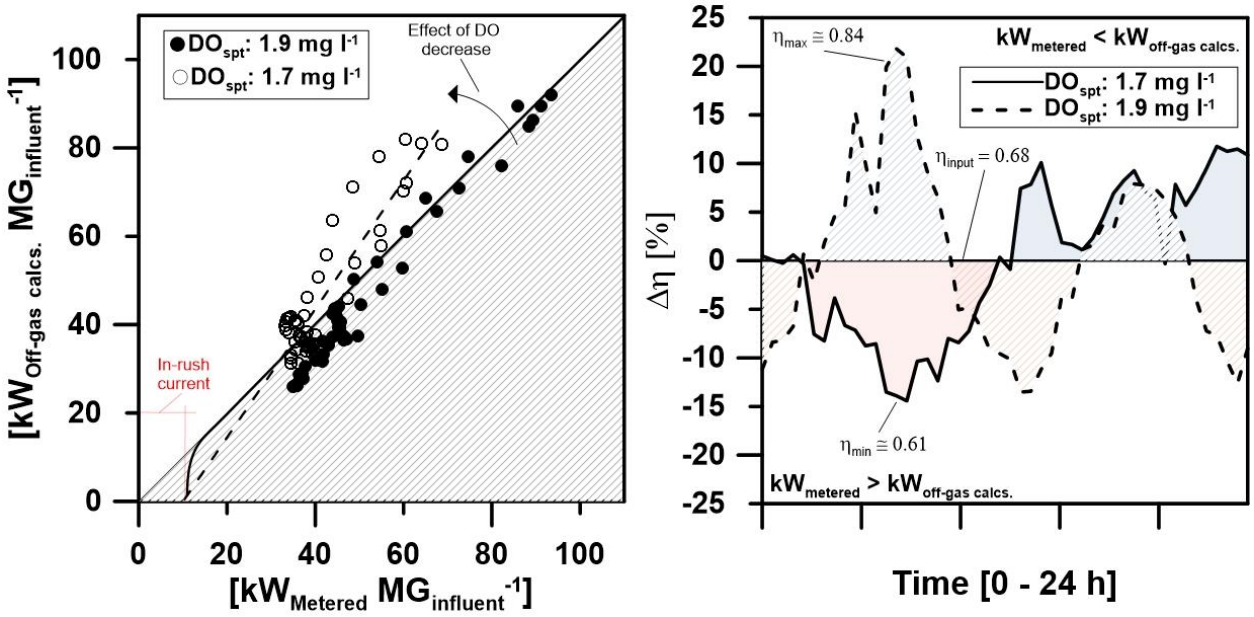

Figures 4.7, 4.8 – Power demand normalized on influent flow is reported in Fig.4.7 (left) independently measured from power metering and derived from off-gas results. The datasets for different DO setpoints show how power demand was over-estimated when DO was reduced. In Fig. 4.8 (right) the differential value between the two measurements is used to define blower efficiency dynamics over the day.

4.5 Summary and conclusions

Real-time respirometric measurements were performed to assess the biological oxygen demand for carbon oxidation and nitrification. Results showed how oxygen demand for carbon and nitrification can be manipulated through the control of process variables such as the C:N ratio, dissolved oxygen and biomass MCRT. Hence, the reduction of DO coupled with real-time monitoring of process state variables may be a viable option to reduce cost for aeration while maintaining effluent quality and/or favour SND, additionally reducing the cost of treatment. The continuous off-gas monitoring allowed to characterize the transient efficiency of oxygen transfer. Good correlation between sOUR and oxygen transfer efficiency was found, similarly to what observed between alpha factor and COD concentration (L. M. Jiang et al. 2017).

A comprehensive analysis of the results allowed to highlight optimization strategies to reduce energy footprint for secondary treatment while ensuring effluent quality. The potential limitations of the proposed methodology were investigated and confirmed the importance of including site-specific constraints in process description and modelling. In conclusion, the coupled monitoring of respirometric rates and aeration efficiency indicators was confirmed to be a powerful tool to diagnose process performances and re-calibrate existing correlations to site-specific conditions.

References

Amerlinck, Y, G Bellandi, A Amaral, S Weijers, and I Nopens. 2016. "Detailed Off-Gas Measurements for Improved Modelling of the Aeration Performance at the WWTP of Eindhoven." *Water Science and Technology* 74 (1): 203–11. https://doi.org/10.2166/wst.2016.200.

Andreottola, G, E Oliveira, P Foladori, R Peterlini, and G Ziglio. 2007. "Respirometric Techniques for Assessment of Biological Kinetics in Constructed Wetland." In *Water Science and Technology*, 56:255–61. https://doi.org/10.2166/wst.2007.512.

APHA. 2005. "Standard Methods for the Examination of the Water and Wastewater." Washington, D.C.

Ayesa, Eduardo. 2006. "Supervisory Control Strategies for the New WWTP of Galindo-Bilbao : The Long Run from the Conceptual Design to the Full-Scale Experimental Validation Supervisory Control Strategies for the New WWTP of Galindo-Bilbao : The Long Run from the Conceptual Desi." *Water Science and Technology* 53: 193–201. https://doi.org/10.2166/wst.2006.124.

Aymerich, I, L Rieger, R Sobhani, D Rosso, and Ll Corominas. 2015. "The Difference between Energy Consumption and Energy Cost: Modelling Energy Tariff Structures for Water Resource Recovery Facilities." *Water Research* 81: 113–23. https://doi.org/10.1016/j.watres.2015.04.033.

Baeza, Juan Antonio, David Gabriel, and J. Lafuente. 2002. "In-Line Fast OUR (Oxygen Uptake Rate) Measurements for Monitoring and Control of WWTP." In *Water Science and*

Technology, 45:19–28. https://doi.org/10.2166/wst.2002.0541.

Baquero-Rodríguez, Gustavo Andrés, Jaime Andrés Lara-Borrero, Daniel Nolasco, and Diego Rosso. 2018. "A Critical Review of the Factors Affecting Modeling Oxygen Transfer by Fine-Pore Diffusers in Activated Sludge." *Water Environment Research* 90 (5): 431–41. https://doi.org/10.2175/106143017x15131012152988.

Baroni, P, G Bertanza, C Collivignarelli, and V Zambarda. 2006. "Process Improvement and Energy Saving in a Full Scale Wastewater Treatment Plant: Air Supply Regulation by a Fuzzy Logic System." *Environmental Technology* 27 (7): 733–46. https://doi.org/10.1080/09593332708618689.

Beccari, M, D Dionisi, A Giuliani, M Majone, and R Ramadori. 2002. "Effect of Different Carbon Sources on Aerobic Storage by Activated Sludge." In *Water Science and Technology*, 45:157–68. https://doi.org/10.2166/wst.2002.0103.

Campos, H. M., and M. Von Sperling. 1996. "Estimation of Domestic Wastewater Characteristics in a Developing Country Based on Socio-Economic Variables." *Water Science and Technology* 34 (3-4–4 pt 2): 71–77. https://doi.org/10.1016/0273-1223(96)00558-6.

Chotkowski, W, M A Brdys, and K Konarczak. 2005. "Dissolved Oxygen Control for Activated Sludge Processes." *International Journal of Systems Science* 36 (12): 727–36. https://doi.org/10.1080/00207720500218866.

Durán, C., Y. Fayolle, Y. Pechaud, A. Cockx, and S. Gillot. 2016. "Impact of Suspended Solids on the Activated Sludge Non-Newtonian Behaviour and on Oxygen Transfer in a Bubble Column." *Chemical Engineering Science* 141: 154–65. https://doi.org/10.1016/j.ces.2015.10.016.

Fan, Haitao, Lu Qi, Guoqiang Liu, Yuankai Zhang, Qiang Fan, and Hongchen Wang. 2017a. "Aeration Optimization through Operation at Low Dissolved Oxygen Concentrations: Evaluation of Oxygen Mass Transfer Dynamics in Different Activated Sludge Systems." *Journal of Environmental Sciences (China)*. https://doi.org/10.1016/j.jes.2016.08.008.

Fan et. al, 2017. "Aeration Optimization through Operation at Low Dissolved Oxygen Concentrations: Evaluation of Oxygen Mass Transfer Dynamics in Different Activated Sludge Systems." *Journal of Environmental Sciences (China)* 55: 224–35. https://doi.org/10.1016/j.jes.2016.08.008.

Germain, E., F. Nelles, A. Drews, P. Pearce, M. Kraume, E. Reid, S. J. Judd, and T. Stephenson. 2007. "Biomass Effects on Oxygen Transfer in Membrane Bioreactors." *Water Research* 41 (5): 1038–44. https://doi.org/10.1016/j.watres.2006.10.020.

Gillot, S., and A. Héduit. 2000. "Effect of Air Flow Rate on Oxygen Transfer in an Oxidation Ditch Equipped with Fine Bubble Diffusers and Slow Speed Mixers." *Water Research* 34 (5): 1756–62. https://doi.org/10.1016/S0043-1354(99)00323-1.

Gillot, Sylvie, and Alain Héduit. 2008. "Prediction of Alpha Factor Values for Fine Pore Aeration Systems." *Water Science and Technology* 57 (8): 1265–69. https://doi.org/10.2166/wst.2008.222.

Goel, Rajeev, Takashi Mino, Hiroyasu Satoh, and Tomonori Matsuo. 1999. "Modeling Hydrolysis Processes Considering Intracellular Storage." *Water Science and Technology* 39 (1): 97–105. https://doi.org/10.1016/S0273-1223(98)00779-3.

Guisasola, Albert, Irene Jubany, Juan A. Baeza, Julián Carrera, and Javier Lafuente. 2005. "Respirometric Estimation of the Oxygen Affinity Constants for Biological Ammonium and

Nitrite Oxidation." *Journal of Chemical Technology and Biotechnology* 80 (4): 388–96. https://doi.org/10.1002/jctb.1202.

Henkel, J., P. Cornel, and M. Wagner. 2011. "Oxygen Transfer in Activated Sludge - New Insights and Potentials for Cost Saving." *Water Science and Technology* 63 (12): 3034–38. https://doi.org/10.2166/wst.2011.607.

Henkel, Jochen, Mladen Lemac, Martin Wagner, and Peter Cornel. 2009. "Oxygen Transfer in Membrane Bioreactors Treating Synthetic Greywater." *Water Research* 43 (6): 1711–19. https://doi.org/10.1016/j.watres.2009.01.011.

Hodgson, B., R. Subramanian, B. Cavanaugh, D. Rosso, K. Brischke, and M. Garrido-Baserba. 2019. "Our Blowers Are Too Large! We're Wasting Too Much Energy!....Hmmm..Maybe Not!" *WEFTEC 2019 - 92nd Annual Water Environment Federation's Technical Exhibition and Conference*, 1415–35.

Holman, J. B., and D. G. Wareham. 2005. "COD, Ammonia and Dissolved Oxygen Time Profiles in the Simultaneous Nitrification/Denitrification Process." *Biochemical Engineering Journal* 22 (2): 125–33. https://doi.org/10.1016/j.bej.2004.09.001.

HU, Jie, Daping LI, Qiang LIU, Yong TAO, Xiaohong HE, Xiaomei WANG, Xudong LI, and Ping GAO. 2009. "Effect of Organic Carbon on Nitriffication Efficiency and Community Composition of Nitrifying Bioffilms." *Journal of Environmental Sciences*. https://doi.org/10.1016/S1001-0742(08)62281-0.

Iranpour, Reza, and Michael K. Stenstrom. 2001. "Relationship Between Oxygen Transfer Rate and Air flow for Fine-Pore Aeration Under Process Conditions." *Water Environment Research* 73 (3): 266–75. https://doi.org/10.2175/106143001x139272.

Jiang, Lu Man, Manel Garrido-Baserba, Daniel Nolasco, Ahmed Al-Omari, Haydee DeClippeleir, Sudhir Murthy, and Diego Rosso. 2017. "Modelling Oxygen Transfer Using Dynamic Alpha Factors." *Water Research* 124: 139–48. https://doi.org/10.1016/j.watres.2017.07.032.

Jiang, Yuyuan, Brian Bebee, Alvaro Mendoza, Alice K. Robinson, Xiaying Zhang, and Diego Rosso. 2018. "Energy Footprint and Carbon Emission Reduction Using Off-the-Grid Solar-Powered Mixing for Lagoon Treatment." *Journal of Environmental Management* 205: 125–33. https://doi.org/10.1016/j.jenvman.2017.09.049.

Jimenez, Mélanie, Nicolas Dietrich, John R Grace, and Gilles Hébrard. 2014. "Oxygen Mass Transfer and Hydrodynamic Behaviour in Wastewater: Determination of Local Impact of Surfactants by Visualization Techniques." *Water Research* 58: 111–21. https://doi.org/10.1016/j.watres.2014.03.065.

Jubany, Irene, Javier Lafuente, Juan A Baeza, and Julián Carrera. 2009. "Total and Stable Washout of Nitrite Oxidizing Bacteria from a Nitrifying Continuous Activated Sludge System Using Automatic Control Based on Oxygen Uptake Rate Measurements." *Water Research* 43 (11): 2761–72. https://doi.org/10.1016/j.watres.2009.03.022.

Karpinska, AM, J Bridgeman - Water research, and undefined 2016. 2016. "CFD-Aided Modelling of Activated Sludge Systems–A Critical Review." *Water Research*, no. 88: 861–79.

Koch, G., M. Kühni, W. Gujer, and H. Siegrist. 2000. "Calibration and Validation of Activated Sludge Model No. 3 for Swiss Municipal Wastewater." *Water Research*. https://doi.org/10.1016/S0043-1354(00)00105-6.

Krampe, J., and K. Krauth. 2003. "Oxygen Transfer into Activated Sludge with High MLSS Concentrations." *Water Science and Technology* 47 (11): 297–303.

https://doi.org/10.2166/wst.2003.0618.

Leu, Shao-yuan, Diego Rosso, Lory E Larson, and Michael K Stenstrom. 2009. “Real-Time Aeration Efficiency Monitoring in the Activated Sludge Process and Methods to Reduce Energy Consumption and Operating Costs.” *Water Environment Research* 81 (12): 2471–81. https://doi.org/10.2175/106143009x425906.

Libra, J. A., C. Sahlmann, A. Schuchardt, J. Handschag, U. Wiesmann, and R. Gnirss. 2005. “Evaluation of Ceramic and Membrane Diffusers under Operating Conditions with the Dynamic Offgas Method.” *Water Environment Research* 77 (5): 447–54. https://doi.org/10.2175/106143005x67359.

Luccarini, Luca, Gianni Luigi Bragadin, Gabriele Colombini, Maurizio Mancini, Paola Mello, Marco Montali, and Davide Sottara. 2010. “Formal Verification of Wastewater Treatment Processes Using Events Detected from Continuous Signals by Means of Artificial Neural Networks. Case Study: SBR Plant.” *Environmental Modelling and Software* 25 (5): 648–60. https://doi.org/10.1016/j.envsoft.2009.05.013.

Marne, Paris Est-créteil Val De. 2013. “Dossier De Paiement” 13 (December): 75012. https://doi.org/10.1061/(ASCE)1076-0342(2007)13.

Marsili-Libelli, S., and F. Tabani. 2002. “Accuracy Analysis of a Respirometer for Activated Sludge Dynamic Modelling.” *Water Research* 36 (5): 1181–92. https://doi.org/10.1016/S0043-1354(01)00339-6.

Mena, P. C., M. C. Ruzicka, F. A. Rocha, J. A. Teixeira, and J. Drahoš. 2005. “Effect of Solids on Homogeneous-Heterogeneous Flow Regime Transition in Bubble Columns.” *Chemical Engineering Science* 60 (22): 6013–26. https://doi.org/10.1016/j.ces.2005.04.020.

Philichi, T. L., and M. K. Stenstrom. 1989. “Effects of Dissolved Oxygen Probe Lag on Oxygen Transfer Parameter Estimation.” *Journal of the Water Pollution Control Federation* 61 (1): 83–86.

Pittoors, Erika, Yaping Guo, and Stijn W.H. Van Hulle. 2014. “Modeling Dissolved Oxygen Concentration for Optimizing Aeration Systems and Reducing Oxygen Consumption in Activated Sludge Processes: A Review.” *Chemical Engineering Communications*. https://doi.org/10.1080/00986445.2014.883974.

Pochana, Klangduen, Jürg Keller, and Paul Lant. 1999. “Model Development for Simultaneous Nitrification and Denitrification.” In *Water Science and Technology*, 39:235–43. https://doi.org/10.1016/S0273-1223(98)00789-6.

Puig, Sebastià, Lluís Corominas, M. Teresa Vives, M. Dolors Balaguer, Jesús Colprim, and Joan Colomer. 2005. “Development and Implementation of a Real-Time Control System for Nitrogen Removal Using OUR and ORP as End Points.” *Industrial and Engineering Chemistry Research* 44 (9): 3367–73. https://doi.org/10.1021/ie0488851.

Raszka, Anna, Monika Chorvatova, and Jiri Wanner. 2006. “The Role and Significance of Extracellular Polymers in Activated Sludge. Part I: Literature Review.” *Acta Hydrochimica et Hydrobiologica* 34 (5): 411–24. https://doi.org/10.1002/aheh.200500640.

Reardon, David J. 1995. “Turning down the Power.” *Civil Engineering* 65 (8): 54–56.

Regmi, Pusker, Mark W Miller, Becky Holgate, Ryder Bunce, Hongkeun Park, Kartik Chandran, Bernhard Wett, Sudhir Murthy, and Charles B Bott. 2014. “Control of Aeration, Aerobic SRT and COD Input for Mainstream Nitritation/Denitritation.” *Water Research* 57: 162–71. https://doi.org/10.1016/j.watres.2014.03.035.

Rosso, D., R. Iranpour, and M. K. Stenstrom. 2005. “Fifteen Years of Offgas Transfer Efficiency Measurements on Fine-Pore Aerators: Key Role of Sludge Age and Normalized Air Flux.” *Water Environment Research* 77 (3): 266–73. https://doi.org/10.2175/106143005x41843.

Sahlmann, C, Judy A Libra, A Schuchardt, U Wiesmann, and R Gnirss. 2004. “A Control Strategy for Reducing Aeration Costs during Low Loading Periods.” *Water Science and Technology* 50 (7): 61–68. https://doi.org/10.2166/wst.2004.0417.

Satoh, H., S. Okabe, N. Norimatsu, and Y. Watanabe. 2000. “Significance of Substrate C/N Ratio on Structure and Activity of Nitrifying Biofilms Determined by in Situ Hybridization and the Use of Microelectrodes.” *Water Science and Technology* 41 (4–5): 317–21. https://doi.org/10.2965/jswe.22.763.

Schuchardt, A, J A Libra, C Sahlmann, U Wiesmann, and R Gnirss. 2007. “Evaluation of Oxygen Transfer Efficiency under Process Conditions Using the Dynamic Off-Gas Method.” *Environmental Technology* 28 (5): 479–89. https://doi.org/10.1080/09593332808618812.

Sin, Gurkan, and Peter A. Vanrolleghem. 2006. “Evolution of an ASM2s-like Model Structure Due to Operational Changes of an SBR Process.” *Water Science and Technology* 53 (12): 237–45. https://doi.org/10.2166/wst.2006.426.

Sin, Gurkan, and Peter A Vanrolleghem. 2004. “A Nitrate Biosensor Based Methodology for Monitoring Anoxic Activated Sludge Activity.” *Water Science and Technology* 50 (11): 125–33. https://doi.org/10.2166/wst.2004.0680.

Sommer, A. E., M. Wagner, S. F. Reinecke, M. Bieberle, F. Barthel, and U. Hampel. 2017. “Analysis of Activated Sludge Aerated by Membrane and Monolithic Spargers with Ultrafast X-Ray Tomography.” *Flow Measurement and Instrumentation* 53: 18–27.

https://doi.org/10.1016/j.flowmeasinst.2016.05.008.

Stenstrom, Michael K., and Richard A. Poduska. 1980. “The Effect of Dissolved Oxygen Concentration on Nitrification.” *Water Research*. https://doi.org/10.1016/0043-1354(80)90122-0.

Third, Katie A, Natalie Burnett, and Ralf Cord-Ruwisch. 2003. “Simultaneous Nitrification and Denitrification Using Stored Substrate (PHB) as the Electron Donor in an SBR.” *Biotechnology and Bioengineering* 83 (6): 706–20. https://doi.org/10.1002/bit.10708.

Thunberg, A, A-m Sundin, and B Carlsson. 2009. “Energy Optimization of the Aeration Process at Käppala Wastewater Treatment Plant.” *10th IWA Conference on Instrumentation, Control and Automation*.

Yinl, Mark T., and and Michael K. Stenstrom. 1996. “HPO-AS PROCESS.” *Journal of Environmental Engineering* 122 (6): 484–92.

Yoo, ChangKyoo, and Min Han Kim. 2009. “Industrial Experience of Process Identification and Set-Point Decision Algorithm in a Full-Scale Treatment Plant.” *Journal of Environmental Management* 90 (8): 2823–30. https://doi.org/10.1016/j.jenvman.2009.04.004.

6. Conclusions

- Cost for aeration in secondary treatment is strongly influenced by daily fluctuations of loading conditions and by the adopted operative conditions (DO, air flow rate).
- **The variable and time-based cost of energy is often most influential than the daily energy consumption pattern**, as the negative effect of low energy efficiency periods is amplified by the highest cost of energy.
- The abatement of cost for energy consumption can be achieved manipulating plant operations in order to minimize peaks of power demand during targeted periods of the daily operations.
- The **continuous characterization of process state variables** describing loading conditions and efficiency of the aeration system **can be adopted as a diagnostic tool** for modelling, design and process control.
- By **coupling different techniques and independent measurements, additional insights about the process can be obtained.** For instance, the difference in the estimation of biomass respirometric rates derived from off-gas measurements and from respirometric test can be used to quantify the degree of under-aeration and optimize the air supply. More, if blower's power metering is performed, the effect of operating conditions on blower's efficiency can be evaluated by calculating the over or under-estimation of blower's power demand from adiabatic formula.
- **Site specific conditions need to be thoroughly evaluated** to increase accuracy for modelling and predictions, as the successful implementation of optimization strategies may be limited on even neutralized by equipment limitations.

The reduction of cost for aeration in secondary treatment of WRRFs can be achieved by intervening on:

- **Influent flow**: peaks in hydraulic and organic load can be curbed through equalization basins and/or strategic return flows with high contaminants concentration. This way, the ineffective air supply to variable oxygen requirements is decreased as the circadian amplification of air flow rate for hydraulic peak is minimized. More, carbon diversion from primary treatment to anaerobic digestion can additionally corroborate the energy optimization, as reducing organic load in primary stage translates in lower oxygen requirements to secondary treatment and higher biogas production.
- **Biomass characteristics (concentration, MCRT)**: the characterization of biomass respiration rates for carbonaceous contaminants and ammonia would allow to identify the optimal operating conditions. As higher removal of surfactants is associated with high MCRTs, the consistent characterization of biomass characteristics and variables describing aeration efficiency would help define most the most desirable wasting rate. More, the analysis of nitrification and the influence of C:N ratio would highlight optimal conditions to perform nitrification and to exploit the maximum biomass treatment capacity, whereas loading conditions can be modified to maintain maximum respiration rates.
- **Optimization of aeration efficiency:** the continuous monitoring of variables describing the efficiency of the aeration system for short (daily) and long-term (seasonal) variability would allow to highlight criticalities resulting in highest oxygen transfer suppression over the daily operations as well as the evaluation of fouling phenomena over time.

7. Future steps

For off-gas testing:

1. Evaluate the minimum hood area per unit of air flow to ensure accurate and representative results and the effect of flow regime on air plume at full-scale;
2. Introduce the continuous analysis of nitrification via off-gas test;
3. Introduce the continuous analysis of GHG emissions via off-gas test;

For respirometric testing:

4. Investigate the effect of dissolved oxygen on respirometric rates, biomass growth and half velocity constants for different MCRTs;
5. Minimize the use of respirometry to calibrate off-gas calculations and limit maintenance and manual labor;

For process characterization and control:

6. Develop a standard methodology to characterize process dynamics is secondary treatment via off-gas and respirometric tests;
7. Develop a standard methodology to continuously characterize settling characteristics and floc volume;
8. Merge the methodologies in a series of logic rules adopting real-time and historical data to re-calibrate and enhance predictions;
9. Implement aeration control based on respirometric and off-gas real time measurements;
10. Quantify savings per year to perform cost/benefit analysis and evaluate capital investment aimed to increase energy efficiency for equipment and operations.
11. Evaluate demand/response measures to curb cost of energy during high peak (solar panels, wind turbine, battery storage, etc).